약학박사 학위논문

Fluoride-assisted LC-ESI-MS/MS analysis of phenolic compounds in human urine

인간 소변 시료 내의 페놀 화합물에 대한 불소 보조 LC-ESI-MS/MS 분석

2023 년 2 월

서울대학교 대학원

약학과 생약학 전공

이 강 미

Fluoride-assisted LC-ESI-MS/MS analysis of phenolic compounds in human urine

인간 소변 시료 내의 페놀 화합물에 대한 불소 보조 LC-ESI-MS/MS 분석

지도교수 오 원 근

이 논문을 약학박사 학위논문으로 제출함

2022 년 12 월

서울대학교 대학원

약학과 생약학전공

이 강 미

이강미의 약학박사 학위논문을 인준함

2023 년 1 월

위 원 장 _____ 진 영 원 _____ (인)

부위원장 _____ 김 철 영 _____ (인)

위 원 _____ 양 희 정 _____ (인)

위 원 _____ 이 재 익 _____ (인)

위 원 _____ 오 원 근 _____ (인)

Abstract

Liquid chromatography (LC)–electrospray ionization (ESI)–mass spectrometry (MS) is conventional analytical platform for the applications in life sciences, such as environmental, pharmaceutical, and biological areas. In accordance with the technology development of our daily life, the demand for more sensitive and powerful analytical methodologies is increasing for advanced information. Therefore, recent analytical trends are focused on multi-class residue analysis only using low volume of micro-sampling, and the core requirement is highly sensitive detection limits of target analytes. In the LC–ESI–MS/MS analysis, mobile phase composition is a key parameter that affects the ionization efficiency and chromatographic behavior of analytes due to the ionization process based on liquid phase spray in ESI. In contrast to the well-known mobile phase additive (i.e., acetic acid or formic acid) for positive ESI, there have been few obvious descriptions for selecting the best mobile phase composition for negative ESI. Although many biomolecules favor positive ESI analysis, there are also a significant number of small molecules that can be easily ionized in negative ESI. Therefore, in the present study, we elucidated the correlation between the mobile phase composition and ionization efficiency in negative ESI mode.

To investigate the effect of mobile phase composition on ionization efficiency, propofol and environmental phenols were analyzed as target substances. Because they have a phenolic structure, which is a weak acid, and thus they are easily ionized into negatively charged ions in ESI. Propofol is a widely used anesthesia agent, but it is often abused for recreational purposes and has become a serious social problem.

Environmental phenols (i.e., bisphenols, parabens, benzophenones, chlorophenols, and alkylphenols) are important endocrine disrupting chemicals that can cause adverse health effects to exposed individuals. However, propofol determination in biological samples suffer from problems associated with its high volatility and poor ionization efficiency in mass spectrometry. Environmental phenols also have limitations in developing a comprehensive and sensitive analytical method using LC-ESI-MS/MS because a significant of phenols, especially alkylphenols, lack ESI sensitivity.

Herein, we have developed a sensitive and accurate fluoride-assisted LC-MS/MS method for the determination of phenolic compounds through systematic investigation of mobile phase composition. The dramatically improved ionization efficiency allowed a simple dilute and shoot assay. For propofol, the optimal concentration of ammonium fluoride in the mobile phase was 1 mM under methanol condition. In the validation, the linearity was good ($R^2 \geq 0.999$) and the intra- and inter-day precisions were between 1.9 and 8.7%. The accuracies ranged from 87.5% to 105.4% and the limits of detection and quantitation for propofol in urine were 0.15 and 0.44 ng/mL, respectively. The developed method was successfully applied to human urine and showed a sufficient sensitivity to determine propofol and its phase II metabolites over 48 h after administration. For environmental phenols, the proposed method was affected by 0.5 mM ammonium fluoride under methanol condition; and it allowed the concurrent ionization of 38 phenols and sensitivity enhancement especially for bisphenols and alkylphenols, which typically have poor ionization efficiency. The developed method was validated and all substances

satisfied higher than 0.99 of R^2 showing good linearity. The intra- and inter-day precisions for the target analytes were between 0.4 and 14.6% and the accuracies ranged from 85.4 to 113.0%, respectively. Furthermore, its application on 80 urine samples obtained from aquatic (swimming) and land (indoor volleyball and outdoor football) athletes found that certain athletes can be exposed to specific environmental phenols, depending on the type of sports activity.

Consequently, the phenol-specialized mobile phase composition significantly improved the inherently poor ionization efficiencies of phenolic compounds with high p*K*a values in negative ESI. Furthermore, the developed method has the potential as a generic analytical platform for phenol analysis that can be very useful for integrating newly identified phenolic compounds.

Keywords : Fluoride, ionization efficiency, propofol, environmental phenols, alkylphenols, negative ionization

Student Number : 2015-30505

Table of Contents

List of Tables

List of Figures

Chapter 1 : Introduction

1.1 Motivation

Liquid chromatography (LC)–electrospray ionization (ESI)– mass spectrometry (MS) is the most widely used technique for the application in environmental, pharmaceutical and biological areas. ESI has powerful advantage to ionize various compounds in liquid samples, even non-volatile and thermally labile bio-molecules that are not amenable to analysis by other conventional techniques (Smith et al., 1990). In particular, tandem mass spectrometry (MS/MS) can selectively detect fragmentation ions exhibiting structural information of target analytes by collision-induced dissociation in three quadrupoles system. This ion purification step allowed to simplify the complicated sample procedure in a broad range of materials, providing a highly sensitive, selective and high throughput analytical tool (Zhang et al., 2016).

However, as researchers who were a pioneering stage of technology development have uncovered the basic mechanisms of biological, environmental, and industrial parts over the decades, based on accumulated observations, more sensitive and powerful analytical technologies are required for advanced information (Seger and Salzmann, 2020). In accordance with the environment complexity of our daily life, the demand for multi-class residue analysis only using low volume of micro-sampling that require lower detection limits of target analytes is very high. And the essential prerequisite for comprehensive and sensitive method is concurrent ionization of multi-residue and high ionization efficiency in ESI source.

As a result, numerous studies have been conducted relative to sensitive enhancement in LC-ESI-MS/MS. To overcome this sensitivity issue, many studies have focused on the development of sample preparation methods prior to LC–ESI–MS/MS to concentrate the targeted analytes and remove the interferences using solid phase extraction (SPE), liquid liquid extraction (LLE) (Ulrich, 2000). Otherwise, derivatization methodology is applied to improve ionization efficiency with the incorporation of a functional group with a permanent charge, especially for analytes that are not efficiently ionized by ESI such as aldehydes, sugars, and steroids (Eggink et al., 2008). However, these methods have limitations as a simple and high-throughput multiresidue analytical technique. The approach to modification of sample preparation is not practical for large-scale epidemiological studies when it comes to the excessive demand for manpower, preparation time, and cost.

Consequently, solving sensitivity problem using other technology is crucial. In the LC–ESI–MS/MS analysis, the additive composition of mobile phase is a key parameter that affects the ionization efficiency and chromatographic behavior of analytes inherently (Wang et al., 2010). Because, ESI source has an ionization process based on liquid phase spray (Wilm, 2011). Therefore, several studies have been conducted on the investigation of mobile phase compositions to improve ionization efficiency. In particular, most of these studies have reported on mobile phase parameters that correlate with the sensitivity of positive ESI since most compounds are easily ionized in positive mode. Generally, the acidic mobile phase can increase the ionization efficiency of target analytes in positive mode by providing sufficient proton sources. As a result, formic acid or acetic acid are

commonly used as mobile phase additive in order to improve the ionization efficiency of analytes such as proteins and organic molecules that have basic functional groups (Cech and Enke, 2001; Hua and Jenke, 2012; Yang et al., 2013). A buffer such as ammonium formate or acetate also could be used as ion pairing reagent to improve chromatographic behavior of analytes in positive mode, because only using acid modifier in mobile phase often give rise to the poor chromatographic properties (Rainville et al., 2012).

However, the mechanism and performance of the negative ESI mode are different from those of the positive mode (Cole and Harrata, 1993). Negative ionization is more susceptible to electric discharge phenomena than positive ionization because electrons that emanate from the sharp edges of the electrospray capillary are easier at negative voltage (Cole and Harrata, 1993). And this leads to unstable formation of anionic adducts. Therefore, negative ionization mode has drawn less attention compared to positive ionization mode. However, it is of significant importance to investigate to improve negative ionization efficiency since numerous small molecules are easily ionized in negative ESI (Thurman et al., 2001). In addition, it is known that negative ionization is less affected by ionization suppression caused by the compounds co-eluting with the analyte (Thurman et al., 2001; Kloepfer et al., 2005). This can be an advantage in quantitative analysis. The following studies have elucidated the correlation between the ionization efficiency in negative mode and the analyte. Henriksen et al. (Henriksen et al., 2005) showed the influence of solution composition and the analyte characteristics in the negative mode. They presented the relationship between response and the logarithm of the

octanol-water partition coefficient (log P) was positively correlated for a number of structurally diverse analytes, but only to a limited extent. Huffman et al. (Huffman et al., 2012) have also studied the effect of polar protic (methanol and water) and polar aprotic (acetonitrile and acetone) solvents on the negative ionization with diverse small, acidic molecules. As in the previous study (Henriksen et al., 2005), they also observed that the response was greater in methanol than acetonitrile for most. However, there was a limitation depending on the structural characteristics of the analyte. Further, Kruve et al. (Kruve et al., 2014) predicted the deprotonation efficiency using the charge delocalization in anions. They observed that charge delocalization in the anion (WAPS) and degree of ionization (α) of the molecule in solution are the most important parameters in negative mode.

Despite several studies examining the correlation between negative ionization and analyte characteristics, there are limitations in optimization methods that can greatly improve the sensitivity in negative ESI. Therefore, in this study, we investigated the mobile phase composition that can maximize the ionization efficiency in negative ESI system.

1.2 Phenolic compounds

Phenols are weakly acidic compounds with high pK_a values; thus, they are preferably ionized in negative ESI. However, even in negative ESI mode in mass spectrometry, considerable phenol scaffold still exhibit low ionization efficiency or are not ionized in the common mobile phase composition due to their structural characteristics. Therefore, in order to investigate the influence of mobile phase

composition on ionization efficiency, phenolic compounds were selected as target analytes. In particular, it was proposed to analyze propofol and environmental phenols, which are gaining worldwide attention. First, single target analysis was performed by applying propofol, a pharmaceutical drug, and multi-residue analysis of environmental phenols, endocrine disrupting compounds, was conducted by extending this system.

1.3 Strategy and objectives

Recently, several studies have indicated that ammonium fluoride (AFL) as a mobile phase additive can enhance ionization efficiencies in negative ESI and it has been applied to various substances with poor ionization efficiency, such as steroids, polycyclic aromatic hydrocarbons, hydroxyl metabolites, and various endogenous metabolites (Yanes et al., 2011; Fiers et al., 2012; Lindner et al., 2017; Mulabagal et al., 2017; Wang et al., 2017; Cheng et al., 2019; Preindl et al., 2019). Furthermore, Yanes et al. (Yanes et al., 2011) reported that AFL increases the ionization efficiency of endogenous metabolites from *E.Coli* in negative ESI; while Preindl et al. (Preindl et al., 2019) reported that AFL enhances the ionization efficiency of xenoestrogens without derivatization. Details of the ionization process by AFL are still a matter of speculation, but it is generally assumed that the strong basicity of the fluoride ion increases the generation of deprotonated molecular ions by capturing a proton from the target molecule in negative ESI mode (Yanes et al., 2011; Takkis et al., 2017; Cheng et al., 2019). Considering the results of previous studies, the use of AFL as

mobile-phase additive is an excellent strategy to enhance an ionization efficiency of phenolic scaffold compounds in negative ESI.

Accordingly, in the present study, we employed AFL along with general mobile phase additive such as ammonium formate, ammonium acetate, acetic acid and formic acid to address the problems encountered in the mass spectrometry-based determination of 1) propofol and 2) environmental phenols. Propofol has the disadvantages of being highly affected by sample preparation methods due to its high volatility. For environmental phenols, the analysis of multiclass phenols is also quite challenged because diverse chemical properties and low biological concentrations of phenols may lead to complicate sample preparation.

However, the optimized mobile phase composition allowed highly sensitive and simple sample preparation procedure for phenolic compounds. For this purpose, we evaluated the ionization efficiency, chromatographic behavior, collision-induced dissociation (CID), and volatility of phenols. Following in-house validation, the developed method was applied to human urine samples and demonstrated the feasibility of generic analytical platform for phenol analysis

Chapter 2. General Experimental Procedure

2.1 Instruments

All analyses were performed using LC-MS/MS. A Thermo Scientific™ Vanquish™ UHPLC system (ThermoFinnigan, San Jose, CA, USA) was connected to a TSQ Altis triple quadrupole mass spectrometer (ThermoFinnigan, San Jose, CA, USA) equipped with a heated ESI source. The mass spectrometer was operated in negative mode (spray voltages; 3.5 kV). The capillary temperature was 320 °C and the vaporizer temperature was 340 °C. Nitrogen gas was used for the sheath gas and the auxiliary gas at flow rates of 60 arbitrary units (arb) and 15 arb, respectively. And 1 arb was used for the sweep gas. All experiments were performed using scheduled selected reaction monitoring (SRM) mode for simultaneous analysis. For HPLC operation, an ACE Excel 2 C18-AR column (150 mm × 2.1 mm I.D.; Advanced Chromatography Technology, Scotland) was used for the LC column. Phenyl bonded phases with ultra pure and ultra inert silica of this column provided superior selectivity for aromatic functionality, especially for phenolic compounds. The mobile phase was consisted of water (A) and methanol/acetonitrile (B) with various additive conditions and the temperature of sampler module was maintained at 10 °C.

2.2 Software

TSQ Altis 3.0 Tune was used for the program of mass parameter optimization, and Xcalibur 4.1 was used for the sequence running operation. For data acquisition and quantification, QuanBrowser 4.1.31.9 was used.

2.3 Reagents

Acetonitrile (ACN), methanol (MeOH), ethyl acetate (EA), and methyl tert-butyl ether (MTBE) were of high-performance liquid chromatography (HPLC)-grade and obtained from Burdick & Jackson (Ulsan, Korea). Ammonium formate (AFO), ammonium acetate (AAC), ammonium fluoride (AFL), formic acid (FA), and acetic acid (AA) were purchased from Sigma-Aldrich (St. Louis, MO, USA). Deionized water was generated using an in-house water purification system (Milli-Q, Bedford, MA, USA) and analytical grade water was obtained from Merck (Darmstadt, Germany).

2.4 Standard solutions

Each stock solution was prepared at a concentration of 1000 μg/mL by dissolving with methanol and stored in −4 ˚C. A mixture of 38 environmental phenols standard solution for phenols analysis was prepared with 10 μL of each 1000 μg/mL stock with 0.62 mL of methanol to 1 mL. The 13 working standard solutions for the calibration curve were prepared with 1, 2, 4, 10, 20, 40, 100, 200, 400, 1 000, 2 000, 4 000, and 10 000 ng/mL concentrations by adding the proper amounts of mixture standard solution and a methanol. The volumes of each working standard solution needed to make the calibration curve is 10 μL into 0.2 mL of urine sample.

2.5 Urine sample storage

All urine samples for the experiment were collected in glass bottles and stored at −20 ˚C until analysis.

2.6 Dilute and shoot assay

For sample preparation, a simple dilute and shoot assay was used. The urine samples were simply diluted with acetonitrile and centrifuged as can be seen from Lee et al (Lee et al., 2011).

Chapter 3. Fluoride assisted analysis I : Propofol

3.1 Introduction

3.1.1 Study background

Propofol (2,6-diisopropyl phenol, **Figure 1**), an intravenous anesthetics, has been widely used for the induction and maintenance of anesthesia due to its short acting effect (Wilson et al., 2010; Bateman and Kesselheim, 2015; Walsh, 2018; Kim et al., 2019). In addition to clinical application, propofol is also used for recreational purpose because of its sedative and relaxing properties and potential sexual illusions and euphoric feelings. However, propofol has several fatal side effects including bradycardia, hypotension, cardiac arrhythmia, somnolence and seizures and has been associated with fatal heart failure and suicide (Wilson et al., 2010; Bateman and Kesselheim, 2015). Despite these potentially fatal toxicity, propofol has short duration of its narcotic effects and is not classified as a controlled substance in most countries, making it easier to abuse than other recreational drugs (Maas et al., 2017a). Also, propofol is probably easy to misuse even by experienced physicians because the therapeutic range between the desired effect and potentially fatal toxicity is very narrow.

Dose of propofol was cleared by metabolism to inactive glucuronide and sulfate adducts (**Figure 1**) with only 1% of the active parent compound in urine. At present, most case of propofol abuse is confirmed through metabolite analysis. Because its phase II metabolites are excreted in large amounts (accounting for more than 50% of the excreted metabolites) and have been successfully determined by LC-ESI-

MS/MS in negative ion mode. However, propofol and its phase I metabolites are difficult to protonate or deprotonated which complicates their detection by LC/MS in either positive or negative ion mode.

Consequently, practical and sensitive analytical methods to investigate the chronic abuse and toxicity of propofol are required.

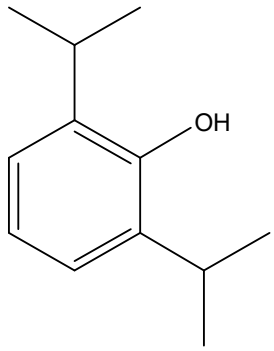

Propofol

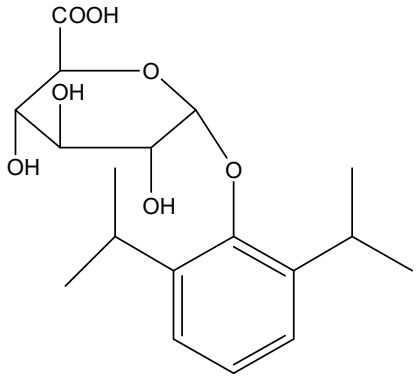

Propofol glucuronide (M1)

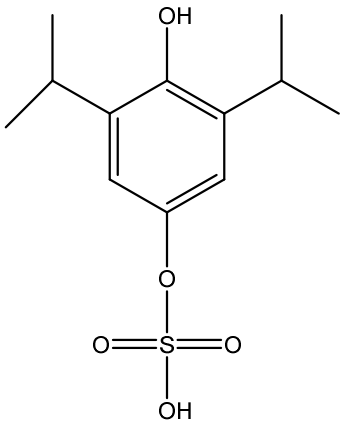

4-(2,6-diisopropyl-1,4-quinol) sulfate(M2)

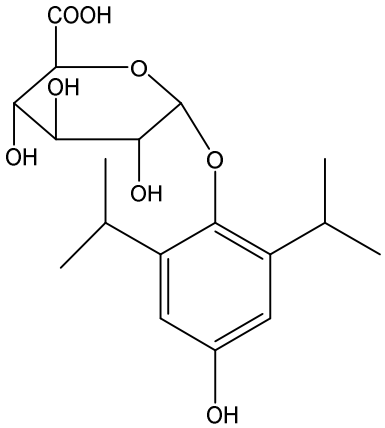

1-(2,6-diisopropyl-1,4-quinol) glucuronide (M3)

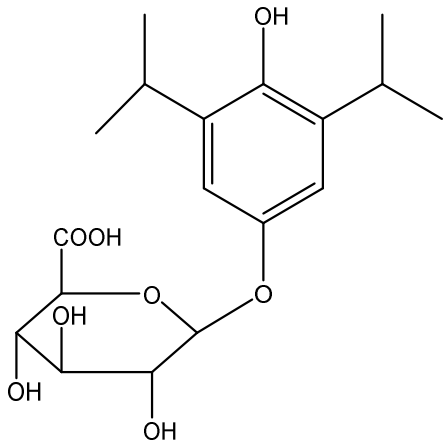

4-(2,6-diisopropyl-1,4-quinol)glucuronide (M4)

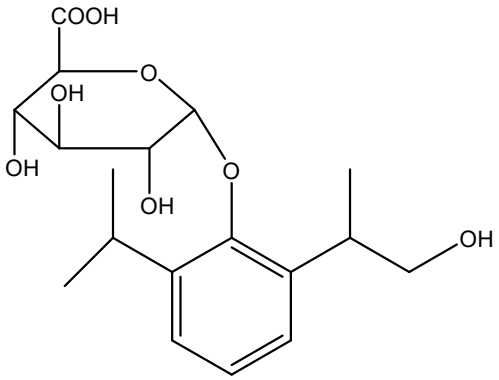

x-(2-(ω-propanol)-6-isoproyl-phenol) glucuronide (M5)

Figure 1. Structure of propofol and its metabolites

3.1.2 Analytical history of propofol

Traditionally, GC/MS platforms have been applied for the determination of propofol due to its high separation ability and detection sensitivity of volatile compounds despite the need for intensive sample preparation such as extraction and derivatization (Favetta et al., 2000; Iwersen-Bergmann et al., 2001). The derivatization step is commonly used by trimethylsilyl reagent to improve the sensitivity of propofol. However, GC/MS has limitations in the analysis of phase II metabolites because glucuronide or sulfate conjugated compounds are incompatible with GC/MS. Therefore, for simultaneous analysis of propofol and its metabolites, LC-MS methods combined with electrospray ionization or atmospheric pressure chemical ionization are gaining attention recently.

Several analytical methods based on liquid chromatography-mass spectrometry (LC-MS/MS) have been reported for the determination of propofol and its metabolites in blood, urine, and hair (Beaudry et al., 2005; Thieme et al., 2009; Vlase et al., 2011; Kim et al., 2013; Vaiano et al., 2014; Khedr et al., 2017; Maas et al., 2017a). However, current analysis of propofol using LC-MS/MS suffers from serious problems associated with its mass spectrometry detection and sample preparation. The detection problem results from the poor ionization efficiency of propofol under in electrospray ionization (ESI).

Propofol has structural characteristics of o-, m- or p-substituted phenols, and phenols are known to readily form negative ions in the gas phase giving the corresponding anion $[M-H]^-$ (Binkley et al., 1992). While propofol can be ionized to the deprotonated molecular ion in negative-mode ESI, its ionization efficiency is

very low, leading to problems with its direct detection in biological matrices. Also, its collision-induced dissociation undergoes poor ionization efficiency and weak fragmentation, which pointed out in the literature, resulting in detection problem (Bajpai et al., 2005).

To overcome the poor ionization efficiency of propofol, derivatization methods using azo-coupling (Vaiano et al., 2014; Vaiano et al., 2017), 3-bromomethyl-propyphenazone (BMP) (Khedr et al., 2017), and 1,2-dimethylimidazole-4-sulfonyl chloride (DMISC) (Maas et al., 2017b) have been developed, with azo-coupling methods being particularly successful in improving the sensitivity of propofol. However, even though very low quantities of propofol can be detected, these derivatization methods require a complex sample preparation procedure. Besides, the derivatization step is not suitable for simultaneous analysis of the phase II metabolites which include glucuronide structure form with propofol.

These derivatization methods including evaporation step lead to another critical problem associated with the intrinsic volatility of propofol, which leads to its uncontrolled loss during sample preparation. Propofol readily evaporates during evaporation process in liquid-liquid extraction (LLE), solid-phase extraction (SPE), or derivatization.

Plummer (Plummer, 1987) and Alaa Kheedr et al. (Khedr et al., 2017) reported the use of quaternary alkyl amines at room temperature to avoid the loss of propofol by evaporation. However, these general ion-pairing methods are unable to completely prevent the loss of propofol. Furthermore, this methodology necessitates careful and time-consuming drying processes to remove the quaternary alkyl amines

because they cause serious signal suppression in ESI (Wu et al., 2004).

Consequently, the development of a reliable, accurate, and sensitive analytical method for propofol determination that does not involve extraction/evaporation steps is urgently required. In the present study, we employed various mobile phase composition to address the problems encountered in the mass spectrometry-based determination of propofol and to develop a highly sensitive and accurate analytical method without sample preparation and derivatization. For this purpose, we evaluated the ionization efficiency, chromatographic behavior, collision-induced dissociation (CID), and volatility of propofol and developed a fluoride-assisted LC–ESI/MS/MS method with direct-injection for the direct quantification of propofol. The resulting fluoride-assisted LC–ESI/MS/MS method was validated and applied to real samples to demonstrate its feasibility.

3.2 Experimental procedures for propofol analysis

3.2.1 Chemicals and reagents

Propofol and $^{13}C_{12}$-Bisphenol A as an internal standard (ISTD) were purchased from Cerilliant (Round Rock, Texas, USA) and Cambridge Isotope Laboratories (Andover, MA, USA). ACN, MeOH, EA, and MTBE were of HPLC-grade and obtained from Burdick & Jackson (Ulsan, Korea). AFO, AAC, AFL, FA, and AA were purchased from Sigma-Aldrich (St. Louis, MO, USA). Deionized water was generated using an in-house water purification system (Milli-Q, Bedford, MA, USA).

3.2.2 Instruments

All analyses were performed using LC-MS/MS. A Thermo Scientific™ Vanquish™ UHPLC system (ThermoFinnigan, San Jose, CA, USA) with an ACE Excel 2 C18-AR column (150 mm × 2.1 mm I.D.; Advanced Chromatography Technology, Scotland) was connected to a TSQ Altis triple quadrupole mass spectrometer (ThermoFinnigan, San Jose, CA, USA) equipped with an ESI source. The mobile phase consisted of water (A) and methanol (B), both of which contained AFL (1 mM). The initial gradient composition (20% B) was maintained for 0.5 min and then linearly increased to 95% B over 9 min and maintained for 2.5 min before being decreased to 2% B over 0.1 min. Then, equilibration was performed for 2.9 min. The flow rate was set to 0.3 mL min^{-1}. The column and sampler module temperature was fixed at 35 °C and 10 °C, respectively. The mass spectrometer was operated in negative mode (spray voltages; 3.5 kV). The capillary temperature was

320 °C and the vaporizer temperature was 340 °C. All experiments were performed using scheduled selected reaction monitoring (SRM) mode for simultaneous analysis. The cycle time was 0.3 sec and the resolution of Q1 and Q3 were used at 0.7 FWHM. The optimized SRMs were *m/z* 177 → 177 for propofol, *m/z* 353 > 177 for propofol glucuronide (M1), *m/z* 273 → 192 for 4-(2,6-diisopropyl-1,4-quinol) sulfate (M2), *m/z* 369 → 193 for the mono hydroxyl propofol-glucuronides (1-(2,6-diisopropyl-1,4-quinol) glucuronide, 4-(2,6-diisopropyl-1,4-quinol) glucuronide, and x-(2-(ω-propanol)-6-isoproyl-phenol) glucuronide (M3–M5)), and *m/z* 239 → 224 for the ISTD. The summary of analytical conditions used in this experiment were shown in **Table 1** and **2**.

Table 1. Optimized operating conditions of LC-ESI/MS/MS for propofol analysis

LC conditions				
Instruments	Thermo Scientific™ Vanquish™ UHPLC system			
Column	ACE Excel 2 C18-AR column (150 mm × 2.1 mm)			
Mobile phase	A : 1 mM ammonium fluoride in DW B : 1 mM ammonium fluoride in MeOH			
Gradient	Time (min)	A (%)	B (%)	Flow rate (mL/min)
	Initial	80	20	0.3
	0.5	80	20	
	9.5	5	95	
	12.0	5	95	
	12.1	80	20	
	15.0	80	20	
MS source parameter				
Instruments	TSQ Altis triple quadrupole mass spectrometer			
Spray voltage	Negative : 3500 V			
Vaporizer temperature	340˚C			
Ion transfer tube temperature	320˚C			
Gas paramether	Sheath/ Aux/ Sweep gas : 60/ 15/ 1arb			
Scan type	Selected reaction monitoring (SRM) mode			
Cycle time	0.3 sec			
Q1/Q3 resolution	0.7 FWHM			
CID gas	1.5 mTorr			

Table 2. Optimized mass parameters and retention times of analytes and internal standards for propofol analysis

Compound	ESI Polarity	Transition [Q1/Q3 (CE)]	Dwell Time (ms)	Retention time/ Monitoring time (min)
Propofol	-	177/177 (15)	41.06	10.8/1.0
M1	-	353/177 (26)	41.06	7.85/2.0
M2	-	273/192 (30)	41.06	6.00/2.0
M3-5	-	369/193 (15)	41.06	6.50/5.0
$^{13}C_{12}$-BPA (ISTD)	-	239/224 (18)	41.06	9.30/1.0

M1 : propofol glucuronide

M2 : 4-(2,6-diisopropyl-1,4-quinol) sulfate

M3 : mono hydroxyl propofol-glucuronides (1-(2,6-diisopropyl-1,4-quinol) glucuronide

M4 : 4-(2,6-diisopropyl-1,4-quinol) glucuronide

M5 : x-(2-(ω-propanol)-6-isoproyl-phenol) glucuronide

3.2.3 Sample collection

Human urine samples obtained from two patients who were infused with propofol were provided by the Medical Center of Kyung Hee University. The dose was approximately 1 g of propofol delivered during a 4 h infusion. Urine samples were collected for the periods 0–6, 6–12, 12–18, 12–24, and 24–48 h after propofol administration and stored at −20 ℃ until analysis.

3.2.4 Ethics

The study was approved by the Institutional Review Board of Korea Institute of Science and Technology (IRB number: 2021-E-002) and has been performed in accordance with ethical standards.

3.2.5 Sample preparation

Urine (0.2 mL) was taken and 20 μL of ACN was added. The samples were vortex-mixed and centrifuged at 13,000 rpm for 10 min (Eppendorf, Hamburg, Germany). The supernatants from each sample were transferred to autosampler vials and 10 μL was injected into the LC/MS/MS system. The Sample preparation step was summarized in **Figure 2**.

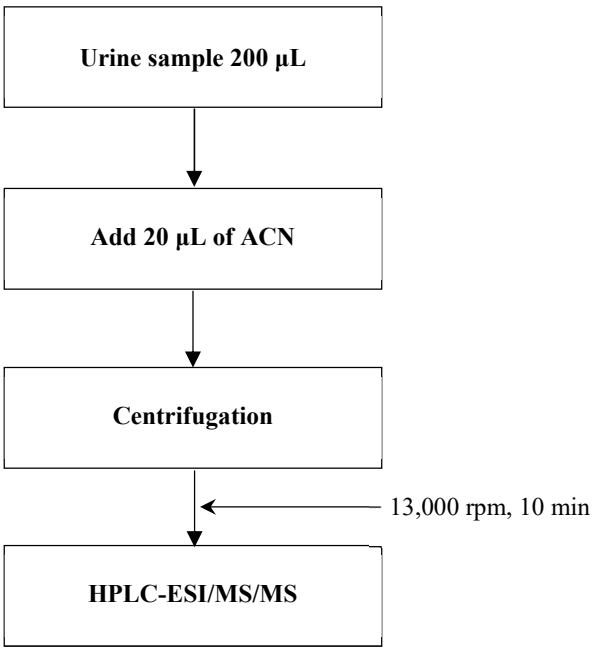

Figure 2. Schematic diagram of sample preparation procedure for propofol

3.2.6 Method validation

The optimized method was validated for linearity, limit of detection (LOD), limit of quantification (LOQ), intra- and inter-day precision, and accuracy. Calibration was performed ranging from 0.5 to 500 ng/mL with an ISTD concentration of 20 ng/mL urine. The linearity was assessed by correlation coefficient (R^2). The validation results were evaluated based on guidelines established by Bioanalytical Method Validation Guidance for Industry (Brodie and Hill, 2002). The LOD and LOQ values are given by the equation from the ICH Q2B guidelines (LOD = 3.3(σ/S) and LOQ= 10(σ/S)), where σ is the standard deviation of the response and S is the slope of the calibration curve (Walfish, 2006). For repeatability, urine samples were analyzed with five replicates in the same run (intra-day precision) and in five separate runs (inter-day precision). The results are represented as the percentage coefficient of variation values of the peak area ratio for the analyte to the ISTD. The accuracy is expressed as the bias of the measured concentration to the expected value. For selectivity, 10 blank urine samples from different individuals were analyzed repeatedly to evaluate the possibly of interfering peaks. The matrix effects (including ion suppression and ion enhancement effects) were investigated for seven different blank samples. The matrix effect was calculated from the peak areas (A) without ISTD correction (matrix effect (%) = ($A_{\text{pure standard}} - A_{\text{spiked sample}}$) × 100/ $A_{\text{pure standard}}$). Recovery was determined by comparing the chromatographic peak areas of the urine samples spiked before sample preparation with the chromatographic peak areas of urine samples spiked after sample

preparation. Three replicates at four different concentrations were analyzed. The QC samples at 0.5, 2, 20 and 200 ng/mL were processed and measured in three replicates.

3.3 Result and discussion

3.3.1 Optimization of propofol-specialized sensitive analytical method

3.3.1.1 Optimization of mobile phase composition

Due to the poor ESI ionization efficiency and volatility of propofol, its direct analysis using LC–ESI/MS/MS is known to be challenging. In LC–ESI/MS/MS analysis, mobile phase composition is a key parameter for achieving the best ionization efficiency and chromatographic behavior of analytes. Herein, we investigated the effects of numerous additives and organic modifiers in the mobile phase to improve the inherently poor ionization efficiency of propofol. AFL, AAC, AFO, AA, FA, and no additive were evaluated under methanol or acetonitrile.

First, the optimal concentration of each additive was determined to compare the relative ionization efficiency of propofol in different mobile phase compositions. As shown in **Figure 3(A)**, all the additives result in better ionization efficiency in methanol than that in acetonitrile, regardless of the type and concentration of the additive. Especially, AFL and AA showed much higher ionization efficiencies in methanol. In methanol, the optimal concentrations of the additives are 1–2 mM for AFL and AAC, 0.1–0.2 mM for AFO, and 0.002–0.005% for AA. When using FA as the additive, propofol is barely detected. These results are consistent with the

literature, which confirms that FA causes strong signal suppression in negative ESI (Wu et al., 2004; Huffman et al., 2012). **Figure 3(B)** shows the relative ionization efficiencies of propofol in the optimized additive concentrations. AFL and AAC generate higher ionization efficiencies than that with no additive. Conversely, AFO, AA, and FA effect lower efficiencies than that observed with no additive. These results reveal that AFL is the most effective additive for the ionization of propofol in negative ESI. **Figure 3(C)** illustrates the chromatographic behavior of propofol with different mobile phase compositions. A chromatographic factor (area/height ratio) was employed to evaluate the relative sharpness of peaks, where narrower peaks have lower values (shown as deeper blue in the figure). Propofol shows better chromatographic behavior in acetonitrile (factor: 2.58–3.36) than in methanol (factor: 2.94–5.51). Furthermore, as the concentration of additives in methanol increase, the peak tends to broaden slightly, and this aspect is more evident in ammonium salt solutions. Overall, however, propofol shows a sharp and symmetric chromatographic peak for all the compositions. Specifically, most of the chromatographic factor values with AFL, which is selected as the mobile-phase additive in the present study, are distributed between 2.58 and 4.53. This is a negligible difference. Consequently, 1 mM AFL and methanol were selected as the optimal mobile phase composition for enhancing the ionization efficiency of propofol.

Regarding the enhancement of the ionization efficiency of propofol by AFL, a series of studies by Cole et al. reported the enhancement of signal intensity by anion attachment and anion-induced deprotonation in negative ESI (Zhu and Cole, 2000, 2001; Cai and Cole, 2002a; Cai et al., 2002; Jiang and Cole, 2005; Wang and Cole,

2009). Based on these studies, we investigated fluoride-ion attachment/induced deprotonation in the enhanced ionization efficiency of propofol. As illustrated in **Figure 4**, in full scan mode, the fluoride adduct ion $[M+F]^-$ at *m/z* 197 as well as the deprotonated molecular ion $[M-H]^-$ at *m/z* 177 is observed. The CID of the fluoride adduct ion at *m/z* 197 gives rise to the product ion at 177.1276 Da, which is equivalent to the calculated mass (177.1279 Da) of deprotonated propofol ($C_{12}H_{17}O$) with an error of 1.176 ppm. The presence of the fluoride adduct ion implies that fluoride-ion attachment/induced deprotonation may be involved in the ionization of propofol. Herein, even though the process of ionization by ammonium fluoride is still subject to speculation, we propose that the fluoride adduct ion of propofol ($[M-H]^-\cdots H^+\cdots[F]^-$) instantly dissociates to deprotonated propofol and neutral hydrogen fluoride ($[M-H]^-$ + HF) owing to the strong gas-phase basicity (1529 kJ mol^{-1}) of the fluoride ion and the stability of hydrogen fluoride.

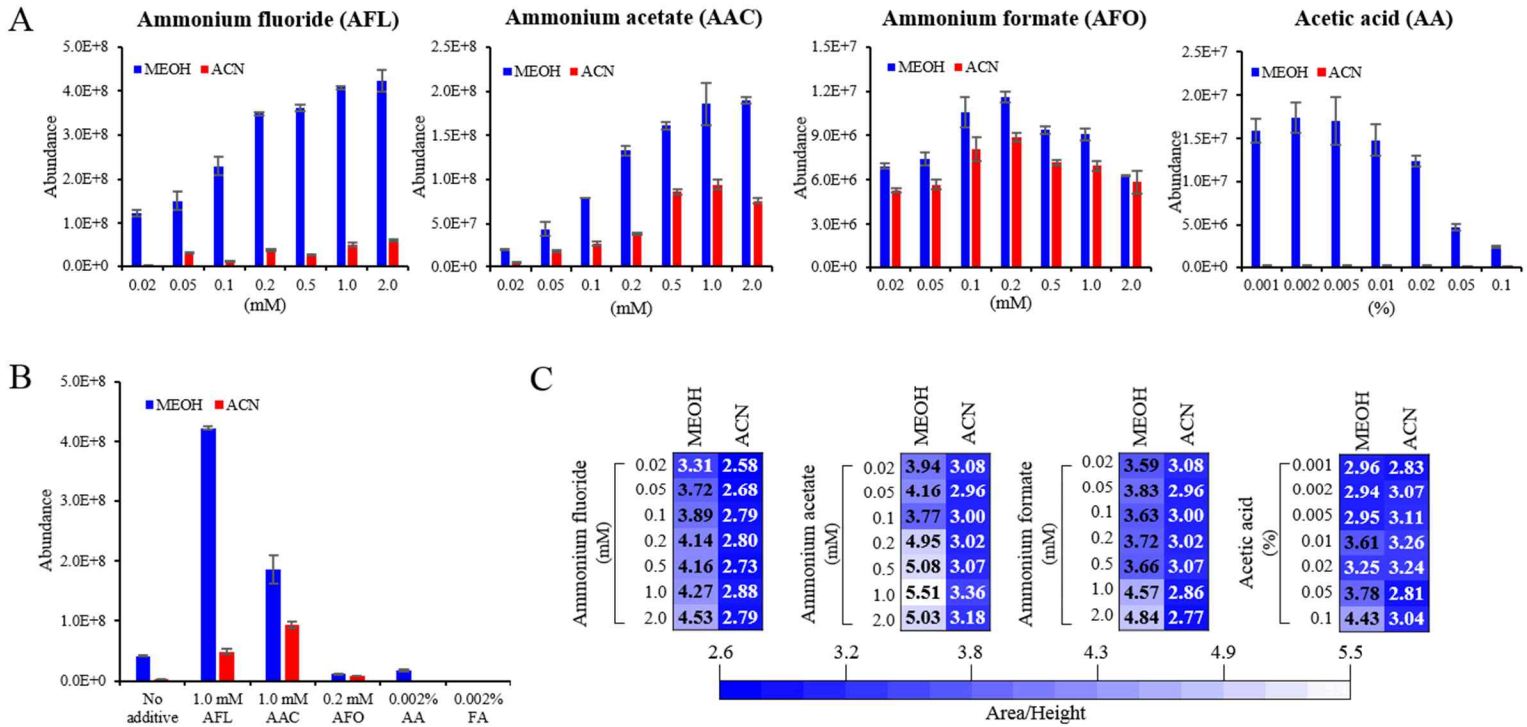

Figure 3. Ionization efficiencies and chromatographic behaviors of propofol under different mobile phase compositions. (A) Optimal concentrations of additives for the ionization of propofol. (B) Relative ionization efficiencies of propofol under the optimized concentrations of mobile phase additives in methanol and acetonitrile. (C) Heat map of chromatographic factor (area/height) values for mobile phase compositions.

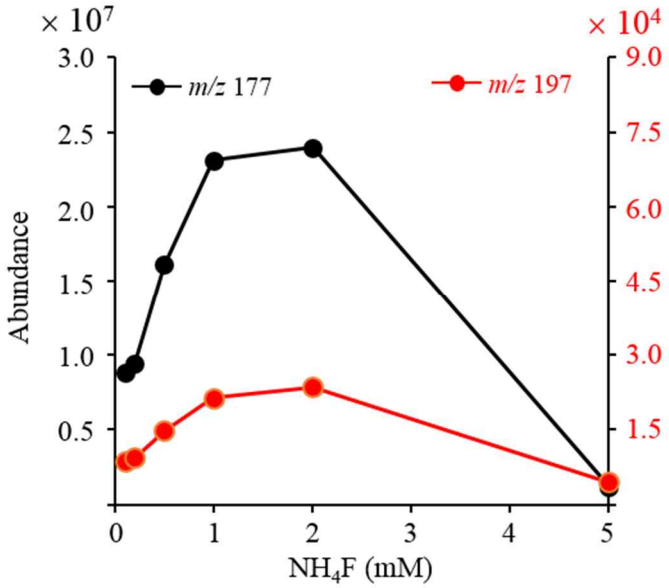

Figure 4. Abundance of the deprotonated molecular ion $[M-H]^-$ at m/z 177 and the fluoride adduct ion $[M+F]^-$ at m/z 197 in fluoride-assisted LC–ESI-MS/MS.

3.3.1.2 Optimization of collision-induced dissociation

Along with its poor ionization efficiency in mass spectrometry, the poor CID of propofol is another crucial problem. As reported by Bajpai et al. (Bajpai et al., 2005), the CID of deprotonated propofol generates a very poor fragmentation profile and weak fragment ion signals. The deprotonated propofol at *m/z* 177 gives rise to only a single major product ion at *m/z* 161, suggesting the neutral loss of a methane molecule (16 Da). However, the product ion at *m/z* 161 shows abnormally low intensity. This seems to be because the dissociation of propofol proceeds by two different cleavage modes, i.e., heterolytic and hemolytic cleavage, simultaneously. Consequently, propofol is unable to yield an "ideal" product ion in tandem mass spectrometry. For this reason, Dziadosz et al. (Dziadosz, 2019) used the acetate adduct ion as precursor ion (Q1) for SRM analysis. They showed that *m/z* 237 (acetate adduct) → 177 (deprotonated propofol) for SRM provides better sensitivity than *m/z* 177 (deprotonated propofol) → 161 (methane loss). Furthermore, Sørensen et al. (Sorensen and Hasselstrom, 2015) and Lin et al (Lin et al., 2021) used the same molecular ion (*m/z* 177 → 177) for the Q1 and Q3 ions because of the scarcity of the product ion. Based on these studies, we investigated the optimal Q1/Q3 transitions and collision energies (CEs) to improve the sensitivity and selectivity for propofol in the SRM analysis. We evaluated *m/z* 177 → 177 and *m/z* 177 → 161 as SRM transitions. **Figure 5(A)** shows the abundance of these SRM transitions at different CEs. The SRM transitions at *m/z* 177 → 177 and *m/z* 177 → 161 show the highest intensities at CEs of 8 and 23 eV, respectively. The SRM transition at *m/z* 177 → 177 shows over 200-fold higher sensitivity than that for *m/z* 177 → 161. As a result, the SRM transition at *m/z* 177 → 177 with a CE of 8 eV was deemed effective for improving sensitivity to propofol. However, as shown in **Figure 5(B)**, the SRM

analysis using *m/z* 177 → 177 with a CE of 8 eV gives rise to serious interference and high background signal in the pooled urine spiked with propofol at 0.5 ng/mL and it is not easy to distinguish the peak of propofol. Hence, the CE for *m/z* 177 → 177 was re-optimized to reduce interference and background. As shown in **Figure 5(B)**, when the collision energy is increased to 15 eV, the interference and background are dramatically decreased while the sensitivity for propofol is maintained. This is because the interfering substances in urine with the same molecular ions and relatively low CEs can be dissociated and removed at an appropriately increased CE that is still too low to dissociate the propofol. Accordingly, the SRM transition at *m/z* 177 → 177 with a CE of 15 eV was selected for quantitative analysis of propofol in real urine. Thus, although the SRM transition using *m/z* 177 → 177 may not be a conventional transition, the present CID optimization as well as fluoride-assisted LC–ESI/MS/MS enables the sensitive and selective determination of propofol without derivatization.

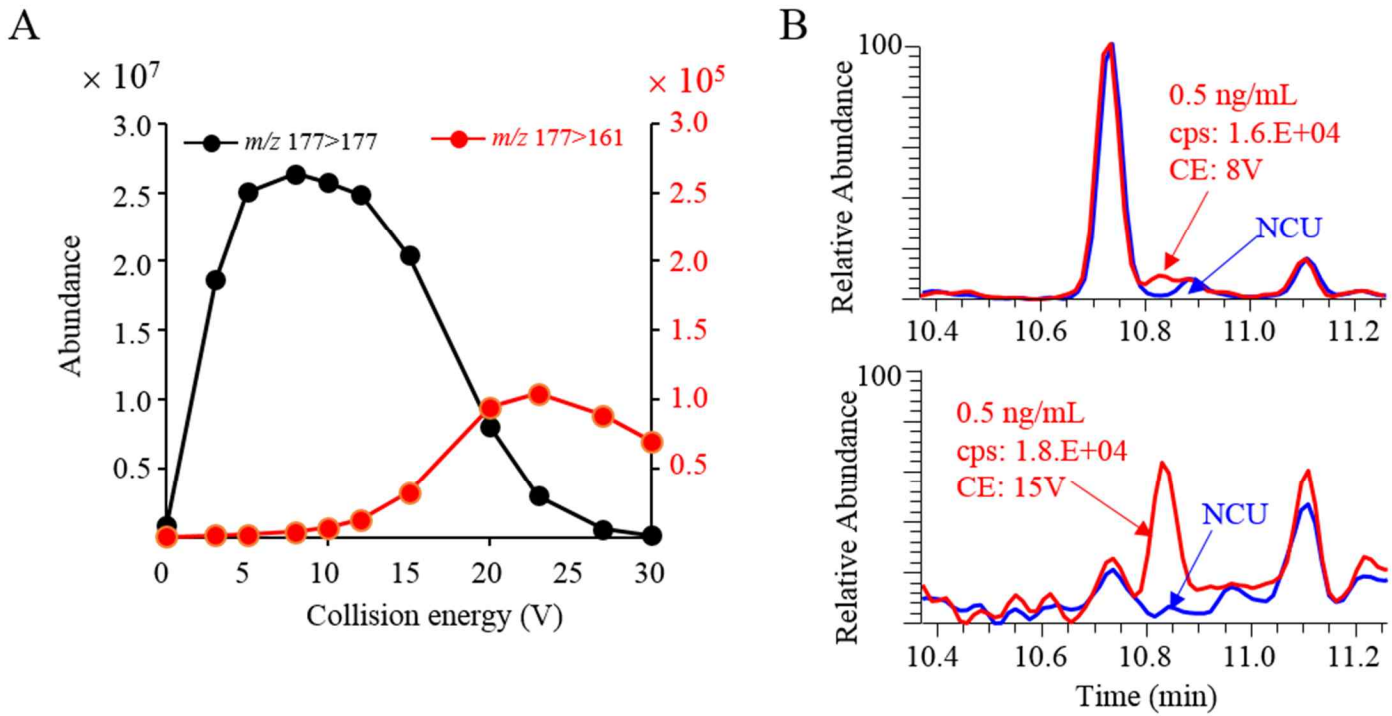

Figure 5. Optimization of the CID of propofol. (A) Relative abundance of different SRM transitions using fluoride-assisted LC–ESI/MS/MS. (B) CE optimization for elimination of background interference in real urine samples (blue line: negative control urine, red line: spiked urine).

3.3.1.3 Volatility of propofol and optimization of sample preparation

As mentioned earlier, several methods based on derivatization to improve the ionization efficiency of propofol have been developed (Beaudry et al., 2005; Thieme et al., 2009; Vlase et al., 2011; Vaiano et al., 2014). However, heating or evaporation processes are required for derivatization, necessitating great care to avoid uncontrolled loss of propofol. Prior to sample preparation optimization, we investigated the influence of organic solvents and temperature on the loss of propofol during evaporation. Four different organic solvents spiked with propofol (100 ng/mL in 5 mL of MTBE, ACN, EA, or MeOH) were tested in these experiments. **Figure 6** illustrates the recoveries of propofol under different evaporation conditions.

In EA and MeOH, over 99.5% of propofol is eliminated under gentle nitrogen evaporation regardless of the evaporation temperature. In MTBE, ~90% of propofol is eliminated and a high standard deviation is observed. This indicates that propofol can be quickly eliminated unless evaporation is stopped immediately as soon as the sample becomes dry. Conversely, the use of ACN at room temperature shows ~75% recovery and a relatively reproducible result. However, the evaporation time for ACN at room temperature is over 2 h, and when the evaporation temperature is increased to 50 °C, the recovery decreases to below 50%. These results strongly indicate that evaporation gives rise to uncontrolled loss of propofol.

In this study, we employed the dilute and shoot method to avoid the uncontrolled loss of propofol and reduce quantitation errors. Urine samples (200 μL) were simply diluted with ACN (20 μL) to remove the minute particles therein and subsequently centrifuged. The resulting supernatants were directly injected into the

HPLC system without dilution or further concentration. In general, it is well known that the dilute and shoot method is simple, rapid, and accurate, but it can be only used when sensitivity is satisfied. As described above, we have developed a highly sensitive and selective analytical method for propofol determination based on fluoride-assisted LC–ESI/MS/MS and CID optimization and it has allowed direct analysis of propofol at low concentrations using direct injection. The developed method is effective for minimizing the uncontrolled loss of propofol and quantitation errors.

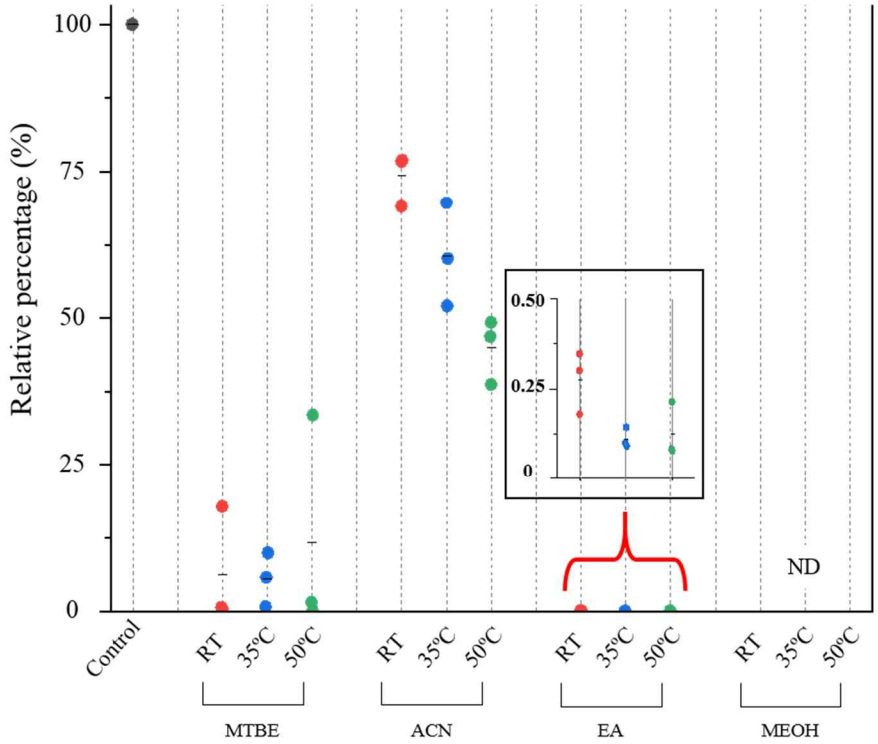

Figure 6. Recoveries of propofol under different solvents and nitrogen evaporation conditions. The small rectangle is an expanded version of EA recoveries. *N.D.* = not detected.

3.3.2 Method performance

3.3.2.1 Method validation

The validation results for the quantitation of propofol are summarized in **Table 3-5**. The peak area ratio of each analyte and its internal standard are fitted to a weightless least-squares model to provide a calibration curve, and the linearity as shown by the correlation coefficient is greater than 0.999. The intra- and inter-day precisions for propofol are between 1.9% and 8.7% and the accuracies range from 87.5% to 105.4%. The values obtained indicate that the method is precise and accurate because the results satisfy the criteria (Walfish, 2006) for all four concentration levels. No interference is observed for drug-free urine samples at the retention time of propofol (10.8 min). The matrix effects, which were calculated for the four different concentrations, range from 3.2% to 26.3%. The recoveries range from 93.3% to 109.7%. This strongly indicates that the present direct-injection method is effective for preventing loss of propofol. The LOD and LOQ values are 0.15 and 0.44 ng/mL, respectively.

Table 3. Validation results of propofol in human urine for intra-day assay (n=5)

Compounds (Abbr.)	Spiked Conc. (ng/mL)	Intra-day (n=5)					Mean	Accuracy (%)	Precision (%)
		Batch-1	Batch-2	Batch-3	Batch-4	Batch-5			
Propofol	0.5	0.53	0.50	0.46	0.49	0.54	0.50	100.8	6.5
	2	1.72	1.76	1.72	1.74	1.80	1.75	87.5	1.9
	20	19.0	17.1	18.0	17.5	19.1	18.1	90.7	5
	200	190	188	218	223	188	201	100.7	8.7

Table 4. Validation results of propofol in human urine for inter-day assay (n=5)

Compounds (Abbr.)	Spiked Conc. (ng/mL)	Intra-day (n=5)					Mean	Accuracy (%)	Precision (%)
		Day-1	Day-2	Day-3	Day-4	Day-5			
Propofol	0.5	0.54	0.53	0.50	0.55	0.51	0.53	105.4	3.5
	2	1.80	1.74	1.77	1.75	1.78	1.77	88.5	4.5
	20	19.1	18.4	19.0	18.4	19.2	18.8	94.0	2.1
	200	188	193	213	204	210	202	100.8	5.3

Table 5. The summary of validation results for propofol

Compound	Spiked Conc. (ng/mL)	Intra-day (n = 5)		Inter-day (n = 5)		Dynamic Range (ng/mL)	R^2	LOD (ng/mL)	LOQ (ng/mL)	Matrix Effect (%)	Recovery (%)
		Accuracy (%)	Precision (%)	Accuracy (%)	Precision (%)						
Propofol	0.5	100.8	6.5	105.4	3.5	0.2-500	0.9996	0.15	0.44	26.3	108.0
	2	87.5	1.9	88.5	4.5					25.1	105.2
	20	90.7	5.0	94.0	2.1					19.8	93.3
	200	100.7	8.7	100.8	5.3					3.2	109.7

3.3.2.2 Analytical performance comparison between methods

Table 6 summarizes the analytical information and results of different LC-MS/MS methods reported in the literature for the determination of propofol and its metabolites. In terms of the sensitivity for propofol, our method (LOQ: 0.44 ng/mL) exhibits 11–568-fold higher sensitivity than those of previously reported methods (LOQ: 5–250 ng/mL) except that for the azo-coupling-derivatization method (LOQ: 0.0004 and 0.1 ng/mL). But the propofol concentration in blood is normally ranged between 3-8 μg/mLfor anesthesia and between 1-2 μg/mL for sedation (Vlase et al., 2011). For this reason, it may be not ideal to simply compare the LOQ in blood and urine. However, our method provides the best sensitivity among the LC–ESI/MS/MS methods without derivatization for the quantitation of propofol and has the advantages such as simple and rapid sample preparation.

Table 6. Summary of previously reported LC-MS/MS methods for the determination of propofol

Derivatization[a]	Sample Preparation	Target analytes [b]	Matrix	LOQ (ng mL^{-1})	Mobile phase [c]	Recovery	Detection ions	Reference
Without	Dilute 1:0.1 with ACN > Direct injection	P, PG, PM	Urine (0.2mL)	0.44	(A) 1mM ammonium fluoride in DW (B) 1mM ammonium fluoride in MEOH	93-110%	177 > 177 (- ESI, SRM)	Present
	Dilute 1:29 with MEOH/H_2O (1:1) > Direct injection	PG, PM	Urine (3 mL)	-	(A) 0.1 mM ammonium acetate in DW (B) MEOH/ACN (50:50)	~90%	-	(Lee et al., 2012)
	Dilute 1:39 with ACN > Direct injection	P	Plasma (0.01 mL)	250	0.025% ammonium hydroxide in 70% ACN	91-93%	177 (- ESI, SIM)	(Shopova et al., 2019)
	LLE > evaporation > reconstitution (0.1 mL)	P	Serum (0.5 mL)	60	10 mM ammonium acetate and 0.1% AA in DW/MEOH (3:97)	57-62%	237 > 177 (- ESI, SRM)	(Dziadosz, 2019)
	SPE > evaporation > reconstitution (0.2 mL)	P, PG	Blood (0.2 mL)	10	(A) 0.02% AA in 10% MeOH (B) 0.02% AA in MeOH/ACN (1:1)	81-85%	177 > 177 (- ESI, SRM)	(Sorensen and Hasselstrom, 2015)
	C18 pipette-tip based SPE > Direct injection	P	Plasma (0.1 mL)	5	(A) 0.1% FA in DW (B) ACN	~24%	177 > 177 (- APCI, SRM)	(Lin et al., 2021)
	SPE > direct injection	P	Plasma (0.6 mL)	18	0.05% ammonium hydroxide in DW and ACN (30:70)	96-108%	177 (- ESI, SIM)	(Maurer et al., 2018)
	SPE > direct injection	P	Plasma (1 mL)	5	0.05% ammonium hydroxide solution/MEOH (2:98)	97-104%	177 > 161 (- APCI, SRM)	(Bajpai et al., 2004)

Table 6. (Continued)

Derivatization[a]	Sample Preparation	Target analytes [b]	Matrix	LOQ (ng mL^{-1})	Mobile phase [c]	Recovery	Detection ions	Reference
Without	SPE > direct injection	P	Plasma (0.5 mL)	10	0.025% ammonium hydroxide in MEOH/DW (75:25)	100%	177 > 177 (- ESI, SRM)	(Cohen et al., 2007)
	SPE > direct injection	PG, PM	Plasma (0.5 mL)	-	100 mM ammonium acetate/ACN/ DW (12:87:1)	85-90%	-	(Cohen et al., 2007)
Azo	Hydrolysis > LLE > evaporation > derivatization > LLE > evaporation > reconstitution (0.1mL)	P	Urine (1 mL)	0.0004	(A) 5 mM FA in DW (B) MEOH	>85%	281 > 176 (- ESI, SRM)	(Vaiano et al., 2015)
	Dilute 1:2 with MEOH > derivatization > LLE > evaporation > reconstitution (0.1mL)	P	Blood (1 mL)	0.1	(A) 5 mM FA in DW (B) MEOH	>87%	281 > 176 (- ESI, SRM)	(Vaiano et al., 2015)
DMISC	Dilute 1:5 with ACN > derivatization > LLE > evaporation > reconstitution (0.1 mL)	P	Serum (0.2 mL)	5	(A) 5mM ammonium formate and 0.1% FA in DW (B) 5mM ammonium formate and 0.01% FA in MEOH	-	337 > 96, 159 (+ ESI, SRM)	(Maas et al., 2017b)
Dansyl	Dilute 1:5 with acetone > derivatization > direct injection	P	Blood, plasma (0.05 mL)	20	ACN and 0.5% FA in DW (80:20)	>90%	412 > 171 (+ ESI, SRM)	(Beaudry et al., 2005)

[a] Derivatization: Azo-coupling (diazonium salt from aniline derivative), NMP (N-methylpyridinium ether derivative), DMISC (1,2-Dimethylimidazole-4-sulfonyl chloride derivative) [b] Target: P (propofol), PG (propofol glucuronide), PM (Conjugated phase I metabolite) [c] Mobile phase: FA (formic acid), AA (acetic acid)

3.3.3 Application to patient after propofol administration

Propofol is mainly metabolized to inactive glucuronide or sulfate-conjugated forms of the parent molecule and its phase I metabolites, such as the mono-hydroxylation, di-hydroxylation, quinol, and quinone forms (Kim et al., 2013; Dziadosz, 2019). The phase II metabolites such as propofol glucuronide are typically present in large amounts in the body and can play an important role in investigating the abuse of propofol as long-term metabolites in forensic investigations. Thus, it is important to simultaneously monitor phase II metabolites as well as propofol. For such simultaneous analyses, both sample preparation without derivatization and high analytical sensitivity are important prerequisites. As shown in **Table 6**, methods based on derivatization are not capable of simultaneously determining propofol and phase II metabolites. Conversely, methods without derivatization (Cohen et al., 2007; Lee et al., 2012) are capable of determining phase II metabolites. However, it is not easy to simultaneously determine propofol and its phase II metabolites owing to poor propofol sensitivity. Sørensen et al. (Sorensen and Hasselstrom, 2015) simultaneously determined propofol and propofol glucuronide in blood, but the LOQ for propofol was quite high (10 ng/mL) for analysis of urine samples with low propofol concentration level. Compared with these previous methods, the present direct-injection fluoride-assisted LC-MS/MS method allows the simultaneous determination of propofol and its phase II metabolites, and this is an additional advantage of the present method.

The developed method was applied to determining propofol and its phase II metabolites in urine samples from volunteers. The urine samples were collected during the two days (1, 6, 12, 18, 24 and 48 h) following administration. In all the urine samples, propofol was quantified and its phase II metabolites were also

simultaneously monitored. Based on the previous report by Lee et al. (Lee et al., 2012), propofol-glucuronide (M1), 4-(2,6-diisopropyl-1,4-quinol) sulfate (M2), and mono-hydroxylated propofol-glucuronides (M3–M5, i.e., 1-(2,6-diisopropyl-1,4-quinol) glucuronide, 4-(2,6-diisopropyl-1,4-quinol) glucuronide, and x-(2-(ω-propanol)-6-isoproyl-phenol) glucuronide) were monitored. In general, glucuronide- or sulfate-conjugated metabolites undergo cleavage involving the neutral loss of glucuronide or sulfate from the deprotonated molecular ion in CID. Based on these fragmentation pathways and previous reports, we optimized and confirmed the SRM transitions for the phase II metabolites. With regard to the mono-hydroxylated propofol-glucuronide metabolites, the exact structures of the metabolites could not be assigned to each peak owing to the absence of standard materials. **Figure 7** shows the representative chromatograms **(A)** and product ion spectrums **(B)** of propofol and its phase II metabolites in the urine samples. The phase II metabolites are successfully determined without interference in negative ESI mode and show good peak shapes and sensitivities. After intravenous administration, propofol in two volunteers showed a maximum concentration of 130.2 ng/mL and 3.7 ng/mL for the earlier collection time (6 h), respectively. Then, the concentration rapidly decreases to 6.9 ng/mL and 0.4 ng/mL at 48 h, as shown in **Table 7**. Considering the LOQ of our method, this result demonstrates that the present method can quantify the propofol in urine over 48 h. The phase II metabolites also show their maximum concentrations for the earlier collection times and are excreted in large amounts for two days (**Figure 8**). This means that propofol is rapidly transformed into phase II metabolites and that these metabolites are suitable as long-term indicators for investigating the abuse of propofol. Specifically, the propofol-glucuronide M1 shows a high abundance at 48 h. The ESI abundances of all of the propofol

metabolites for two volunteers are shown in **Table 8**. Even though urine is not the best matrix to monitor the abuse of propofol, the sensitivity of our method enabled its monitoring over several days. Thus, the present fluoride-assisted LC–ESI/MS/MS method combined with dilute and shoot assay enables us to quantify propofol over two days with high sensitivity and selectivity and to simultaneously monitor its phase II metabolites.

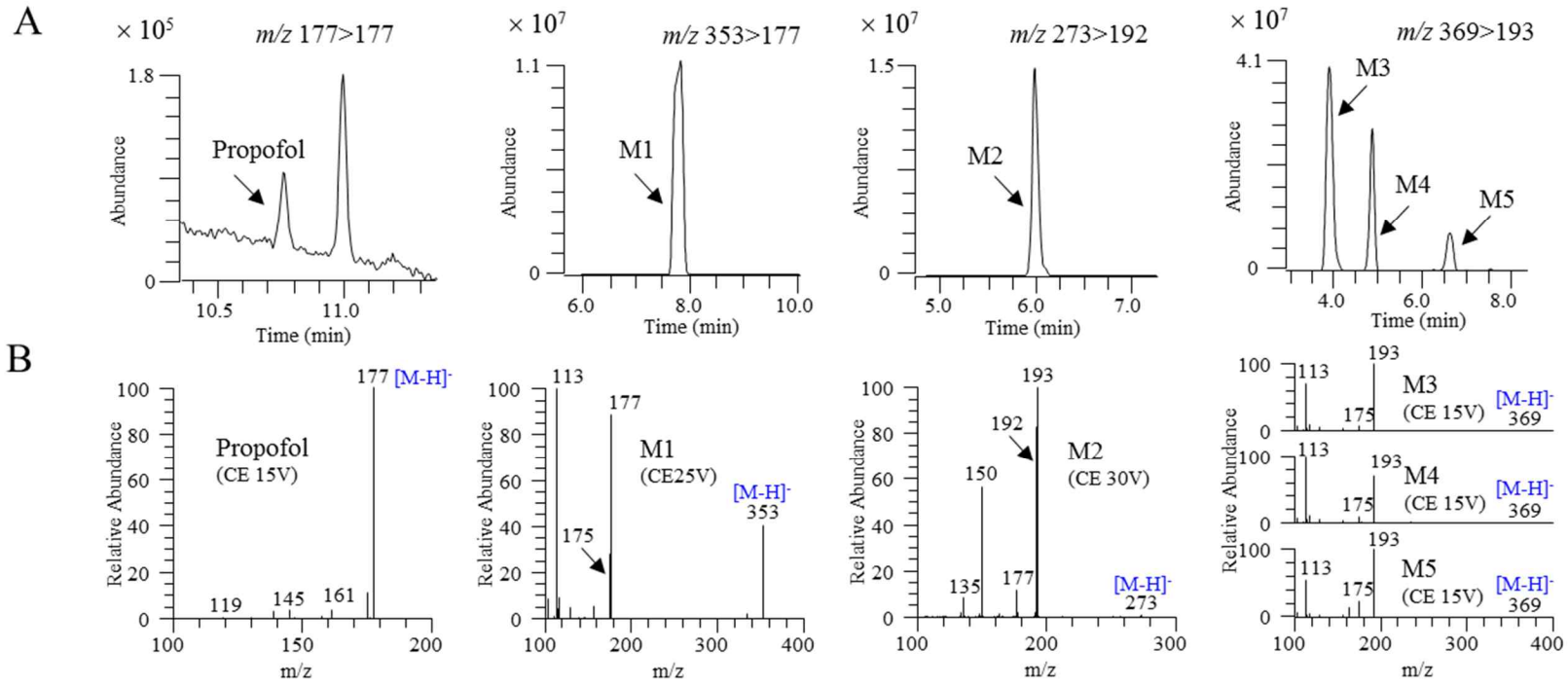

Figure 7. Application to urine samples. Representative chromatograms (A) and product ion scan spectrums (B) for propofol and its phase II metabolites in urine from volunteer-2 at 24h (M1: Propofol-glucuronide, M2: Mono-hydroxylated propofol-sulfate, M3~5: Mono-hydroxylated propofol-glucuronide).

Table 7. Urinary concentration-time profiles of propofol in two volunteers

Excretion time (h)	Propofol concentration (ng/mL)	
	Volunteer-1	Volunteer-2
Before	0	0
1	126.1	3.2
6	130.2	3.7
12	30.9	1.2
18	20.1	1.5
24	12.3	1.6
48	6.9	0.4

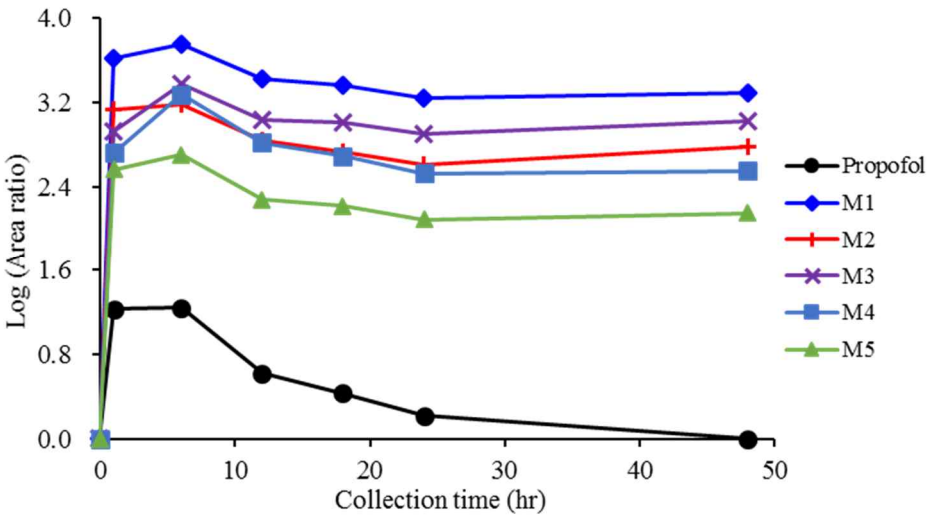

Figure 8. Excretion profiles for propofol and its metabolites from volunteer-1 (M1: Propofol-glucuronide, M2: Mono-hydroxylated propofol-sulfate, M3~5: Mono-hydroxylated propofol-glucuronide).

Table 8. Urine collection time and ESI abundance profiles of propofol metabolites in two volunteers

Collection times (h)	M1		M2		M3		M4		M5	
	Volunteer-1	Volunteer-2	Volunteer-1	Volunteer-2	Volunteer-1	Volunteer-2	Volunteer-1	Volunteer-2	Volunteer-1	Volunteer-2
Before admin.	0	0	0	0	0	0	0	0	0	0
1	1275253776	383471197	408576385	131816875	255208263	91937004	160048603	56058710	110784467	22596026
6	1199299159	419181752	312419961	113173541	489816843	86263036	392076284	42272985	104662099	20840601
12	842425628	159079765	221377068	71497540	346656350	48143597	206741223	22633466	59371736	7282687
18	699198258	136305665	162294837	51502884	305453295	32393822	149240858	14906209	49279644	5238626
24	589527581	121640829	136082471	61449237	265353272	33091614	113577523	18354881	41035338	6629791
48	362073852	73823987	111934975	30904894	197212344	14079449	66574611	8040960	26168918	2958014

M1: Propofol-glucuronide

M2: Mono-hydroxylated propofol-sulfate

M3-5: Mono-hydroxylated propofol-glucuronide

3.4 Conclusions

In this study, three serious problems associated with propofol determination methods, i.e., uncontrolled loss in sample preparation, poor ionization efficiency, and poor CID in mass spectrometry, were overcome. Accordingly, we have developed a highly sensitive and accurate fluoride-assisted LC–ESI/MS/MS method for the determination of propofol. The present method allows the direct quantitation of propofol and the simultaneous determination of its phase II metabolites.

We have demonstrated that the present method is effective for investigating of metabolism, toxicity, and misuse of propofol. Furthermore, ionization via fluoride-ion attachment/induced deprotonation may be universally applied to improving the inherently poor ionization efficiency of numerous phenolic compounds with high p*K*a values.

Chapter 4. Fluoride assisted analysis II : Environmental phenols

4.1 Introduction

4.1.1 Study background

Environmental phenols (**Figure 9**) such as bisphenols, benzophenones, parabens, alkylphenols, and chlorophenols, are widely used in various industrial fields such as food processing, pharmaceutical materials, personal care products, and antioxidants (Kunisue et al., 2012; Frederiksen et al., 2013; Asimakopoulos et al., 2016; Xue et al., 2017; Fan et al., 2019; Li et al., 2019c; Cornwall, 2020).

Bisphenols are a representative environmental phenol which is used in manufacturing of polycarbonate plastic and epoxy resins and present in a wide range of food packaging, personal care products and toys (Asimakopoulos et al., 2016; Xue et al., 2017; Cornwall, 2020). The combination of triclosan and triclocarban is used as a broad antiseptic in soap, toothpaste, and home disinfectant formulations (Asimakopoulos et al., 2016; Li et al., 2019c). Meanwhile, alkylphenols are major degradation products of alkylphenol polyoxyethylene ethers used as surfactants in domestic and industrial care products (Fan et al., 2019). Furthermore, benzophenones are used as sunscreen agents and parabens as antimicrobial preservatives in various personal care products (Kunisue et al., 2012; Frederiksen et al., 2013; Asimakopoulos et al., 2016; Xue et al., 2017).

Owing to its common use in industries, we are exposed to environmental phenols through a variety of routes, including ingestion, inhalation, or dermal contact (Frederiksen et al., 2013; Li et al., 2019b). Such an exposure can potentially lead to neurodevelopmental, reproductive, and respiratory disorders (Sohoni et al., 2001;

Chen et al., 2016; Gao et al., 2021). To safeguard the health of humans, it is therefore important to constantly measure the exposure of humans to these environmental phenols and determine the association between human exposures and potential risks to human health.

4.1.2 Analytical history of environmental phenols

Numerous analytical approaches, such as chromatography mass spectrometry (Xiao et al., 2011; Chen et al., 2012a; Zhou et al., 2013; Moos et al., 2014; Zhou et al., 2014; Heffernan et al., 2016; Jimenez-Diaz et al., 2016; Rocha et al., 2018; Sanchis et al., 2019; Bocato et al., 2020; Silveira et al., 2020; Ao et al., 2021; Lee et al., 2022; Sukuroglu et al., 2022), fluorescence (Orzel and Swit, 2021), electro sensing assays (Zhang et al., 2021; Neven et al., 2022) or raman spectroscopic (Zhang et al., 2017; Lei et al., 2018) have been used for detecting phenols.

Among them, electrospray ionization mass spectrometry (ESI-MS) coupled with ultra-high pressure liquid chromatography (UHPLC) is the most widely used technique due to its powerful advantage to ionize various compounds in liquid samples, providing a sensitive and high-throughput multi-residue analytical methods. A number of exposome methodologies based on LC–ESI–MS/MS have been reported in human biological samples such as blood (Sosvorova et al., 2017; Gely et al., 2021), breast milk (Zimmers et al., 2014; Tuzimski et al., 2019), saliva (Kingman et al., 2012; Berge et al., 2017) and urine (Bocato et al., 2020; Silveira et al., 2020). Especially, urine has been the best choice of matrix due to its non-invasive and cost effective collection as well as the short biological half-lives (<24h) of urinary phenols (Teeguarden et al., 2015).

However, current analysis methods of urinary phenols have limitation in simultaneous analyzing multiple categories of phenols. Because environmental phenols have widely different physico-chemical properties and low concentration (ng/mL) in biological samples (Ao et al., 2021), which lead to two serious problems; the concurrent ionization and low sensitivity problem of multiclass phenols in ESI. Among two serious problems, the concurrent ionization of multiclass phenols is a core requirement for the successful establishment of multiclass analytical method. Majority of the bisphenols, and particularly para-alkylphenols exhibit low ionization efficiency or are not ionized in the common mobile phase composition (Peng et al., 2016). Also, the ionization efficiency of bisphenols and para-alkylphenols is extremely different depending on the mobile phase compositions.

To overcome the concurrent ionization issue of phenols, majority of reported methodologies have employed water and methanol mobile phase system without additive (Xiao et al., 2011; Chen et al., 2012a; Zhou et al., 2014; Rocha et al., 2018; Sanchis et al., 2019; Bocato et al., 2020; Silveira et al., 2020; Ao et al., 2021). Such no additive condition has allowed the concurrent ionization of a wide range phenols, but still have limitations in covering the concurrent ionization of all multiclass phenols as well as another critical problem associated with the low sensitivity.

On the other hand, sample preparation methods such as SPE or LLE have applied to increase sensitivity (Xiao et al., 2011; Yang et al., 2014; Jimenez-Diaz et al., 2016; Bocato et al., 2020; Silveira et al., 2020). Otherwise, more than two methodologies were applied to evaluate of multi-environmental phenols exposure (Peng et al., 2016; Zhu et al., 2021). However, these traditional extraction methods and structure-specific individual methods are not practical for large-scale epidemiological studies when it comes to the excessive demand for analytical

instruments, manpower, sample preparation time, and cost (Grzeskowiak et al., 2016). For this reason, the analysis of alkylphenols are still preferred GC-MS method (Li et al., 2013; Chung and Ding, 2018), otherwise only nonylphenol (NP) with relatively high biological concentrations was included in multi-residue analysis using LC-ESI-MS/MS (Xiao et al., 2011; Sukuroglu et al., 2022).

Currently, most of the reported methodologies have focused on analyzing exposure to parabens, benzophenones, and a few bisphenols, which have inherently good ionization efficiencies, unlike that of alkylphenols. (Moos et al., 2014; Jimenez-Diaz et al., 2016; Sosvorova et al., 2017; Xue et al., 2017; Sanchis et al., 2019; Bocato et al., 2020; Ao et al., 2021; Gely et al., 2021). Therefore, to establishing a comprehensive and sensitive analytical method for multiple classes of phenols requires the development of a phenol-specialized mobile phase whose composition addresses both problems of concurrent ionization and lack of sensitivity.

For the establishment of comprehensive and sensitive analytical method for multiclass phenols, it is of great importance to develop a phenol-specialized mobile phase composition satisfying both the concurrent ionization and sensitivity enhancement. This study aimed to develop a phenol-specialized mobile phase composition for use in a comprehensive and sensitive LC–ESI–MS/MS methodology for the simultaneous quantitation of multiple classes of environmental phenols, including bisphenols, alkylphenols, parabens, benzophenones, and chlorophenols, in human urine. To the best of our knowledge, this is the first study to develop a methodology capable of assessing most phenols from five different classes. We applied our methodology to assess the sports-related health risks of athletes by analyzing the urine samples of 80 athletes engaged in aquatic and land sports activities.

Bisphenols

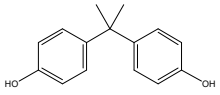

BPA

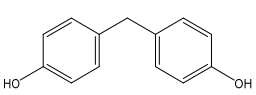

BPF

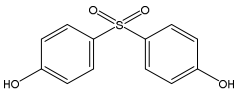

BPS

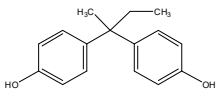

BPB

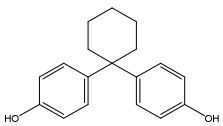

BPZ

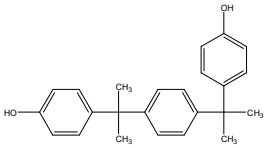

BPP

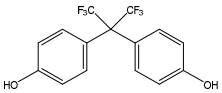

BPAF

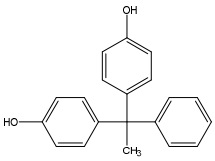

BPAP

Benzophenones

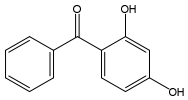

BP-1

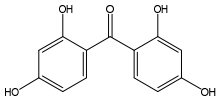

BP-2

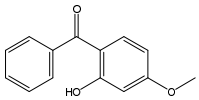

BP-3

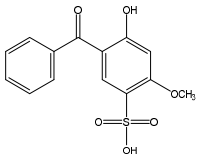

BP-5

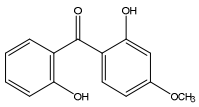

BP-8

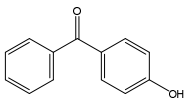

4-HBP

Alkylphenols

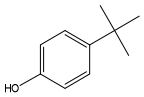

4-TBP

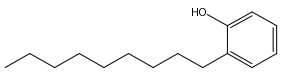

NP

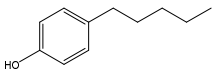

4-BP

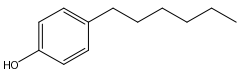

4-PP

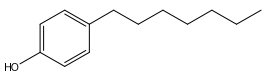

4-HP

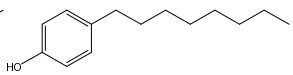

POP

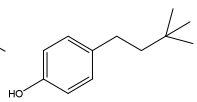

PTOP

Figure 9. Structure of environmental phenols

Parabens

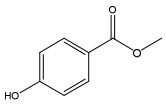

MP

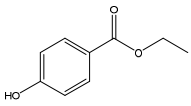

EP

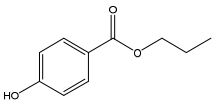

PP

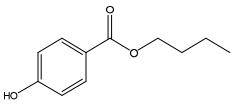

BP

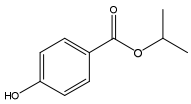

iPP

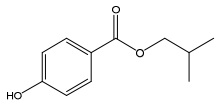

iBP

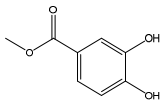

MPA

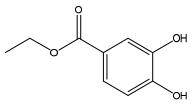

EPA

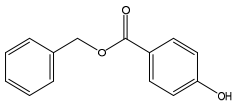

B4-HBZ

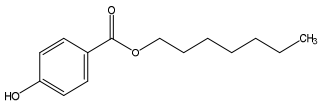

H4-HBZ

Chlorophenols

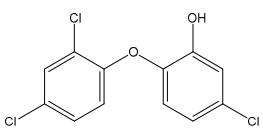

TCS

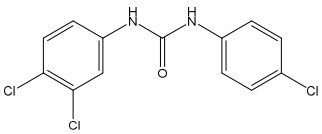

TCC

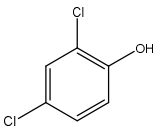

2,4-DCP

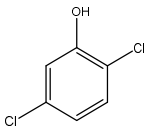

2,5-DCP

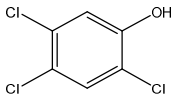

2,4,5-TCP

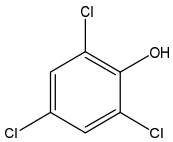

2,4,6-TCP

Others

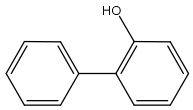

OPP

Figure 9. (Continued)

4.2 Experimental procedures for environmental phenols analysis

4.2.1 Chemicals and reagents

All 38 phenols and 11 internal standards were purchased from Cambridge Isotope Laboratories (Andover, MA, USA), Sigma Aldrich (St. Louis, MO, USA), or Toronto Research Chemicals (Toronto, Canada). The compound names, abbreviations, chemical formula, and molar weight of the analytes are listed in **Table 9**. Acetonitrile (ACN), methanol (MeOH), ethyl acetate (EA) and methyl tert-butyl ether (MTBE) of high performance liquid chromatography grade were obtained from Burdick & Jackson (Ulsan, Korea). Ammonium formate (AFO), ammonium acetate (AAC), ammonium fluoride (AFL) and acetic acid (AA), and formic acid (FA) were purchased from Sigma Aldrich (St. Louis, MO, USA). Analytical grade water was obtained from Merck (Darmstadt, Germany). β-Glucuronidase (4.5 standard units)/arylsulfatase (14 standard units) from *Helix pomatia* was obtained from Roche (Mannheim, Germany). Artificial urine was obtained from BIOZOA (Seoul, Korea). The Standard Reference Materials (SRMs), SRM 3672 (Organic Contaminants in Smoker's Urine) and SRM 3673 (Organic Contaminants in Non-Smoker's Urine), were obtained from the National Institute of Standards and Technology (NIST; Gaithersburg, MD, USA).

Table 9. Information on names, abbreviations, chemical formula, molecular weight and suppliers of analytes and internal standards

Compound	Abbr.	Formula	MW	Supplier	CAS No.
Bisphenol A	BPA	C15H16O2	228.29	Sigma Aldrich	80-05-7
Bisphenol F	BPF	C13H12O2	200.23	Sigma Aldrich	620-92-8
Bisphenol S	BPS	C12H10O4S	250.27	Sigma Aldrich	80-09-1
Bisphenol B	BPB	C16H18O2	242.31	Sigma Aldrich	77-40-7
Bisphenol Z	BPZ	C18H20O2	268.35	Sigma Aldrich	843-55-0
Bisphenol P	BPP	C24H26O2	346.46	Sigma Aldrich	2167-51-3
Bisphenol AF	BPAF	C15H10F6O2	336.23	Sigma Aldrich	1478-61-1
Bisphenol AP	BPAP	C20H18O2	290.36	Sigma Aldrich	1571-75-1
Benzophenone-1	BP-1	C13H10O3	214.22	Sigma Aldrich	131-56-6
Benzophenone-2	BP-2	C13H10O5	246.22	Sigma Aldrich	131-55-5
Benzophenone-3	BP-3	C14H12O3	228.24	Sigma Aldrich	131-57-7
Benzophenone-5	BP-5	C14H12O6S	308.31	TRC	4065-45-6
Benzophenone-8	BP-8	C14H12O4	244.24	Sigma Aldrich	131-53-3
4-Hydroxy benzophenone	4-HBP	C13H10O2	198.22	Sigma Aldrich	1137-42-4
Methyl paraben	MP	C8H8O3	152.15	Sigma Aldrich	99-76-3
Ethyl paraben	EP	C9H10O3	166.17	Sigma Aldrich	120-47-8
Propyl paraben	PP	C10H12O3	180.20	Sigma Aldrich	94-13-3
Butyl paraben	BP	C11H14O3	194.23	Sigma Aldrich	94-26-8
isopropyl paraben	iPP	C10H12O3	180.20	Sigma Aldrich	4191-73-5
isobutyl paraben	iBP	C11H14O3	194.23	Sigma Aldrich	4247-02-3
4-tert-butylphenol	4-TBP	C10H14O	150.22	Sigma Aldrich	98-54-4
ortho-Phenyl phenol	OPP	C12H10O	170.21	Sigma Aldrich	90-43-7
4-Butylphenol	4-BP	C10H14O	150.22	Sigma Aldrich	1638-22-8
4-pentylphenol	4-PP	C11H16O	164.24	Sigma Aldrich	14938-35-3
4-hexylphenol	4-HP	C12H18O	178.27	Sigma Aldrich	2446-69-7

Table 9. (Continued)

Compound	Abbr.	Formula	MW	Supplier	CAS No.
4-tert-octylphenol	PTOP	C14H22O	206.32	Sigma Aldrich	140-66-9
Nonylphenol	NP	C15H24O	220.35	Sigma Aldrich	84852-15-3
4-octylphenol	POP	C14H22O	206.32	Sigma Aldrich	1806-26-4
Methyl -protocatechuate	MPA	C8H8O4	168.15	Sigma Aldrich	2150-43-8
Ethyl -protocatechuate	EPA	C9H10O4	182.17	Sigma Aldrich	3943-89-3
Triclosan	TCS	C12H7Cl3O2	287.54	Sigma Aldrich	3380-34-5
Triclocarben	TCC	C13H9Cl3N2O	315.58	Sigma Aldrich	101-20-2
Benzyl-4-hydroxybenzoate	B4-HBZ	C14H12O3	228.24	Sigma Aldrich	94-18-8
Heptyl-4-hydroxybenzoate	H4-HBZ	C14H20O3	236.31	Sigma Aldrich	1085-12-7
2,4-Dichlorophenol	2,4-DCP	C6H4Cl2O	163.00	Sigma Aldrich	120-83-2
2,5-Dichlorophenol	2,5-DCP	C6H4Cl2O	163.00	Sigma Aldrich	583-78-8
2,4,5-Trichlorophenol	2,4,5-TCP	C6H3Cl3O	197.45	Sigma Aldrich	95-95-4
2,4,6-Trichlorophenol	2,5,6-TCP	C6H3Cl3O	197.45	Sigma Aldrich	88-06-2
ISTD					
$^{13}C_{12}$-Bisphenol A	$^{13}C_{12}$-BPA	^{13}C12C3H16O2	240.20	CIL	263261-65-0
$^{13}C_{12}$-Bisphenol F	$^{13}C_{12}$-BPF	^{13}C12C1H12O2	212.14	CIL	1410794-08-9
$^{13}C_{12}$-Bisphenol S	$^{13}C_{12}$-BPS	^{13}C12H10O4S	262.18	CIL	1991267-29-8
$^{13}C_{4}$-Bisphenol P	$^{13}C_{4}$-BPP	^{13}C20C4H26O2	350.43	TRC	Unlabelled
$^{13}C_{12}$-Triclosan	$^{13}C_{12}$-TCS	^{13}C12H7Cl3O2	301.45	CIL	1365620-36-5
D_3-Benzophenone-3	D_3-BP-3	C14H9D3O3	231.26	TRC	Unlabelled
D_4-Heptyl-4-hydroxybenzoate	D_4-H4-HBZ	C14H16D4O3	240.33	TRC	Unlabelled
$^{13}C_6$-Methyl paraben	$^{13}C_6$-MP	^{13}C6C2H8O3	158.10	CIL	1581694-95-2
$^{13}C_6$-Ethyl paraben	$^{13}C_6$-EP	^{13}C6C3H10O3	17213	CIL	Unlabelled
$^{13}C_6$-Propyl paraben	$^{13}C_6$-PP	^{13}C6C4H12O3	186.16	CIL	Unlabelled
$^{13}C_6$-Butyl paraben	$^{13}C_6$-BP	^{13}C6C5H14O3	200.18	TRC	1416711-53-9

4.2.2 Instruments

All LC–ESI–MS/MS experiments were conducted on a Thermo Scientific™ Vanquish™ UHPLC system from Thermo Finnigan (San Jose, CA, USA) with an ACE Excel 2 C18-AR column (150 × 2.1 mm inner diameter) from Advanced Chromatography Technology (Reading, UK), which was connected to a TSQ Altis Triple Quadrupole Mass Spectrometer (Thermo Finnigan, San Jose, CA, USA) with an ESI source. The mobile phase consisted of water (A) and MeOH (B), both of which contained 0.5 mM AFL. The initial gradient composition (2% B) was rapidly increased to 25% B over 0.1 min and then increased to 95% B over 7.9 min. The 95% B was maintained for 3.5 min before being decreased to 2% B over 0.1 min. Subsequently, column conditioning was performed for 3.4 min (total running time: 15 min). The flow rate and column temperature were set to 0.35 mL/min and 35 °C, respectively. The ESI was operated in the negative ionization mode with spray voltage = 3.5 kV. The capillary and vaporizer temperatures were 320°C and 340°C, respectively. Nitrogen was used as sheath gas and auxiliary gas, and the flow rates were 60 and 15 arbitrary units, respectively. The experiments were conducted using the selected reaction monitoring mode. The optimized instrumental conditions and the selected reaction monitoring parameters are presented in **Table 10** and **11**. Optimization of the mobile-phase composition was performed using an LC-20AD XR ultrafast liquid chromatography (UFLC) system (Shimadzu, Kyoto, Japan) coupled to a Q Exactive quadrupole orbitrap mass spectrometer from Thermo Finnigan (San Jose, CA, USA) under the same analytical condition and scan mode.

Table 10. Optimized operating conditions of LC-ESI/MS/MS for environmental phenols analysis

LC conditions				
Instruments	Thermo Scientific™ Vanquish™ UHPLC system			
Column	ACE Excel 2 C18-AR column (150 mm × 2.1 mm)			
Mobile phase	A : 0.5 mM ammonium fluoride in DW B : 0.5 mM ammonium fluoride in MeOH			
Gradient	Time (min)	A (%)	B (%)	Flow rate (mL/min)
	Initial	98	2	0.35
	0.5	75	25	
	8.0	5	95	
	11.5	5	95	
	11.6	98	2	
	15.0	98	2	
MS source parameter				
Instruments	TSQ Altis triple quadrupole mass spectrometer			
Spray voltage	Negative : 3500 V			
Vaporizer temperature	340˚C			
Ion transfer tube temperature	320˚C			
Gas paramether	Sheath gas : 60 arb Aux gas : 15 arb Sweep gas : 1 arb			
Scan type	Selected reaction monitoring (SRM) mode			

Table 11. Optimized mass parameters and retention times of environmental phenols

Analytes (Abbr.)	ESI Polarity	Transition [Q1/Q3 (CE)]	Dwell Time (ms)	Retention time/ Monitoring time (min)	Matched ISTD
BPA	-	227.1/133 (25)	9.24	7.58/1.0	$^{13}C_{12}$-BPA
BPF	-	199.1/93 (21)	17.13	6.73/1.0	$^{13}C_{12}$-BPF
BPS	-	249.1/108 (26)	25.86	5.46/1.0	$^{13}C_{12}$-BPS
BPB	-	241.2/212 (18)	9.24	8.09/1.0	$^{13}C_{12}$-BPA
BPZ	-	267.2/173 (27)	9.37	8.83/1.0	$^{13}C_{12}$-BPA
BPP	-	345.2/330 (26)	8.47	9.73/1.0	$^{13}C_{12}$-BPP
BPAF	-	335.2/265 (22)	9.24	8.12/1.0	$^{13}C_{12}$-BPA
BPAP	-	289.2/274 (20)	9.69	8.63/1.0	$^{13}C_{12}$-BPA
BP-1	-	213.2/135 (27)	9.24	8.08/1.0	$^{13}C_{12}$-BPA
BP-2	-	245.2/135 (15)	9.24	6.40/1.0	$^{13}C_{12}$-BPA
BP-3*	+	229.2/151 (18)	8.47	9.47/1.0	D_3-BP-3
BP-5	-	307.2/211 (37)	25.86	5.50/1.0	$^{13}C_{12}$-BPA
BP-8	-	243.2/123 (18)	9.24	8.53/1.0	$^{13}C_{12}$-BPA
4-HBP	-	197.2/92 (31)	9.75	7.41/1.0	$^{13}C_{12}$-BPA
MP	-	151.1/92 (21)	25.69	5.71/1.0	$^{13}C_6$-MP
EP	-	165.1/92 (23)	17.13	6.59/1.0	$^{13}C_6$-EP
PP	-	179.1/92 (23)	9.24	7.45/1.0	$^{13}C_6$-PP
BP	-	193.1/92 (25)	9.24	8.15/1.0	$^{13}C_6$-BP
iPP	-	179.1/92 (23)	9.24	7.20/1.0	$^{13}C_6$-PP
iBP	-	193.1/92 (25)	9.24	8.02/1.0	$^{13}C_6$-BP
4-TBP	-	149.2/133 (21)	9.24	8.03/1.0	$^{13}C_{12}$-BPA
OPP	-	169.2/93 (27)	9.24	8.11/1.0	$^{13}C_{12}$-BPA
4-BP	-	149.2/106 (20)	9.24	8.46/1.0	$^{13}C_{12}$-BPA
4-PP	-	163.3/106 (17)	8.47	9.03/1.0	$^{13}C_{12}$-BPA
4-HP	-	177.3/106 (18)	8.47	9.50/1.0	$^{13}C_{12}$-BPA
PTOP	-	205.1/133 (25)	8.47	9.62/1.0	$^{13}C_{12}$-BPA
NP	-	219.0/133 (25)	9.39	10.03/1.0	$^{13}C_{12}$-BPA
POP	-	205.0/106 (22)	9.39	10.25/1.0	$^{13}C_{12}$-BPA
MPA	-	167.1/108 (21)	25.87	4.86/1.0	$^{13}C_6$-MP
EPA	-	181.1/108 (23)	20.60	5.78/1.0	$^{13}C_6$-EP
TCS	-	287.0/35 (10)	8.47	9.90/1.0	$^{13}C_{12}$-TCS
TCC	-	313.2/160 (11)	8.47	9.75/1.0	$^{13}C_{12}$-BPA
B4-HBZ	-	227.2/92 (24)	9.24	8.39/1.0	D_4-H4-HBZ
H4-HBZ	-	235.2/92 (27)	8.47	9.66/1.0	D_4-H4-HBZ
2,4-DCP	-	161.1/125 (16)	9.24	7.90/1.0	D_4-H4-HBZ
2,5-DCP	-	161.1/125 (16)	9.24	7.68/1.0	D_4-H4-HBZ
2,4,5/2,4, 6-TCP	-	195.1/159 (20)	9.37	8.81/1.0	$^{13}C_{12}$-BPA

Table 11. (Continued)

Analytes (Abbr.)	ESI Polarity	Transition [Q1/Q3 (CE)]	Dwell Time (ms)	Retention time/ Monitoring time (min)	Matched ISTD
ISTD					**ISTD**
$^{13}C_{12}$-BPA	-	239.2/224 (18)	9.24	7.59/1.0	$^{13}C_{12}$-BPA
$^{13}C_{12}$-BPF	-	211.2/99 (18)	17.13	6.74/1.0	$^{13}C_{12}$-BPF
$^{13}C_{12}$-BPS	-	261.1/114 (28)	25.86	5.47/1.0	$^{13}C_{12}$-BPS
$^{13}C_{4}$-BPP	-	349.4/333(26)	8.47	9.73/1.0	$^{13}C_{4}$-BPP
$^{13}C_{12}$-TCS	-	299.1/35 (10)	8.47	9.91/1.0	$^{13}C_{12}$-TCS
D_3-BP-3*	+	232.3/154 (19)	8.47	9.45/1.0	D_3-BP-3*
D_4-H4-HBZ	-	239.3/96 (28)	8.47	9.65/1.0	D_4-H4-HBZ
$^{13}C_6$-MP	-	157.1/98 (21)	25.69	5.71/1.0	$^{13}C_6$-MP
$^{13}C_6$-EP	-	171.1/98 (23)	17.13	6.59/1.0	$^{13}C_6$-EP
$^{13}C_6$-PP	-	185.2/98 (23)	9.75	7.42/1.0	$^{13}C_6$-PP
$^{13}C_6$-BP	-	199.1/98 (25)	9.23	8.13/1.0	$^{13}C_6$-BP

* : The positive mode was more superior when considering the peak sensitivity and interference in our analysis conditions, although the ionization efficiency was great for both positive and negative modes.

4.2.3 Sample collection

The urine samples from volunteer athletes were obtained according to the Guidelines for Urine Sample Collection described by the World Anti-Doping Agency. Upon collection, the samples were labeled with anonymized alpha-numeric format, refrigerated, and then transported to the Doping Control Laboratory in Korea. The samples were stored at −20 °C prior to use.

4.2.4 Ethics

The study was approved by the Institutional Review Board of Korea Institute of Science and Technology (IRB number: 2021-E-005) and performed in accordance with ethical standards.

4.2.5 Sample preparation

Urine sample (0.2 mL), internal standard solution (10 μL), and water (0.1 mL) were transferred to a glass tube. Two hundred microliters of 0.2 M acetate buffer at pH 5.0 and 20 μL β-glucuronidase/arylsulfatase (20 μL) were added, and then the mixture was incubated at 55 °C for 2 h. ACN (0.1 mL) was then added, and the mixture was centrifuged at 13,000 rpm for 10 min using an Eppendorf centrifuge (Hamburg, Germany). Finally, the supernatant was transferred to an autosampler vial and 10 μL was injected into the LC–ESI–MS/MS system for analysis. The Sample preparation step was summarized in **Figure 10**.

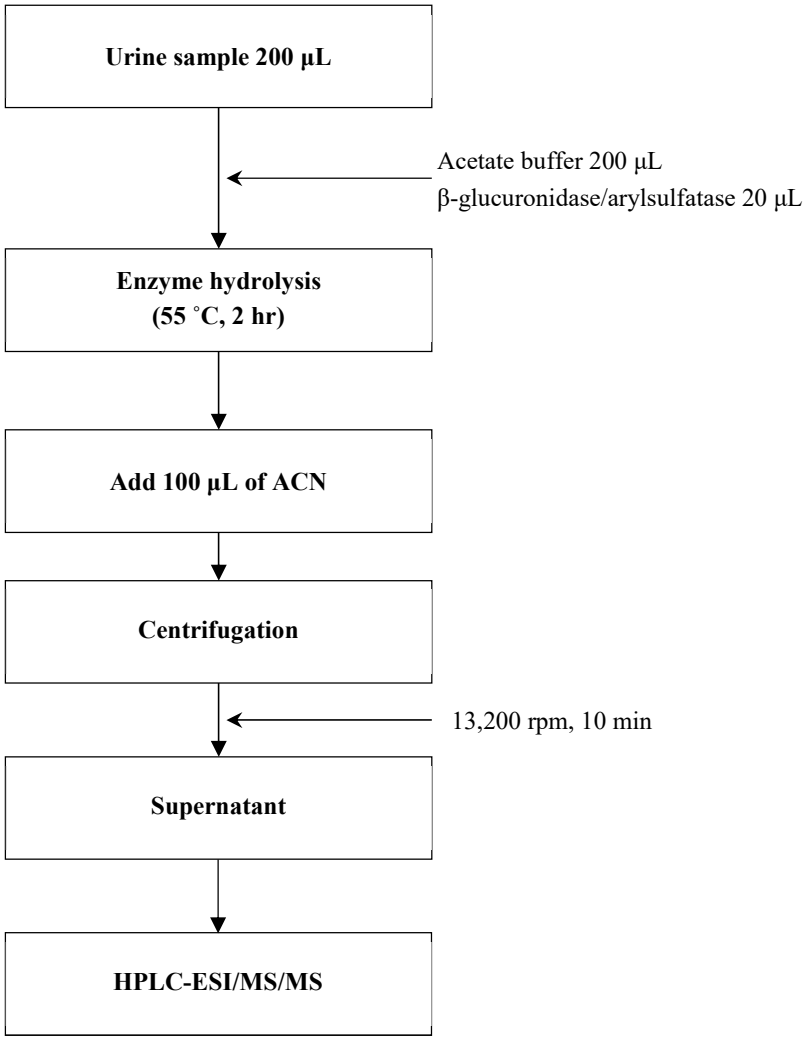

Figure 10. Schematic diagram of sample preparation procedure for environmental phenols

4.2.6 Method validation

The method was validated for linearity, limit of detection (LOD), limit of quantification (LOQ), matrix effects, intra- and inter-day precision, and accuracy. The concentration range studied for the analytes was 0.05 to 500 ng/mL, with ISTD in artificial urine. The linearity was evaluated using the correlation coefficient (R^2). The LOD and LOQ values were calculated using the equations from the ICH guideline: LOD = 3.3(σ/S) and LOQ = 10(σ/S), where σ and S denote the standard deviation of the response and the slope of the calibration curve, respectively (Walfish, 2006). The validation results for linearity, LOD, and LOQ were evaluated according to the guidelines established by Bioanalytical Method Validation Guidance for Industry (Brodie and Hill, 2002). For precision, urine samples are analyzed five replicates in the same run (intra-day precision) and in five separate runs (inter-day precision) at three concentrations for each phenols (0.5 (or 2.0), 20 and 200 ng/mL). The results were expressed as the percentage coefficient of variation values of the peak area ratio for the analyte to the internal standard. The accuracy was expressed as the bias of the measured concentration to the expected value. The matrix effect (%) was calculated using the following equation (1) (Ao et al., 2021).

$$\text{Matrix effect (\%)} = \frac{X1-X2}{X3} \times 100 \quad (1)$$

Here, X1 is the peak area of post-extraction spiked matrix, X2 is the peak area of blank matrix, X3 is the peak area of standard solvent solution.

4.2.7 Statistical analysis

According to the modified 80% rule (Yang et al., 2015), only environmental phenols with less than 20% missing values in the any group were processed for

further analysis. Missing values for each compound were replaced by LOD/2 values and then transformed into the natural-log (Ln) scale. The Levene's test was employed to assess the equality of variances. In cases of a normal distribution, one-way analysis of variance and Scheffe *post hoc* analysis were conducted. If the environmental phenols had no normal distribution, nonparametric tests, including the Kruskal–Wallis test and the Bonferroni adjusted *P*-value were used. With the statistical analyses conducted, comparison of environmental phenols having significant changes among three different disciplines were clearly evaluated. All statistical analyses were conducted using the SPSS statistical software program version 23 from IBM (New York, USA).

4.3 Results and discussion

4.3.1 Discovery of phenol-specialized mobile phase composition

4.3.1.1 Mobile phase composition for concurrent ionization

Among five phenol classes (bisphenols, parabens, benzophenones, chlorophenols and alkylphenols), majority of the bisphenols, and particularly para-alkylphenols, were poorly or are not ionized in the commonly used mobile phase. Therefore, the concurrent ionization of all five classes of phenols is a core prerequisite for the successful development of a comprehensive analytical method for multiple classes of phenols.

To determine the optimum mobile phase composition for the concurrent ionization of phenols, we investigated the relationship between the mobile phase composition and ionization efficiency of phenols. Ammonium fluoride, ammonium acetate, ammonium formate, acetic acid, formic acid, and no additive condition were evaluated as mobile phase additives under water/methanol and water/ACN system. We evaluated the ionization efficiency with the area abundance of analytes according to various additive conditions with water/MeOH system and water/ACN system.

Based on this evaluation, as shown in **Figures 11** to **12**, a heat map was presented in which the blue color becomes deeper as the ESI abundance increases, to compare ionization efficiencies at a glance. **Figures 11** and **12** showed the signal abundance in the water/MeOH system and water/ACN system, respectively. Overall, a deeper blue color was seen in the heatmap of the water/MeOH system (**Figures 11)**, optimal concentration of each additive was determined to compare accurately

the relative ionization efficiency of phenols (excluded isomers) in different mobile phase compositions.

Under the water/MeOH system (**Figures 11)**, the optimum concentration ranges of the additives were 0.2-0.5 mM for AFL, 1.0-2.0 mM for AAC and AFO, 0.05-0.1% for AA and 0.002-0.01% for FA (the green square box). The best optimal concentration (the arrow) was selected as 0.5 mM for AFL, 2.0 mM for AAC, 2.0 mM for AFO, 0.01% for FA, and 0.05% for AA. The best optimal concentration of each additive was also consistent in the water/ACN system (**Figures 12)**. We summarized the optimized concentration for each additive in the heatmap (**Figure 13**). Obviously, methanol modifier showed better ionization efficiency compared to acetonitrile regardless of additive, therefore, the water/MeOH system was determined as organic modifier for phenols analysis.

On the basis of these results, we investigated the concurrent ionization coverage of phenols in each optimized mobile phase composition. As illustrated in **Figure 14**, FA and AA showed an incomplete concurrent ionization coverage, and most of bisphenols and alkylphenols exhibited poor ionization efficiency or were not ionized in these compositions. In particular, the poor ionization efficiency by formic acid was consistent with previous reporting that formic acid diminished negative ESI response of phenolic compounds (Wu et al., 2004). Therefore, they were not suitable as mobile phase composition for the concurrent ionization.

AFO, AAC, and no additive conditions showed a complete concurrent ionization coverage for all phenols, but still poor or low ionization efficiency for most of the bisphenols and alkylphenols. On the other hand, AFL showed good ionization efficiency for most phenols, including bisphenols and alkylphenols, as well as high concurrent ionization coverage. Consequently, AAC, AFO, AFL, and

no additive condition were the candidate mobile phase compositions allowing for the concurrent ionization of multiple classes of phenols.

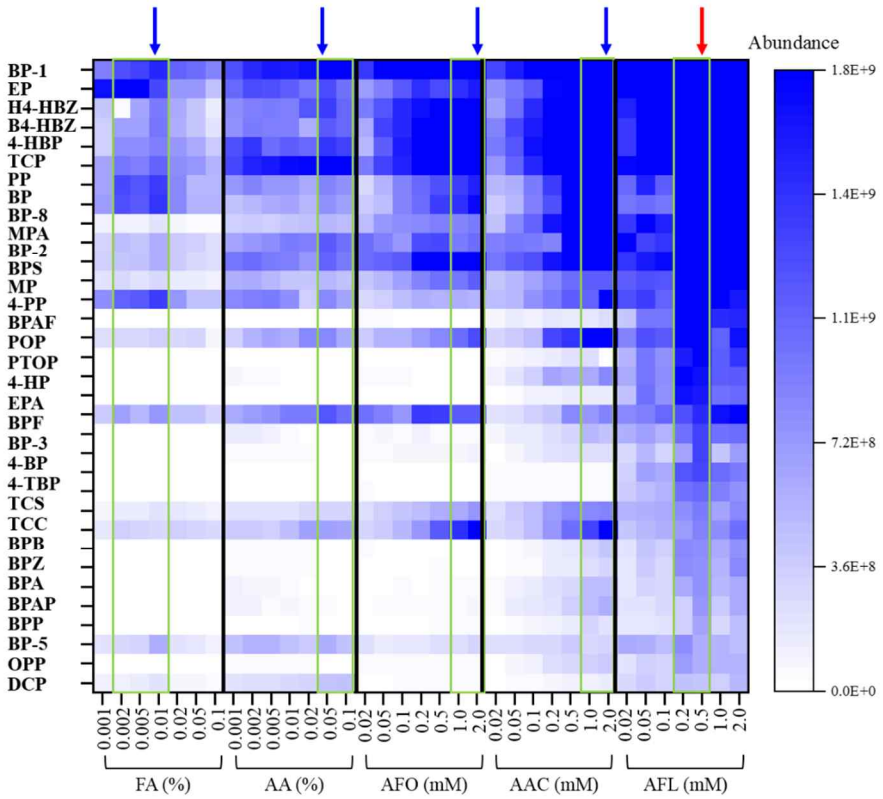

Figure 11. Heatmap of the signal abundance of the analyzed phenols according to the mobile-phase additive concentration using water/MeOH system. The square boxes (green) present the optimum concentration ranges, and the arrows point at the optimized concentration of each additive.

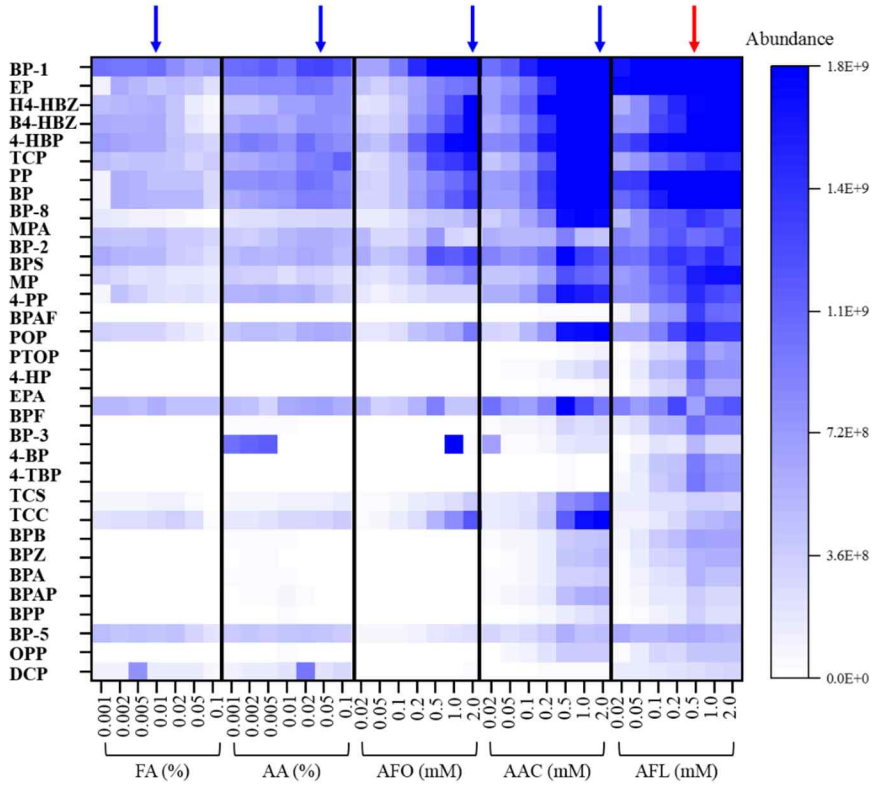

Figure 12. Heatmap of the signal abundance of the analyzed phenols according to the mobile-phase additive concentration using water/ACN system. The arrows point at the optimized concentration of each additive.

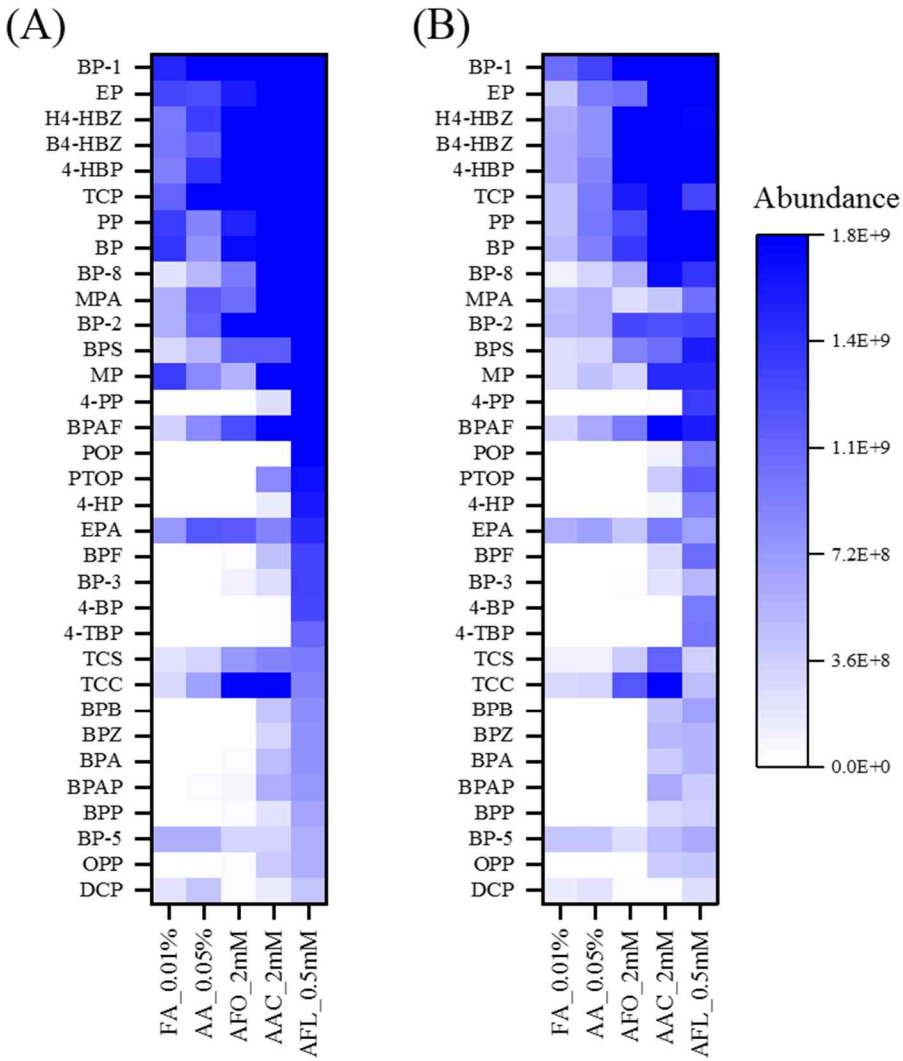

Figure 13. Heatmap of the signal abundance of the analyzed phenols under the optimized concentrations of mobile-phase additives using (A) water/MeOH and (B) water/ACN system.

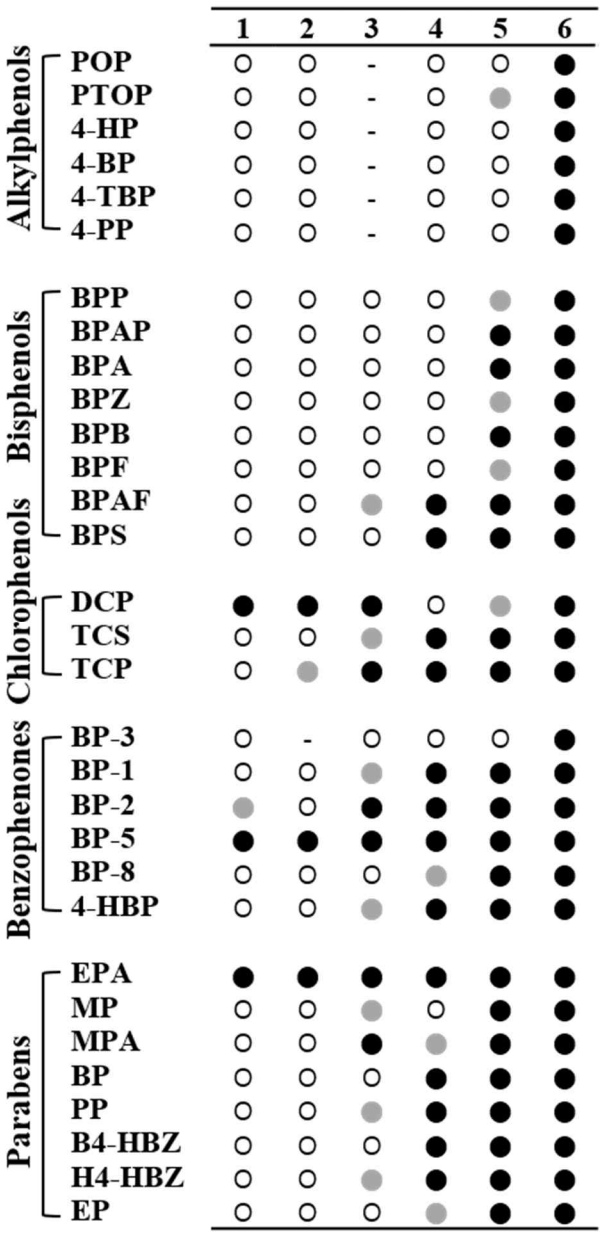

Figure 14. The coverage for concurrent ionization in the optimized mobile phase compositions in the water/MeOH system (-: no ionization, ○: poor ionization, ●: low ionization, ●: good ionization; 1 = no additive, 2 = 0.01% formic acid, 3 = 0.05% acetic acid, 4 = 2.0 mM ammonium formate, 5 = 2.0 mM ammonium acetate, 6 = 0.5 mM ammonium fluoride).

4.3.1.2. Mobile phase composition for sensitivity enhancement

Sensitivity enhancement is another core requirement for phenol analysis. Therefore, we investigated the relative sensitivity enhancement of phenols in mobile phases with AAC, with AFL, and with no additive; which had a complete concurrent ionization coverage. Although the ionization efficiency with no additive was somewhat low, this condition was included along with AFL and AAC because it has been commonly used in previous reports.

Figure 15 illustrates the ionization efficiencies of phenols without additive, with AAC, and with AFL using the water/MeOH (**Figure 15(A)**) and water/ACN (**Figure 15(B)**) system. Several interesting results were observed regarding the effect of mobile phase composition on the enhancement of the ionization efficiency of phenols. First, AAC and the no additive condition exhibited similar ionization efficiencies in water/MeOH and water/ACN system, or slightly enhanced efficiencies in the water/MeOH system. This indicates that the ionization efficiencies in the no additive and AAC conditions were not influenced by the organic solvent in the mobile phase. Second, in the water/ACN system, the no additive, AAC, and AFL conditions had similar ionization efficiencies, except in several phenols. Meanwhile, in water/MeOH system, only AFL dramatically enhanced of ionization efficiency compared to the no additive and AAC conditions, a result that was not observed in the water/ACN system. Therefore, AFL was the only additive that enhanced the ionization efficiency of phenols and MeOH was required for this effect.

The water/MeOH system without any additive is the most commonly reported method used to analyze phenols. Therefore, we compared the sensitivity enhancement of AFL and AAC relative to the no additive condition.

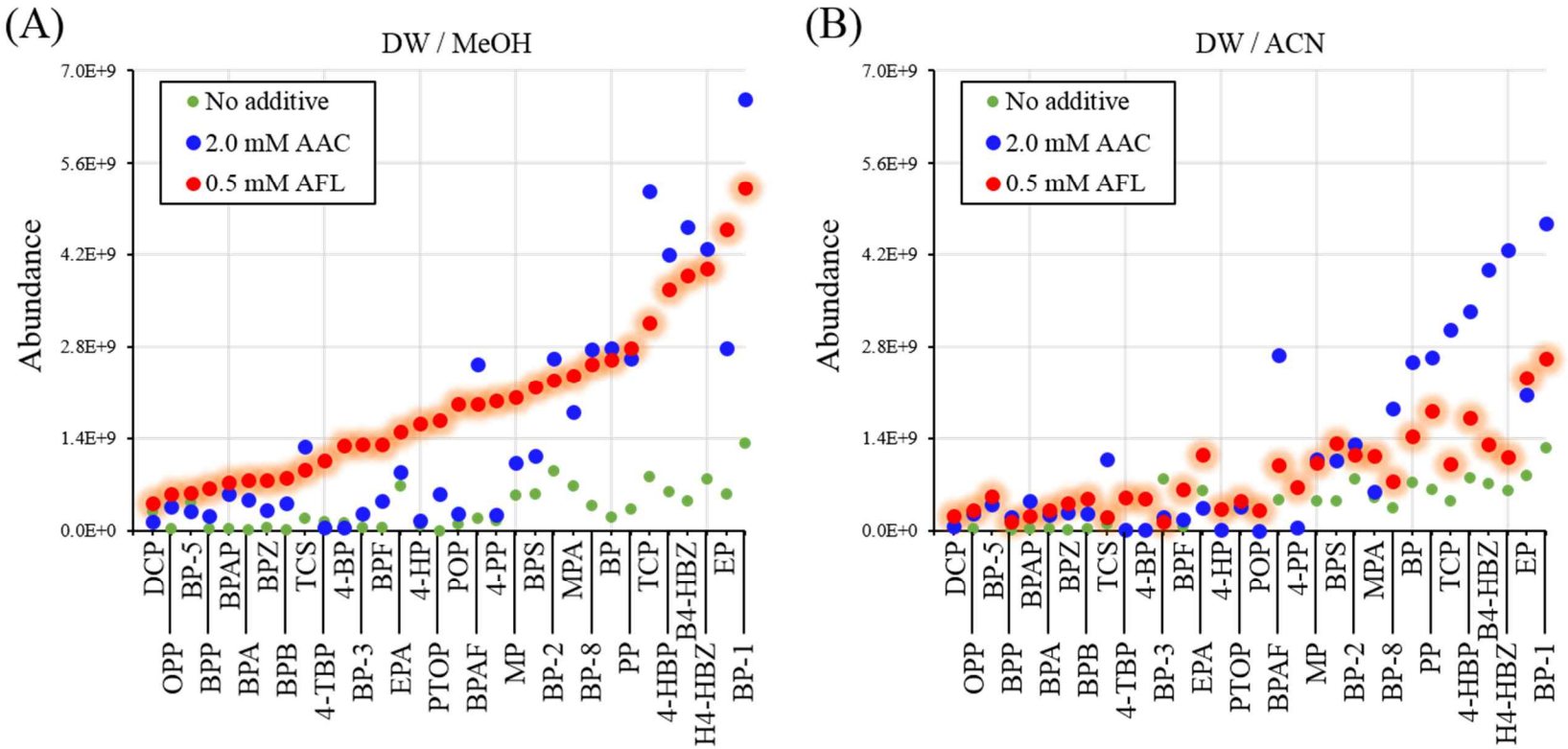

Figure 15. The ionization efficiency of phenols under the optimized mobile phase composition in (A) water/MeOH and (B) water/ACN system

Figure 16 presents the sensitivity enhancement of AFL and AAC relative to the no additive treatment in four phenol classes. In parabens and benzophenones, AAC and AFL had similar sensitivity enhancement ratios. However, in bisphenols (with inherently low ionization efficiency), the use of AFL resulted in 17–39-fold sensitivity enhancement, compared to the no additive treatment. In addition, the use of AFL for alkylphenols, which also have inherently poor ionization efficiency, also resulted in 8–20-fold sensitivity enhancement compared to the no additive treatment. Thus, AFL was an effective additive for alkylphenols and bisphenols. In terms of sensitivity enhancement, AFL was an excellent mobile phase additive compared to the no additive treatment, which has been commonly used in previous reported methods. Our results indicate that 0.5 mM AFL in water/MeOH system is a phenol-specialized mobile phase composition that provides both concurrent ionization and sensitivity enhancement.

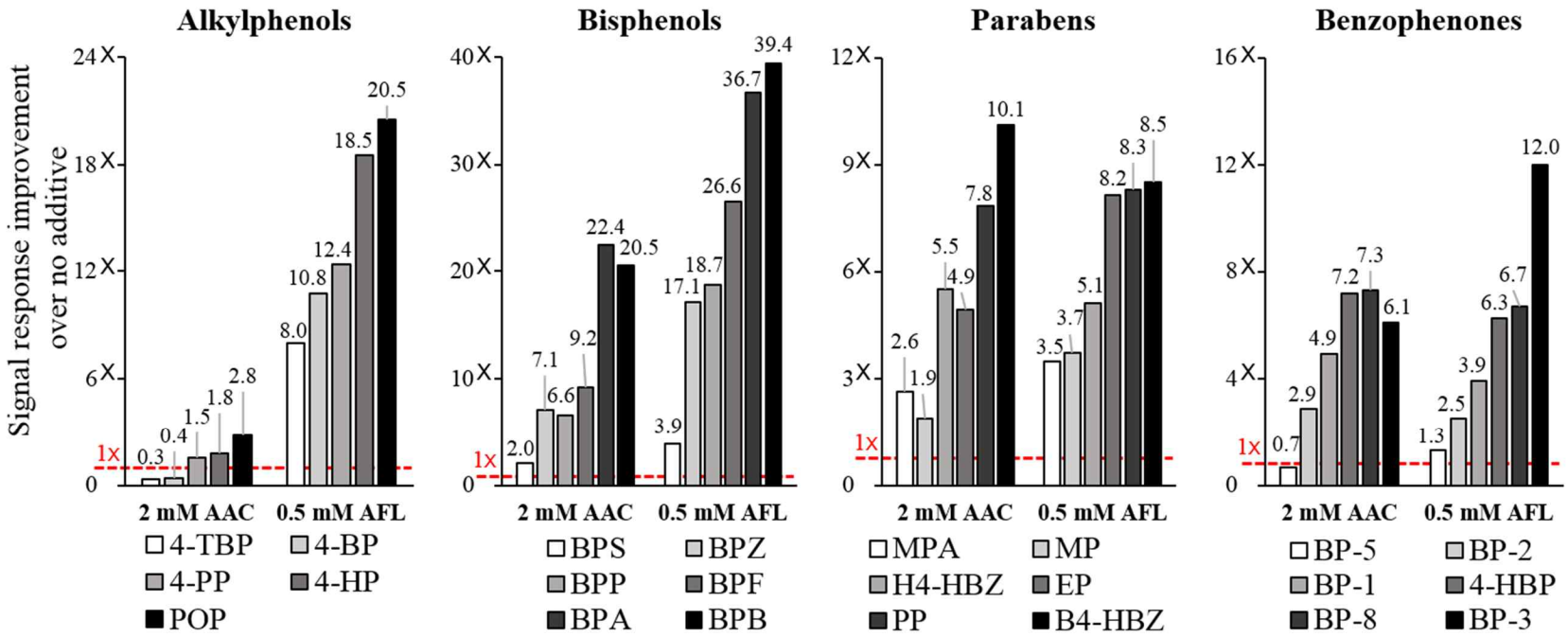

Figure 16. Sensitivity enhancement ratio of AAC and AFL over no additive condition under water and MeOH system

4.3.1.3. Relationship between pK_a and ionization efficiency

The above results suggest that the effect of AFL on ionization efficiency was affected by the structure of phenols. Bisphenols and alkylphenols are well-known to have a slightly higher pK_a value and very poor ionization efficiency compared to other phenols (Castro et al., 2003; Wu et al., 2013; Regueiro et al., 2015). Because analyte pK_a is an important factor that can predict the ESI response, we plotted the signal abundance against the pK_a values of phenols. The phenols with heteroatoms or additional functional groups in the basic structure were excluded because the molecular volume or polarity has also been found to be an important factor affecting the ESI response (Wu et al., 2004; Henriksen et al., 2005).

As presented in **Figure 17**, benzophenones and parabens, which have relatively low pK_a values (7-9), exhibited higher signals regardless of the type of additive. Conversely, the bisphenols and alkylphenols, which have relatively high pK_a values (9-11), showed a large difference in the signals depending on the additive. With AFL (**Figure 17(A)**), the signals for the bisphenols and alkylphenols increased as their pK_a values increased. In contrast, with AFO and AAC (**Figure 17(B)**), the signals for the bisphenols and alkylphenols decreased as their pK_a values increased. The no additive condition also exhibited similar behavior to AFL, but the signal response was much lower than AFL.

This distinctive phenomenon of the effect of AFL may originate from the strong gas-phase proton affinity of fluoride (F^-). In the gas phase, the deprotonation of an analyte may depend on the gas-phase proton affinity of the anion generated from the mobile phase. Ideally, the mobile phase for negative ESI should produce anions with a high gas-phase proton affinity value (Wu et al., 2004) without producing a high pH. The gas-phase proton affinity value of fluoride (F^-) is 1530.5

kJ/mol, which was higher than that for acetate (1427 kJ/mol) and formate (1416 kJ/mol) (Cai and Cole, 2002b). Therefore, we believe that F^- was able to increase the level of deprotonated phenol in the gas phase due to its high proton affinity. **Figure 13** shows that the ionization efficiency results (AFL > AAC > AFO) of phenols are consistent with the gas-phase proton affinities of the anions. Consequently, the anion attachment and their gas-phase proton affinity play an important role in enhancing the ionization efficiency of phenols in negative ESI, and we suggest that AFL can be effective in improving the inherently poor ionization efficiency of phenolic compounds with high pK_a values.

Consequently, the anion attachment and their gas-phase proton affinity play an important role in the enhancement of ionization efficiency of phenols in negative ESI and we suggest that AFL can be effective to improve the inherently poor ionization efficiency of phenolic compounds with high pK_a value.

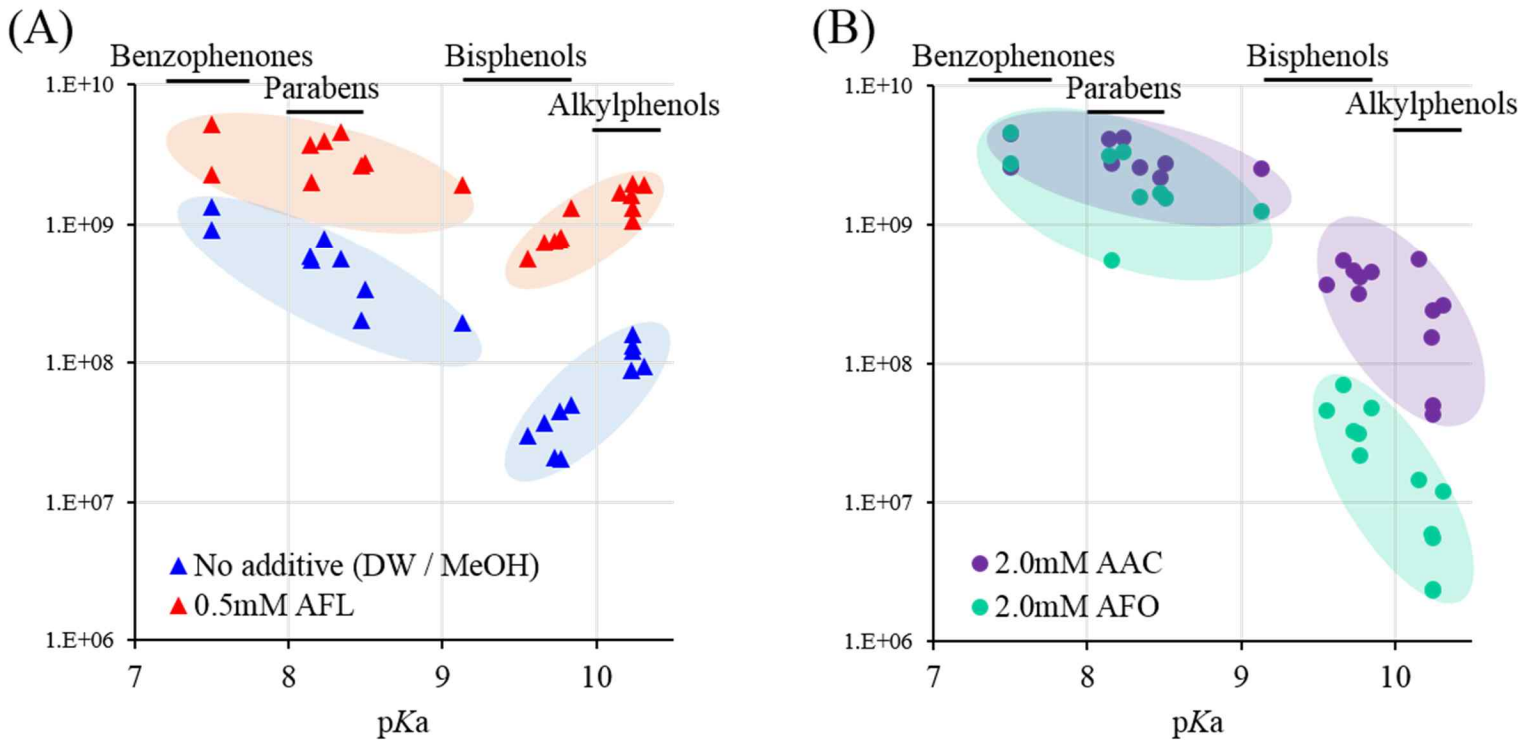

Figure 17. The relationship between the ionization efficiency and pK_a of phenols (A) in no additive and AFL, and (B) in AAC and AFO

4.3.1.4. Ion suppression and sensitivity in real urine samples

Ion suppression by the matrix in ESI is a well-known serious problem that reduces the sensitivity of analytes. Therefore, we investigated the ionization efficiency of phenols in real urine samples using mobile phases with no additive, with AAC, and with AFL.

We analyzed the real urine after sample preparation by spiked all phenols at 10 ng/mL. In the case of actual human urine samples, the concentration of all substances could not be controlled equally because they were already exposed to various environmental phenols (i.e. BP-3, MPA, etc.). Instead, the same sample vial was repeatedly analyzed according to the mobile phase condition, and the abundance according to the additive was observed to compare the degree of ion suppression.

Compared to the results of a standard mixture without a urine matrix (**Figure 15(A)**), the use of AAC in the mobile phase resulted in severe signal suppression for most phenols in a real urine sample (**Figure 18)**. Even alkylphenols were not detected, as shown in the expanded window in **Figure 18**. This is similar to results reported in other previous studies (Peng et al., 2016; Ao et al., 2021). Analysis with no additive had better sensitivity than that with AAC, which resulted in a severe suppression; furthermore, the former had a capacity to detect alkylphenols (**Figure 18**). These results explain why many studies have used mobile phases with no additive. However, in contrast to AAC, AFL improved analysis sensitivity even with a matrix effect in the urine sample. Similar to the results of the analysis of a standard mixture (**Figure 15(A)**), the signal abundance with AFL was significantly improved 3–20 times, especially for alkylphenols and bisphenols. Hence, the best mobile phase composition when analyzing real urine is 0.5 mM AFL in water and MeOH.

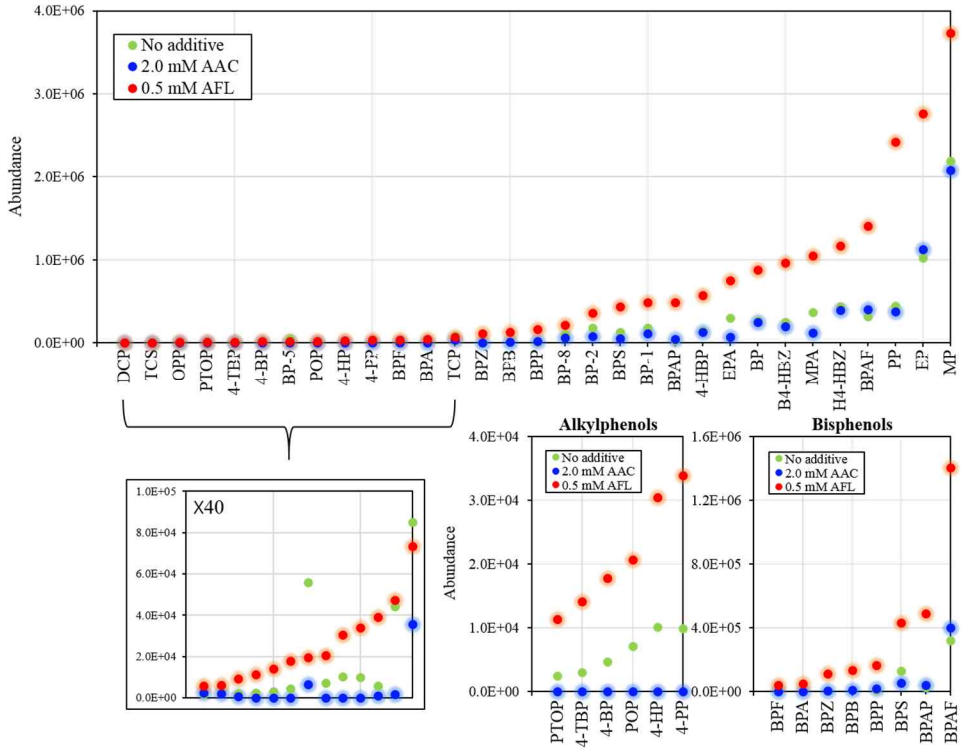

Figure 18. The ionization efficiency of phenols under no additive, AAC, and AFL condition in real urine sample. The right bottom is the expanded window for alkylphenols and bisphenols. Green, blue, and red color represent no additive, AAC, and AFL, respectively

4.3.2 Comprehensive and sensitive analytical method for multiclass phenols

4.3.2.1 Mass spectrometry and chromatography optimization

A chromatographic factor (area/height ratio) was used to evaluate the peak shape, where narrower peaks have lower values and broader peaks have higher values.

Finally, we presented a heatmap for the relative chromatographic behavior of phenols in the optimized additive concentrations as illustrated in **Figure 19**. The narrower peak has deeper blue color and broader peak has deeper red in the heatmap. Red spots were given for peaks that were not detected (e.g., those found in FA, AA, and AFO). **Figure 19(A) and (B)** presents the chromatographic factor in water/MeOH and water/ACN system, respectively. For most phenols, the peak shape was slightly sharper in the water/ACN system. However, there are more substances that cannot be detected than the water/MeOH system, indicating that the water/ACN system is not suitable for phenol analysis.

In the water/MeOH system, most of the analytes tested showed sharp and symmetrical peaks with all the additives used. In particular, AFL additive was the only condition in which red color (broader peak shape) was not seen. The chromatographic factor values with AFL as additive were between 2.4 and 5.4 showing good chromatographic behavior, except for analytes BP-5 and MPA (both with a higher factor of 7). BP-5 and MPA rather showed sharper peak shapes in FA and AA additives, but those additives were not suitable for multiclass phenols analysis because there were many substances that could not be detected. Nevertheless, there was no significant problem in quantitative analysis for BP-5 and

MPA. Therefore, on the basis of 0.5 mM AFL in water/MeOH system as phenol-specialized mobile-phase composition, we developed a comprehensive and sensitive analytical method for simultaneous quantitation of multiclass phenols in human urine. The optimized mass parameters and retention times of analytes are presented in **Table 4**.

Figure 20(A) presents the total ion chromatograms of 38 phenols under optimized conditions. Good chromatography was achieved within 15 min, without splitting, broadening, and tailing of peaks. No significant interference from the urine matrix were observed at the retention time of the analytes. **Figure 20(B)** shows structural isomers in the same selected reaction monitoring transitions, namely, isobutyl- and butylparaben, isopropyl- and propylparaben, and 2,4-DCP and 2,5-DCP. These isomers were satisfactorily separated *via* chromatography. Representative chromatograms for each phenol used in this study are shown in **Figure 21**. The chromatograms were obtained after sample preparation by spiked standard mixure of phenols at 10 ng/mL in artificial human urine.

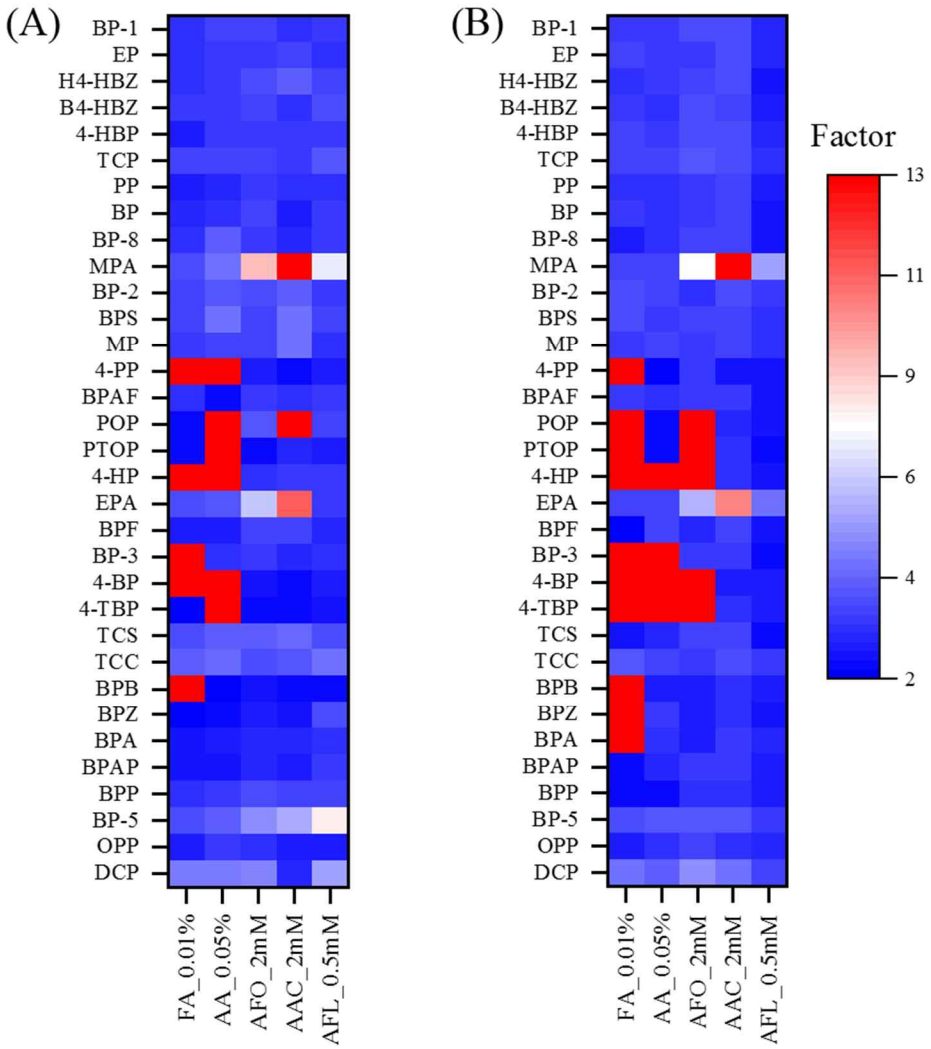

Figure 19. Heatmap of the chromatographic factors in the optimized additive concentrations in (A) water/MeOH system and (B) water/ACN system. The narrower peak (lower value) has deeper blue color and broader peak (higher value) has deeper red in the heatmap. Red spots were given for analytes that were not detected.

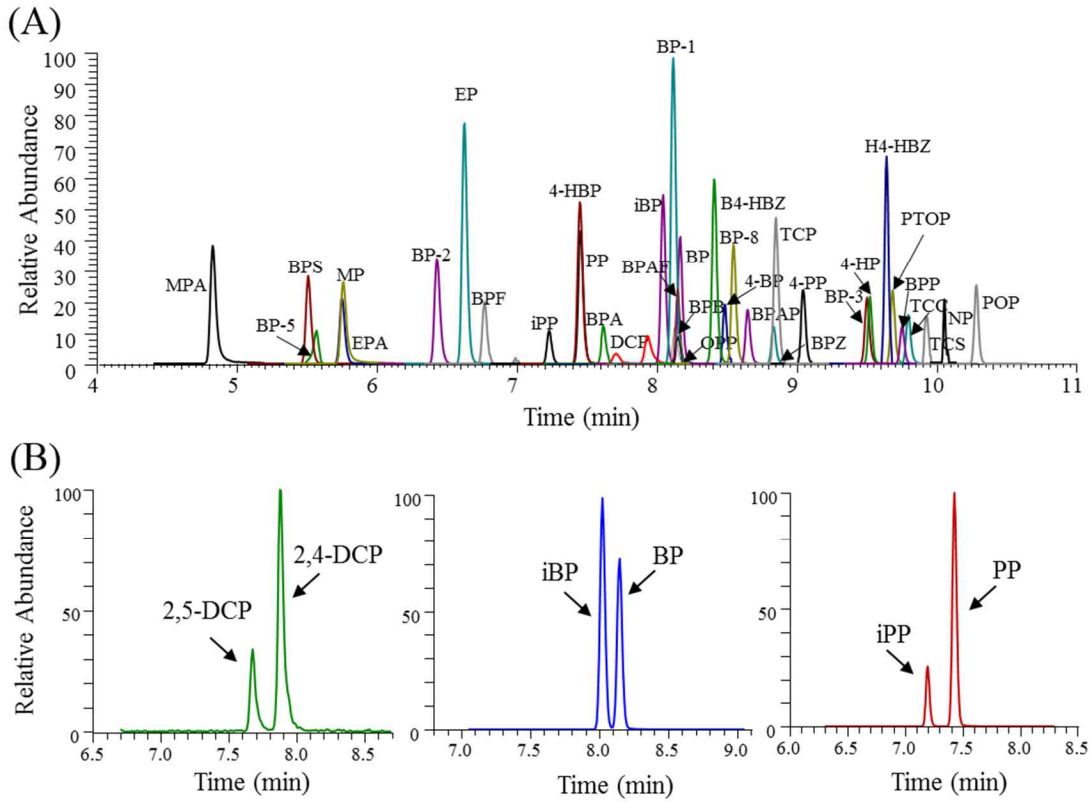

Figure 20. (A) The total ion chromatogram showing separation of 38 phenols in 15 min. (B) The optimized separation of 2,5- and 2,4-DCP; isobutylparaben (iBP) and butylparaben (BP); isopropylparaben (iPP) and propylparaben (PP) in LC–ESI–MS/M

Bisphenols

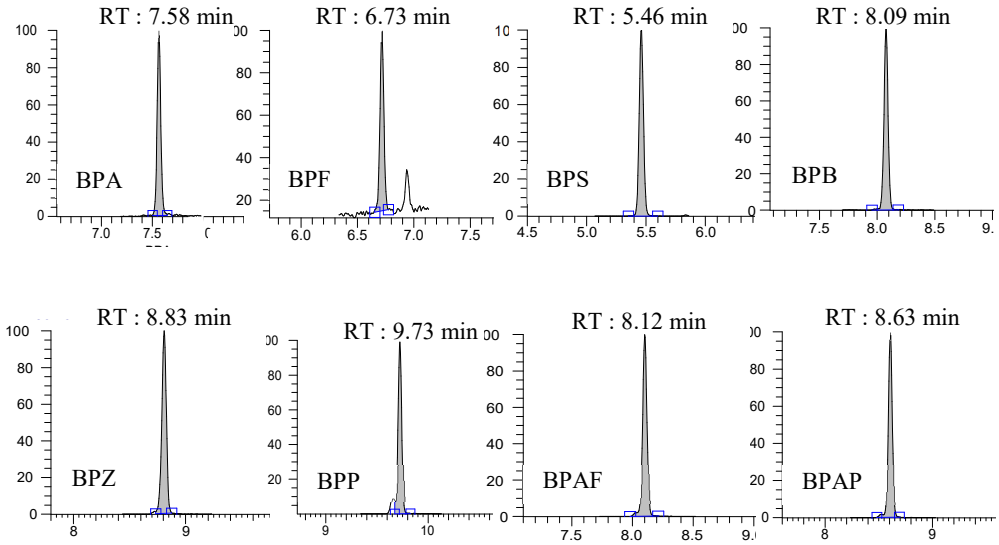

Benzophenones

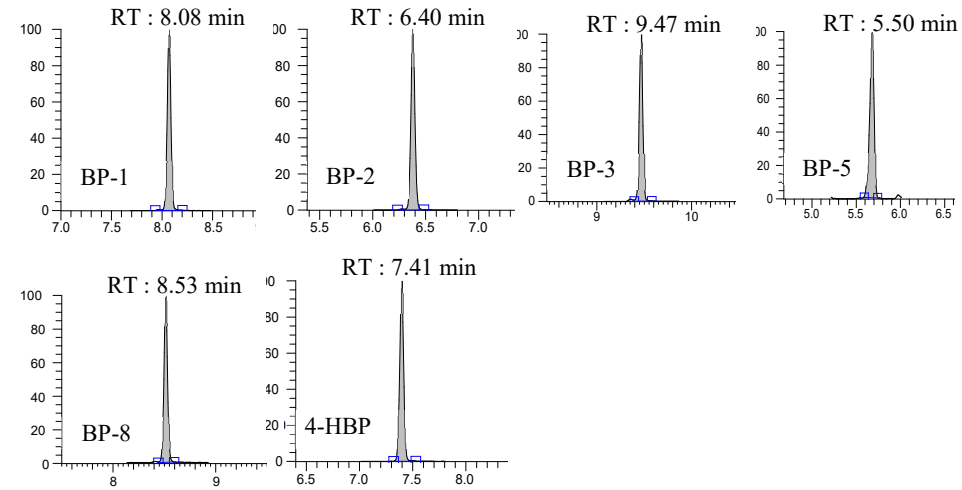

Chlorophenols

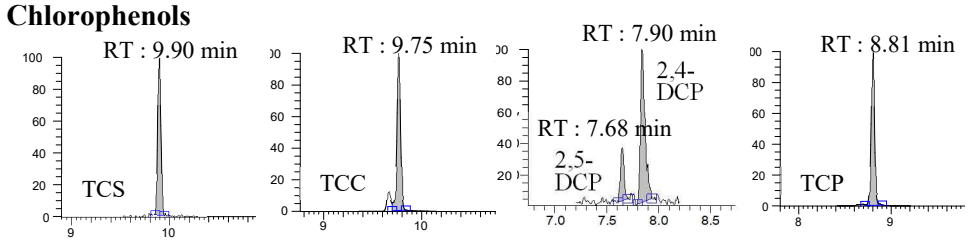

Figure 21. Representative chromatograms for each phenol at 10 ng/mL in artificial urine

Parabens

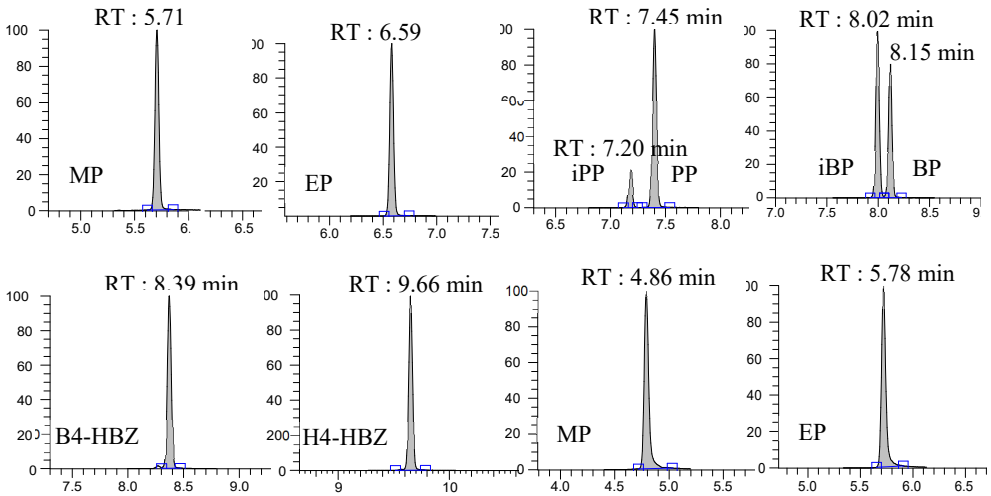

Alkylphenols

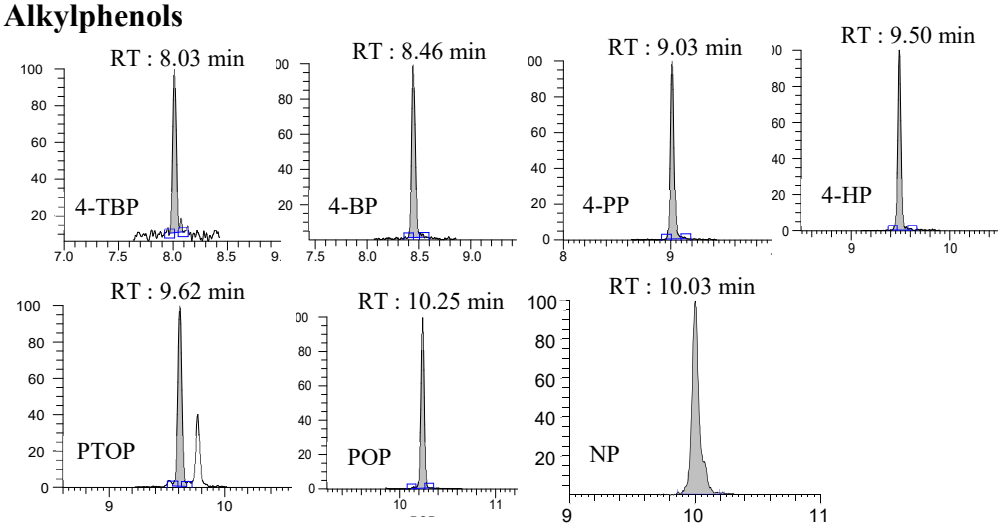

Others

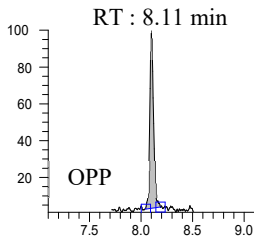

Figure 21. (Continued)

4.3.2.2. Sample preparation optimization

4.3.2.2.1 Comparison of volatility

Exposure assessment studies require not only high sensitivity but also fast and cost effective sample preparation steps. Most researchers analyzing multiple phenols have mainly used SPE or LLE after enzyme hydrolysis to achieve high sensitivity. In general, the SPE and LLE methods include an evaporation step to concentrate target analytes, which can potentially lead to uncontrolled loss of analytes, especially for volatile substances. Therefore, prior to optimizing sample preparation, we investigated the volatility of phenols using diverse evaporation conditions.

Four typical organic solvents (5 mL of MTBE, ACN, EA, and MeOH) that were fortified with 10 ng/mL of all phenols were evaluated in this experiment. Then, the samples were evaporated at three different temperature conditions (room temperature (RT), 35°C, 35°C). When use high temperature condition, the solution evaporates quickly and the sample preparation time can be shortened. However, in the case of substances with high volatility, the loss is large and the uncertainty in quantitative analysis is increased. **Table 12** shows the mean values of the evaporation recoveries for each phenol under various conditions by repeating the experiment three times.

We grouped the phenols into four classes (bisphenols, benzophenones and parabens, chlorophenols, and alkylphenols) depending on their structure. And the recovery of each compound was plotted according to the organic solvent and evaporation temperature as shown in **Figure 22**. Majority of bisphenols showed good recoveries of more than 75%, regardless of the conditions. Benzophenones and parabens had recovery values of more than 50%. However, the overall recoveries for

chlorophenols and alkylphenols were lower than 50% or showed large deviations, suggesting high volatility. The recoveries at low temperature with ACN were high for all the analytes; however, ACN is not a common extracting solvent, and the evaporation time lasted 95 min. In conclusion, SPE or LLE, including the evaporation process, should be avoided during sample preparation of multiple classes of phenols. Therefore, we adopted a simple and economical dilute and shoot assay for our developed method.

Table 12. The mean values of evaporation recoveries of phenols under various conditions (n=3)

Compounds (Abbr.)	Organic solvent for extraction with various evaporate temperature											
	MTBE			ACN			EA			MeOH		
	RT	35°C	50°C	RT	35°C	50°C	RT	35°C	50°C	RT	35°C	50°C
Bisphenols												
BPA	94.3	97.6	104.1	102.2	104.0	110.2	110.4	108.1	104.4	101.1	94.3	99.2
BPF	90.0	97.0	101.3	99.0	107.0	106.0	98.0	98.0	97.0	88.0	84.0	89.0
BPS	80.0	89.0	93.0	78.0	80.0	95.0	96.0	96.0	96.0	99.0	94.0	94.0
BPB	74.0	84.0	86.0	85.0	90.0	91.0	86.0	87.0	86.0	80.0	77.0	80.0
BPAF	85.0	92.0	93.0	100.0	105.0	107.0	100.0	99.0	96.0	94.0	91.0	90.0
BPAP	82.0	91.0	109.8	96.0	93.0	96.0	101.0	97.0	98.0	91.0	88.0	90.0
BPZ	84.0	97.0	98.0	96.0	99.0	99.0	97.0	100.0	99.0	89.0	87.0	90.0
BPP	75.0	81.0	85.0	99.0	102.0	94.0	92.0	92.0	90.0	83.0	79.0	82.0
Benzophenones & parabens												
BP-3	76.4	79.5	82.4	92.1	92.5	79.6	95.3	81.3	57.5	57.1	44.3	50.0
BP-2	87.8	93.7	104.9	101.1	104.6	70.1	107.7	101.9	97.6	74.2	62.3	75.7
4-HBP	78.0	84.0	87.0	92.0	94.0	90.0	89.0	89.0	87.0	88.0	83.0	80.0
BP-5	84.0	92.0	94.0	93.0	95.0	98.0	94.0	96.0	95.0	88.0	96.0	94.0
BP-1	79.0	84.0	90.0	103.0	106.0	90.0	92.0	92.0	89.0	85.0	79.0	76.0
BP-8	75.0	78.0	86.0	106.0	109.0	73.0	87.0	84.0	74.0	87.0	80.0	80.0
MP	67.0	72.0	70.0	110.0	109.0	73.0	89.0	75.0	51.0	61.0	52.0	53.0

RT : room temperature

Table 12. (Continued)

Compounds (Abbr.)	Organic solvent for extraction with various evaporate temperature											
	MTBE			ACN			EA			MeOH		
	RT	35°C	50°C	RT	35°C	50°C	RT	35°C	50°C	RT	35°C	50°C
Benzophenones & parabens												
EP	74.0	79.0	77.0	101.0	101.0	69.0	91.0	81.0	59.0	66.0	55.0	57.0
PP	70.0	76.0	75.0	101.0	100.0	75.0	83.0	78.0	61.0	67.0	57.0	55.0
BP	79.0	86.0	87.0	104.0	104.0	84.0	88.0	87.0	75.0	80.0	70.0	68.0
iPP	68.0	73.0	73.0	100.0	99.0	72.0	83.0	75.0	56.0	63.0	52.0	52.0
iBP	77.0	83.0	84.0	103.0	104.0	82.0	87.0	85.0	71.0	76.0	67.0	64.0
Chlorophenols												
TCS	81.2	91.7	96.3	110.7	120.7	72.8	96.6	98.1	90.6	93.5	78.8	78.8
TCC	91.9	103.8	107.4	97.0	99.5	108.4	105.3	110.2	113.6	112.8	110.4	106.9
2,5-DCP	0.0	16.2	14.1	76.9	69.9	24.9	19.9	0.0	0.0	41.8	8.9	25.4
2,4-DCP	13.8	18.1	22.9	72.5	67.0	21.5	22.1	13.2	5.6	35.2	9.6	22.6
TCP	36.2	43.8	45.1	84.8	83.2	33.2	53.7	37.9	12.9	57.6	48.1	52.4
Alkylphenols												
4-TBP	22.2	28.0	39.0	99.3	90.3	30.8	41.2	14.3	0.0	30.2	16.0	0.0
OPP	19.1	28.1	31.9	99.3	101.6	35.4	52.8	24.0	0.0	31.5	14.3	11.4
4-BP	14.3	27.5	31.1	91.3	82.6	27.4	44.3	19.2	1.5	28.2	8.1	6.1
4-PP	28.3	40.4	42.7	92.3	87.2	37.3	61.7	38.6	4.6	30.3	13.7	9.3

RT : room temperature

Table 12. (Continued)

Compounds (Abbr.)	Organic solvent for extraction with various evaporate temperature											
	MTBE			ACN			EA			MeOH		
	RT	35°C	50°C	RT	35°C	50°C	RT	35°C	50°C	RT	35°C	50°C
Alkylphenols												
4-HP	45.3	54.2	51.8	83.2	81.4	47.7	71.6	55.5	16.7	35.3	18.0	14.5
PTOP	51.1	55.0	51.3	87.3	82.5	62.1	74.3	61.6	23.2	32.6	18.9	18.5
NP	59.0	61.2	55.2	82.5	87.8	62.4	86.5	73.5	42.1	43.3	35.1	30.3
POP	47.8	50.4	44.4	58.9	61.6	45.9	67.3	61.1	34.9	33.0	25.3	18.5

RT : room temperature

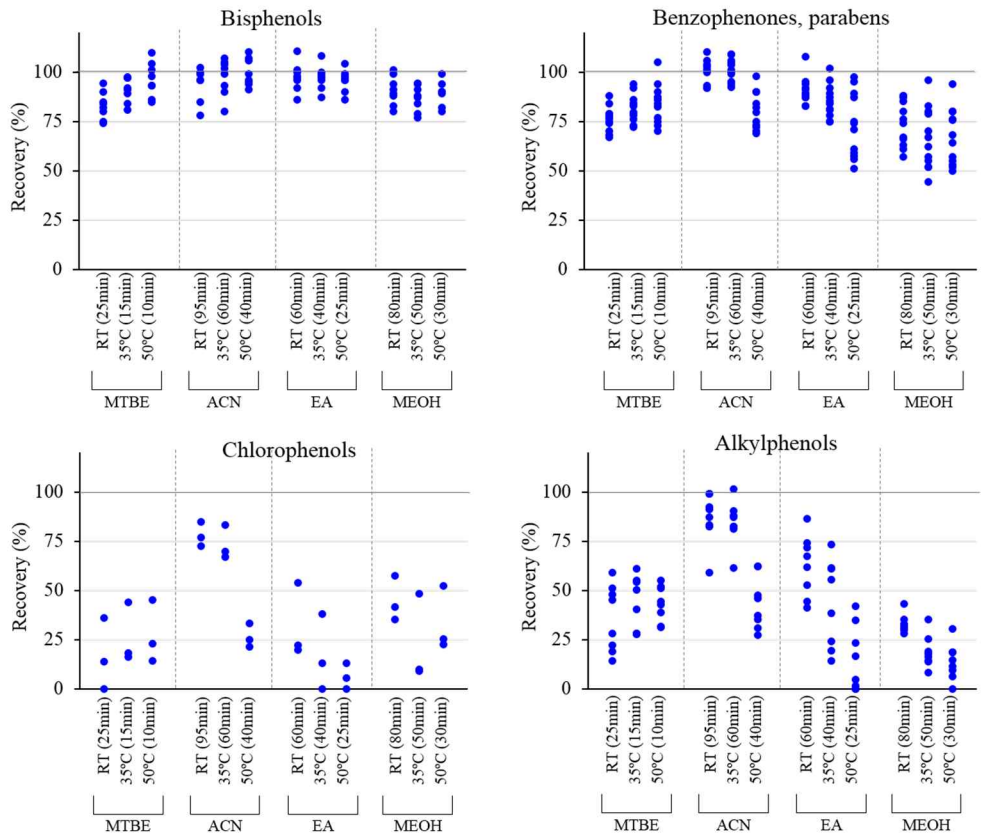

Figure 22. Recoveries of phenols by class under various evaporation conditions

4.3.2.2.2 Enzyme selection

Exogenous compounds are generally excreted as phase I or phase II metabolites such as glucuronide and sulfate conjugates form in urine. Therefore, numerous studies have been used *E. coli* β-glucuronidase or *Helix pomatia* β-glucuronidase/sulfatase in order to hydrolyze EDC metabolites. CDC NHANENS and related studies have used H-1 (Chen et al., 2012b) or H-2 (Wang et al., 2013; Yao et al., 2018) type of *Helix pomatia* β-glucuronidase/sulfatase to hydrolyze phenols and parabens. For BPA, as representative bisphenols, only less than 3 % of BPA is excreted as sulfate form in humans (Vokel et al., 2002; Thayer et al., 2015). However, the sulfate conjugate form composes about 40% of the paraben metabolites except for BP according to literature (Dewalque et al., 2014) and which means that the hydrolysis with *E. coli* β-glucuronidase is not suitable to provide accurate quantitation for parabens. In this study, we have reached the accurate quantitation result for parabens in NIST SRMs with *Helix pomatia* β-glucuronidase/sulfatase. For enzymatic hydrolysis completion, we compared different conditions (37°C for overnight *vs* 55°C for 2 hr) of this step with using analysis of pooled urine sample repeatedly. There was no significant difference of the concentration of bisphenols and parabens between two conditions (data were not shown). Therefore, we adapted 55°C for 2 hr condition to save the time. Additionally, we have also monitored enzyme hydrolysis marker by adding 4-methylumbelliferryl glucuronide into the internal standard mixture solution.

4.3.2.2.3 Contamination control

The other major issue of quantitation of environmental phenols is exogenous contamination during sample preparation, affecting the accuracy and precision of quantitation results to analysis of phenols. As mentioned earlier, environmental phenols are ubiquitous in various plastic products including laboratory supplies as well as even in the air (Sanchis et al., 2019). The background contamination that occur in analytical procedure might cause wrong accumulation of longitudinal data in human exposome study. Accurate quantitation of the trace level of target analytes is still of importance in exposome study, because even low level of environmental exposures are probably vulnerable when people are constantly exposed to environmental toxic substances (Li et al., 2019a; Li et al., 2019c).

An initial effort to minimize exogenous contamination, all laboratory plastic wares were avoided during sample handling. All glassware were washed with 1% of detergent water and pure water, and rinsed with acetone and covered with an aluminum foil. We also observed notable contamination of water solvent obtained from a lavoratory Milli-Q-filtration system. To avoid these contamination, all solvents for sample preparation and mobile phase were replaced with ultrapure HPLC grade water. After glassware wash and high purity solvents change, phenols and parabens, especially for BPA, was dramatically eliminated to about 40-95% (**Table 13**). Any remaining background concentrations of target chemicals were insignificant. In our preliminary experiments, however, PA (3,4-dihydroxybenzoic acid) and 4-HBA (4-hydroxybenzoic acid) were found in hundreds to thousands of ng/mL in the *Helix pomatia* β-glucuronidase/sulfatase. Thus, those compounds were excluded from the analysis.

Table 13. Relative background contamination (%)

Compounds (Abbr.)	Before change	Glassware wash & solvent change
BPA	100	4
BP-3	100	60
MP	100	11
EP	100	30
PP	100	24
BP	100	23
TCC	100	25

4.3.3 Method performance

4.3.3.1. Method validation

We validated our method by analyzing artificial human urine samples, and the results are shown in **Table 14-16**. The intra- and inter-day accuracies and precisions for the target analytes were obtained by evaluating three different concentrations of QC samples (LQC, MQC, and HQC) as shown in **Table 14** and **15**. The accuracy values for all the analytes were between 85.4% and 113.0%, and the precision values were between 0.4% and 14.6%. These values satisfied the criteria for all of the QC levels (Walfish, 2006). Other validation results including linearity, LOD, LOQ, and matrix effect are represented in **Table 16**. The R^2 values obtained for all the calibration curves for the 38 analytes were more than 0.99 providing good linearity. The LOD values were between 0.03 and 0.33 ng/mL, and the LOQ values were between 0.10 and 0.99 ng/mL. Considering the previously reported human exposome data (Yang et al., 2014; Zhou et al., 2014; Ye et al., 2015; Bocato et al., 2020), our LODs were acceptable for simultaneous determination of phenols including alkylphenols. The values of matrix effect ranged from 84.8% to 120.8% at 20 ng/mL of spiked levels. Matrix effect is expressed as the percentage enhancement (>100%) or suppression (<100%). According to the literature (Walorczyk, 2014), the determination of matrix effect in the range between 80% and 120% is considered as insignificant. For this study, 32 phenols showed insignificant influence of the matrix effect. On the other hand, strong signal enhancement for BP-5, MPA, EPA, and BPP and signal suppression for BPS and 2,4-DCP were observed. Inclusion of isotope-labelled ISTD 13C12-BPS allowed matrix effect correction and enabled

accurate analysis of BPS in urine. Therefore, the matrix effect can be greatly improved when the stable isotope-labelled ISTDs for other substances are available.

Table 14. Validation results of environmental phenols in human urine for intra-day assay (n=5)

Compounds (Abbr.)	Spiked Conc. (ng/mL)	Intra-day (n=5)					Mean	Accuracy (%)	Precision (%)
		Batch-1	Batch-2	Batch-3	Batch-4	Batch-5			
	0.5	0.53	0.50	0.52	0.48	0.53	0.51	102.0	3.9
BPA	20	18.2	18.0	18.0	18.0	18.0	18.0	90.2	0.5
	200	200	202	200	200	200	200	100.2	0.4
	0.5	0.50	0.48	0.53	0.49	0.48	0.49	98.8	4.5
BPF	20	18.0	17.4	17.6	18.0	17.4	17.7	88.4	1.7
	200	200	202	198	200	204	201	100.4	1.1
	0.5	0.53	0.54	0.55	0.54	0.54	0.54	108.0	1.3
BPS	20	19.0	18.8	18.8	19.0	18.8	18.9	94.4	0.6
	200	202	202	202	202	198	201	100.6	0.9
	0.5	0.48	0.49	0.53	0.50	0.51	0.50	99.8	3.4
BPB	20	22.0	22.0	22.0	21.8	22.2	22.0	110.0	0.6
	200	214	208	210	214	212	212	105.8	1.2
	0.5	0.45	0.45	0.46	0.46	0.46	0.45	90.4	1.0
BPZ	20	18.2	18.8	18.4	18.4	18.2	18.4	92.0	1.3
	200	186	192	192	188	188	189	94.6	1.4
	0.5	0.46	0.44	0.42	0.44	0.44	0.44	87.2	3.3
BPP	20	19.4	19.2	19.6	19.2	18.8	19.2	96.2	1.5
	200	204	200	202	202	200	202	100.8	0.8

Table 14. (Continued)

Compounds (Abbr.)	Spiked Conc. (ng/mL)	Intra-day (n=5)					Mean	Accuracy (%)	Precision (%)
		Batch-1	Batch-2	Batch-3	Batch-4	Batch-5			
	0.5	0.46	0.45	0.45	0.45	0.45	0.45	89.8	0.9
BPAF	20	20.2	20.6	20.4	20.0	20.6	20.4	101.8	1.3
	200	206	206	198	202	206	204	101.8	1.8
	0.5	0.57	0.56	0.51	0.51	0.50	0.53	105.8	5.8
BPAP	20	18.4	18.4	18.2	18.0	18.4	18.3	91.4	1.0
	200	194	196	196	192	192	194	97.0	1.0
	0.5	0.51	0.49	0.51	0.51	0.49	0.50	100.0	2.3
BP-1	20	20.4	19.8	20.2	20.2	20.2	20.2	100.8	1.1
	200	228	224	224	226	228	226	113.0	0.9
	0.5	0.44	0.44	0.44	0.45	0.45	0.44	87.8	1.2
BP-2	20	22.0	21.4	21.8	22.0	22.2	21.9	109.4	1.4
	200	220	214	218	218	218	218	108.8	1.0
	0.5	0.51	0.50	0.50	0.51	0.49	0.50	100.0	1.6
BP-3	20	20.4	20.2	20.2	20.2	20.4	20.3	101.4	0.5
	200	202	200	202	198	200	200	100.2	0.8
	0.5	0.43	0.43	0.43	0.43	0.43	0.43	85.4	0.6
BP-5	20	17.2	17.2	17.0	17.2	17.0	17.1	85.6	0.6
	200	190	206	194	192	194	195	97.6	3.2

Table 14. (Continued)

Compounds (Abbr.)	Spiked Conc. (ng/mL)	Intra-day (n=5)					Mean	Accuracy (%)	Precision (%)
		Batch-1	Batch-2	Batch-3	Batch-4	Batch-5			
	0.5	0.44	0.46	0.45	0.50	0.46	0.46	92.2	5.0
BP-8	20	17.0	16.8	17.0	17.0	17.0	17.0	85.8	2.2
	200	174	176	180	178	176	177	88.4	1.3
	0.5	0.57	0.47	0.50	0.55	0.48	0.51	102.4	8.5
4-HBP	20	22.6	22.2	22.2	22.2	22.4	22.3	111.6	0.8
	200	220	218	220	220	222	220	110.0	0.6
	0.5	0.54	0.52	0.54	0.54	0.52	0.53	106.0	1.8
MP	20	19.6	19.2	19.4	19.4	19.6	19.4	97.2	0.9
	200	196	202	196	196	196	197	98.6	1.4
	0.5	0.54	0.53	0.53	0.53	0.53	0.53	105.8	0.8
EP	20	19.2	19.0	19.4	19.2	19.4	19.2	96.2	0.9
	200	198	198	196	198	200	198	99	0.7
	0.5	0.47	0.48	0.48	0.47	0.48	0.47	94.6	1.6
PP	20	18.6	18.8	18.8	18.8	18.8	18.8	93.8	0.5
	200	196	202	202	196	198	199	99.4	1.5
	0.5	0.55	0.52	0.54	0.55	0.53	0.54	107.0	2.0
BP	20	18.8	19.0	19.0	19.0	19.0	19.0	94.8	0.5
	200	196	202	202	202	202	201	100.4	1.3

Table 14. (Continued)

Compounds (Abbr.)	Spiked Conc. (ng/mL)	Intra-day (n=5)					Mean	Accuracy (%)	Precision (%)
		Batch-1	Batch-2	Batch-3	Batch-4	Batch-5			
	0.5	0.50	0.50	0.49	0.50	0.49	0.49	98.8	1.7
iPP	20	19.0	18.6	18.6	18.8	18.6	18.7	93.6	1.0
	200	218	224	224	224	222	222	111.2	1.2
	0.5	0.46	0.48	0.46	0.46	0.46	0.46	92.6	1.4
iBP	20	19.0	19.0	19.2	19.0	19.0	19.0	95.2	0.5
	200	210	208	210	210	210	210	104.8	0.4
	0.5	0.47	0.55	0.47	0.59	0.55	0.53	105.2	10.2
4-TBP	20	20.2	19.0	20.2	20.0	20.8	20.0	100.2	3.3
	200	206	202	194	196	200	200	99.8	2.4
	0.5	0.49	0.58	0.52	0.48	0.48	0.51	102.0	8.3
OPP	20	19.8	19.2	19.8	19.6	20.8	19.8	99.2	3.0
	200	198	200	200	198	198	199	99.4	0.6
	0.5	0.46	0.55	0.55	0.55	0.46	0.51	102.4	9.7
4-BP	20	20.4	19.4	20.6	20.4	20.4	20.2	101.2	2.4
	200	196	200	200	194	194	197	98.4	1.5
	0.5	0.46	0.55	0.55	0.55	0.46	0.51	91.4	7.4
4-PP	20	20.4	19.4	20.6	20.4	20.4	20.2	86.0	2.7
	200	196	200	200	194	194	197	96.4	3.5

Table 14. (Continued)

Compounds (Abbr.)	Spiked Conc. (ng/mL)	Intra-day (n=5)					Mean	Accuracy (%)	Precision (%)
		Batch-1	Batch-2	Batch-3	Batch-4	Batch-5			
	0.5	0.44	0.43	0.43	0.45	0.44	0.44	87.4	1.9
4-HP	20	17.8	18.0	18.2	18.4	18.8	18.2	91.2	2.1
	200	192	192	202	206	206	200	99.8	3.6
	0.5	0.47	0.50	0.49	0.51	0.51	0.49	98.8	3.2
PTOP	20	21.0	21.6	22.2	21.8	20.2	21.4	106.8	3.7
	200	220	220	216	208	212	215	107.6	2.4
	0.5	0.46	0.48	0.46	0.46	0.51	0.47	94.0	4.8
NP	20	20.4	20.0	19.6	19.0	19.2	19.6	98.2	2.9
	200	188	206	186	184	194	192	95.8	4.6
	0.5	0.48	0.43	0.49	0.47	0.47	0.47	93.0	4.5
POP	20	17.2	16.8	18.0	17.0	17.2	17.2	86.2	2.6
	200	186	148	182	188	186	178	89.0	9.5
	0.5	0.53	0.54	0.52	0.53	0.52	0.53	105.2	1.2
MPA	20	19.0	18.4	18.6	18.8	18.8	18.7	93.6	1.2
	200	196	204	204	204	204	202	101.2	1.8
	0.5	0.50	0.49	0.48	0.48	0.48	0.48	96.6	1.9
EPA	20	19.8	19.8	19.6	19.8	19.6	19.7	98.6	0.6
	200	214	210	210	212	212	212	105.8	0.8

Table 14. (Continued)

Compounds (Abbr.)	Spiked Conc. (ng/mL)	Intra-day (n=5)					Mean	Accuracy (%)	Precision (%)
		Batch-1	Batch-2	Batch-3	Batch-4	Batch-5			
TCS	0.5	0.53	0.51	0.50	0.55	0.55	0.53	105.0	3.9
	20	17.0	17.2	17.8	17.6	17.6	17.4	87.2	1.9
	200	194	196	200	204	198	198	99.2	1.9
TCC	0.5	0.55	0.49	0.50	0.52	0.51	0.51	102.2	4.3
	20	21.8	22.0	22.0	21.8	21.8	21.9	109.4	0.5
	200	220	222	224	220	206	218	109.2	3.3
B4-HBZ	0.5	0.47	0.47	0.49	0.49	0.47	0.48	95.2	2.3
	20	20.0	20.2	20.2	20.0	20.0	20.1	100.4	0.5
	200	198	212	200	194	196	200	100.0	3.5
H4-HBZ	0.5	0.44	0.44	0.43	0.43	0.43	0.43	86.2	1.0
	20	20.2	20.2	20.4	20.0	20.2	20.2	101.0	0.7
	200	214	214	210	212	212	212	106.2	0.8
2,4-DCP	0.5	0.53	0.59	0.57	0.54	0.50	0.54	108.8	6.9
	20	22.2	23.0	22.6	21.8	20.8	22.1	110.4	3.8
	200	210	230	210	212	214	215	107.6	3.9
2,5-DCP	2	1.98	2.26	1.84	2.00	1.92	2.00	100.0	7.9
	20	20.8	21.8	20.2	21.4	19.6	20.8	103.8	4.3
	200	186	184	176	168	170	177	88.4	4.6
2,4,5- & 2,4,6-TCP	0.5	0.42	0.44	0.45	0.46	0.45	0.44	88.0	4.2
	20	17.0	17.4	17.0	17.2	17.4	17.2	86.0	1.2
	200	174	178	174	178	176	176	88.0	1.1

Table 15. Validation results of environmental phenols in human urine for inter-day assay (n=5)

Compounds (Abbr.)	Spiked Conc. (ng/mL)	Inter-day (n=5)					Mean	Accuracy (%)	Precision (%)
		Day-1	Day-2	Day-3	Day-4	Day-5			
	0.47	0.52	0.49	0.49	0.51	0.53	100.2	4.5	0.47
BPA	18.2	18.4	17.4	17.8	17.4	18.2	89.6	2.7	18.2
	184	178	220	216	186	200	96.8	8.7	184
	0.48	0.53	0.49	0.53	0.50	0.50	100.6	4.3	0.48
BPF	19.2	19.0	18.0	18.2	18.0	18.5	92.4	3.1	19.2
	196	194	192	192	200	195	97.4	1.7	196
	0.58	0.45	0.57	0.45	0.53	0.51	102.6	12.6	0.58
BPS	18.4	17.4	17.4	17.2	19.0	17.9	89.4	4.4	18.4
	200	190	200	192	202	197	98.4	2.7	200
	0.46	0.45	0.45	0.45	0.48	0.46	91.2	3.0	0.46
BPB	23.0	23.0	20.6	18.8	22.0	21.5	107.4	8.3	23.0
	214	216	188	212	214	209	104.4	5.6	214
	0.43	0.45	0.47	0.44	0.45	0.45	89.0	2.9	0.43
BPZ	22.8	22.6	19.4	20.2	18.2	20.6	103.2	9.7	22.8
	214	222	186	208	186	203	101.6	8.1	214
	0.46	0.57	0.55	0.49	0.46	0.50	100.6	10.4	0.46
BPP	21.4	17.0	17.6	17.2	19.4	18.5	92.6	10.1	21.4
	204	192	212	188	204	200	100.0	4.9	204

Table 15. (Continued)

Compounds (Abbr.)	Spiked Conc. (ng/mL)	Inter-day (n=5)					Mean	Accuracy (%)	Precision (%)
		Day-1	Day-2	Day-3	Day-4	Day-5			
	0.5	0.45	0.44	0.44	0.44	0.46	0.44	88.4	1.9
BPAF	20	22.8	22.6	21.2	19.4	20.2	21.2	106.2	7.0
	200	206	204	206	212	206	207	103.4	1.5
	0.5	0.52	0.58	0.57	0.48	0.41	0.51	101.8	13.4
BPAP	20	21.6	20.6	18.2	18.4	18.4	19.4	97.2	8.0
	200	212	194	182	198	194	196	98.0	5.5
	0.5	0.55	0.43	0.43	0.44	0.51	0.47	93.8	11.7
BP-1	20	23.0	23.0	20.4	19.8	23.6	22.0	109.8	7.9
	200	210	204	186	188	228	203	101.6	8.5
	0.5	0.57	0.57	0.53	0.43	0.44	0.51	101.0	13.6
BP-2	20	22.6	22.0	19.0	22.0	22.0	21.5	107.6	6.7
	200	212	196	192	204	220	205	102.4	5.6
	0.5	0.51	0.53	0.50	0.46	0.51	0.50	99.6	4.8
BP-3	20	18.2	17.8	17.8	17.0	20.4	18.2	91.2	7.0
	200	182	190	182	198	202	191	95.4	4.8
	0.5	0.49	0.57	0.43	0.45	0.50	0.49	97.0	11.5
BP-5	20	20.0	20.0	17.2	18.0	17.2	18.5	92.4	7.7
	200	218	212	190	188	198	201	100.6	6.6

Table 15. (Continued)

Compounds (Abbr.)	Spiked Conc. (ng/mL)	Inter-day (n=5)					Mean	Accuracy (%)	Precision (%)
		Day-1	Day-2	Day-3	Day-4	Day-5			
	0.5	0.47	0.53	0.42	0.50	0.44	0.47	93.8	9.5
BP-8	20	19.8	20.4	17.2	18.6	17.0	18.6	93.0	8.2
	200	212	206	178	196	174	193	96.6	8.7
	0.5	0.44	0.46	0.56	0.50	0.57	0.51	101.0	11.7
4-HBP	20	23.4	23.0	18.8	19.4	22.6	21.4	107.2	10.1
	200	210	200	218	206	220	211	105.4	3.9
	0.5	0.49	0.55	0.42	0.45	0.54	0.49	97.6	11.2
MP	20	17.4	17.0	17.4	17.4	19.6	17.8	88.8	5.9
	200	180	170	196	208	196	190	95.0	7.9
	0.5	0.58	0.58	0.43	0.45	0.54	0.51	102.4	13.7
EP	20	17.6	17.8	18.2	17.4	19.2	18.0	90.2	4.0
	200	192	196	204	198	198	198	98.8	2.2
	0.5	0.57	0.51	0.43	0.44	0.47	0.48	96.4	11.8
PP	20	18.4	18.2	17.4	17.2	18.6	18.0	89.8	3.5
	200	200	198	198	192	196	197	98.4	1.5
	0.5	0.50	0.56	0.43	0.43	0.55	0.49	98.6	12.5
BP	20	18.0	18.2	18.2	17.4	18.8	18.1	90.6	2.8
	200	196	192	214	196	196	199	99.4	4.4

Table 15. (Continued)

Compounds (Abbr.)	Spiked Conc. (ng/mL)	Inter-day (n=5)					Mean	Accuracy (%)	Precision (%)
		Day-1	Day-2	Day-3	Day-4	Day-5			
	0.5	0.53	0.51	0.50	0.47	0.50	0.50	99.6	4.4
iPP	20	20.2	20.6	17.6	18.2	19.0	19.1	95.6	6.7
	200	210	204	188	198	218	204	101.8	5.6
	0.5	0.45	0.49	0.42	0.43	0.46	0.45	89.6	6.0
iBP	20	22.8	22.2	21.0	19.4	19.0	20.9	104.4	8.0
	200	210	198	202	188	210	202	100.8	4.6
	0.5	0.54	0.48	0.45	0.50	0.47	0.49	97.4	6.6
4-TBP	20	21.2	18.6	20.4	17.4	20.2	19.6	97.8	7.8
	200	208	176	202	202	206	199	99.4	6.5
	0.5	0.53	0.57	0.53	0.46	0.49	0.51	102.8	8.5
OPP	20	17.4	19.4	17.2	18.6	19.8	18.5	92.4	6.3
	200	176	176	210	196	198	191	95.6	7.8
	0.5	0.50	0.43	0.52	0.44	0.46	0.47	93.6	8.6
4-BP	20	17.0	17.6	17.0	17.0	20.4	17.8	89.0	8.3
	200	174	186	186	198	196	188	94.0	5.1
	0.5	0.57	0.48	0.45	0.50	0.48	0.49	98.4	9.1
4-PP	20	19.0	17.4	16.8	17.6	16.4	17.4	87.2	5.7
	200	224	194	190	206	170	197	98.4	10.2

Table 15. (Continued)

Compounds (Abbr.)	Spiked Conc. (ng/mL)	Inter-day (n=5)					Mean	Accuracy (%)	Precision (%)
		Day-1	Day-2	Day-3	Day-4	Day-5			
	0.5	0.56	0.52	0.48	0.43	0.44	0.48	96.4	11.7
4-HP	20	16.6	19.0	17.4	17.0	17.8	17.6	87.8	5.2
	200	202	224	192	204	192	203	101.4	6.5
	0.5	0.54	0.56	0.45	0.50	0.47	0.50	100.6	9.2
PTOP	20	19.6	22.2	18.2	18.2	21.0	19.8	99.2	8.9
	200	202	220	188	180	220	202	101.0	9.0
	0.5	0.51	0.56	0.46	0.52	0.54	0.51	102.8	7.6
NP	20	18.4	19.2	20.4	20.2	19.0	19.4	97.2	4.3
	200	188	222	188	186	170	191	95.4	10.0
	0.5	0.47	0.46	0.42	0.45	0.48	0.45	90.4	4.7
POP	20	17.8	17.0	17.2	18.2	17.2	17.5	87.4	2.9
	200	194	230	212	200	186	204	102.2	8.4
	0.5	0.44	0.58	0.50	0.46	0.53	0.50	99.4	11.2
MPA	20	17.4	17.2	17.8	17.8	19.0	17.8	89.2	3.9
	200	200	190	216	212	196	203	101.4	5.4
	0.5	0.57	0.57	0.47	0.51	0.50	0.52	104.2	8.5
EPA	20	17.4	18.0	17.4	18.6	19.8	18.2	91.2	5.5
	200	188	188	188	214	214	198	99.2	7.2

Table 15. (Continued)

Compounds (Abbr.)	Spiked Conc. (ng/mL)	Inter-day (n=5)					Mean	Accuracy (%)	Precision (%)
		Day-1	Day-2	Day-3	Day-4	Day-5			
TCS	0.5	0.46	0.43	0.51	0.50	0.53	0.48	96.6	8.4
	20	18.4	17.2	17.4	17.4	17.0	17.5	87.4	3.1
	200	176	176	202	198	194	189	94.6	6.5
TCC	0.5	0.43	0.43	0.47	0.42	0.55	0.46	91.2	11.7
	20	22.6	22.2	21.8	19.4	23.8	22.0	109.8	7.4
	200	216	216	196	188	220	207	103.6	6.9
B4-HBZ	0.5	0.54	0.43	0.52	0.43	0.47	0.48	95.0	10.4
	20	20.0	20.6	17.8	19.6	20.0	19.6	98.0	5.4
	200	198	210	192	208	198	201	100.6	3.8
H4-HBZ	0.5	0.45	0.53	0.55	0.43	0.44	0.48	95.4	12.2
	20	22.8	18.0	17.4	18.6	20.2	19.4	97.0	11.2
	200	204	192	194	214	214	204	101.8	5.2
2,4-DCP	0.5	0.46	0.53	0.47	0.56	0.53	0.51	101.2	8.2
	20	18.6	19.0	19.0	19.8	22.2	19.7	98.6	7.4
	200	172	174	194	202	210	190	95.2	8.9
2,5-DCP	2	1.90	2.30	2.24	2.28	1.98	2.14	107.0	8.7
	20	21.0	18.2	20.2	21.0	20.8	20.2	101.2	5.9
	200	212	190	204	212	186	201	100.4	6.1
2,4,5- & 2,4,6-TCP	0.5	0.58	0.57	0.42	0.52	0.43	0.50	100.2	14.6
	20	20.6	18.6	17.0	17.2	16.8	18.0	90.2	8.8
	200	218	190	178	194	174	191	95.4	9.1

Table 16. Validation results of environmental phenols in human urine for linearity, LOD, LOQ, and matrix effect

Compounds (Abbr.)	Dynamic Range (ng/mL)	LOD (ng/mL)	LOQ (ng/mL)	R^2	Matrix Effect (%)
BPA	0.05-500	0.08	0.24	0.9996	8.6
BPF	0.05-500	0.10	0.31	0.9993	6.6
BPS	0.05-500	0.07	0.21	0.9994	6.4
BPB	0.05-500	0.10	0.29	0.9943	0.1
BPZ	0.05-500	0.12	0.37	0.9961	8.8
BPP	0.05-500	0.13	0.39	0.9998	2.0
BPAF	0.05-500	0.11	0.33	0.9987	14.6
BPAP	0.05-500	0.13	0.39	0.9992	3.1
BP-1	0.05-500	0.06	0.18	0.9941	10.4
BP-2	0.05-500	0.10	0.31	0.9978	26.3
BP-3	0.05-500	0.03	0.10	0.9995	5.5
BP-5	0.05-500	0.13	0.39	0.9906	67.6
BP-8	0.05-500	0.07	0.20	0.9973	26.2
4-HBP	0.05-500	0.06	0.19	0.9952	5.2
MP	0.05-500	0.09	0.27	0.9996	5.2
EP	0.05-500	0.11	0.33	0.9997	6.9
PP	0.05-500	0.05	0.16	0.9995	6.9
BP	0.05-500	0.10	0.30	0.9996	4.9
iPP	0.05-500	0.12	0.37	0.9941	9.3
iBP	0.05-500	0.12	0.37	0.9998	10.0
4-TBP	0.50-500	0.16	0.49	0.9995	-45.9
OPP	0.05-500	0.13	0.39	0.9990	-34.9
4-BP	0.05-500	0.14	0.44	0.9995	-41.4
4-PP	0.20-500	0.15	0.47	0.9993	-13.7
4-HP	0.20-500	0.16	0.48	0.9988	23.2
PTOP	0.05-500	0.13	0.38	0.9980	81.4
NP	0.05-500	0.16	0.48	0.9929	64.8
POP	0.05-500	0.17	0.50	0.9941	61.2
MPA	0.20-500	0.12	0.37	0.9992	104.2
EPA	0.05-500	0.12	0.36	0.9994	82.1
TCS	0.50-500	0.15	0.46	0.9989	4.6
TCC	0.05-500	0.13	0.39	0.9913	11.5
B4-HBZ	0.05-500	0.09	0.27	0.9998	14.8
H4-HBZ	0.05-500	0.11	0.33	0.9982	2.9
2,4-DCP	0.10-500	0.14	0.43	0.9886	-50.1
2,5-DCP	1.00-500	0.33	0.99	0.9951	-79.4
TCP	0.05-500	0.08	0.26	0.9996	-52.0

4.3.3.2. Accuracy verification using NIST SRM urines

Although the accuracy and precision of our developed method was satisfactory, its ability to analyze real urine sample may not be accurate because the artificial urine used in the validation experiment has different characteristics from real urine. Therefore, we tested method accuracy in NIST SRM samples, which have certified values. We consider the results of this test as a more important indicator of quantitation accuracy.

Table 17 shows the accuracy and precision results (n=5) for the detected phenols in the NIST SRM samples. The results indicated high accuracy (from 92.7% to 111%) with good precision (from 2.20% to 8.14%) for certified substances. Although the NIST SRMs provided certified values only for eight phenols, we could detect other additional 18 phenols including several alkylphenols due to the high sensitivity of our method. The detailed concentrations for these additional phenols are in **Table 18**. Based on these results, we provided the relative concentration profile of multiclass phenols in NIST SRM 3672 and 3673 (**Figure 23**). In both SRM samples, benzophenones (BP-1 and BP-3), which are the main components of sunscreen, had the highest percentage, followed by parabens, which are widely used as a preservative. For BP-1, the concentration was 40–50 ng/mL, which was much higher than that of other phenols. The concentration of BP-1 is associated with BP-3 metabolism. Considering a previous report (Ye et al., 2015) and the concentration of BP-3 in the NIST SRM samples, this result seems to be quite reliable.

Based on the detection of additional phenols, we expect that our method can play an important role in exposure research fields. Overall, the results suggest that our developed method is sufficiently sensitive and accurate to simultaneously identify and quantify multiple classes of phenols in real urine.

Table 17. Accuracy and precision results for certified substance in NIST SRM 3672 (Smokers' urine) and NIST SRM 3673 (Nonsmokers' urine)

Compounds (Abbr.)	SRM	Certified Value (ng/mL)	Inter-day (n=5)					Mean	Accuracy (%)	Precision (%)
			Day-1	Day-2	Day-3	Day-4	Day-5			
BPA	3672	3.11	3.41	3.42	2.86	3.42	3.08	3.24	104.0	7.91
	3673	2.00	2.30	2.28	2.25	2.21	1.87	2.18	109.1	8.14
BP-3	3672	195	197	202	189	182	191	192.3	98.6	4.10
	3673	279	270	282	273	266	275	273.2	97.9	2.20
MP	3672	115	125	119	129	122	121	123.3	107.2	3.14
	3673	81.0	86.8	82.4	92.7	91.2	88.9	88.4	109.1	4.60
EP	3672	8.27	8.27	8.42	8.25	8.00	7.40	8.07	97.6	4.98
	3673	10.5	9.99	10.28	10.66	10.40	9.31	10.1	96.5	5.07
PP	3672	17.9	20.0	20.1	19.6	18.9	18.1	19.3	108.0	4.29
	3673	22.0	24.2	24.4	24.4	23.6	21.7	23.6	107.4	4.89
BP	3672	11.3	12.9	12.6	12.7	12.6	12.0	12.6	111.1	2.80
	3673	1.13	1.09	1.02	1.12	1.02	0.99	1.05	92.7	5.32
TCS	3672	18.0	18.0	17.8	19.5	17.3	16.4	17.8	98.9	6.31
	3673	6.39	5.83	6.77	6.66	6.15	5.90	6.26	98.0	6.95
2,5-DCP	3672	1.80	1.90	1.94	1.94	1.85	2.06	1.94	107.6	4.01

Table 18. The concentration and precision results for other detected substances in NIST SRM 3672 (Smokers' urine) and NIST SRM 3673 (Nonsmokers' urine)

Compounds (Abbr.)	SRM	Calculated Concentration (ng/mL)					Mean (ng/mL)	Precision (%)
		day-1	day-2	day-3	day-4	day-5		
BPF	3672	2.32	2.10	2.09	2.37	2.02	2.18	7.09
	3673	2.67	2.80	2.55	2.80	2.49	2.66	5.29
BPS	3672	0.29	0.30	0.25	0.28	0.25	0.27	7.48
	3673	0.15	0.14	0.16	0.17	0.15	0.15	7.35
BP-1	3672	43.69	45.46	44.87	43.43	48.78	45.24	4.74
	3673	50.80	50.20	56.13	53.98	54.03	53.03	4.67
BP-8	3672	0.10	0.11	0.10	0.08	0.09	0.09 *	9.15
	3673	0.10	0.10	0.09	0.09	0.10	0.10 *	7.62
4-HBP	3672	1.21	1.19	1.31	1.30	1.41	1.28	6.77
	3673	0.85	0.84	0.91	0.95	0.75	0.86	9.07
4-TBP	3672	5.90	5.59	5.58	5.60	5.82	5.70	2.63
	3673	3.14	3.04	3.31	3.55	3.31	3.27	5.92
iPP	3672	3.20	3.28	3.30	2.80	3.46	3.21	7.67
	3673	3.68	3.48	3.90	3.25	3.48	3.56	6.93
iBP	3672	0.69	0.72	0.72	0.69	0.62	0.69	6.01
	3673	0.23	0.23	0.26	0.25	0.21	0.23 *	8.73
OPP	3672	0.14	0.14	0.15	0.14	0.17	0.15 *	9.75
	3673	0.35	0.36	0.34	0.38	0.41	0.37	6.99
4-PP	3672	0.23	0.21	0.25	0.25	0.26	0.24 *	9.58
	3673	0.10	0.08	0.08	0.09	0.09	0.09 *	7.15
PTOP	3672	0.89	0.84	0.82	0.86	0.93	0.87	4.99
	3673	0.73	0.71	0.75	0.86	0.73	0.76	7.97
NP	3672	0.82	0.89	0.80	0.83	0.84	0.83	4.08
	3673	0.73	0.70	0.69	0.64	0.64	0.68	6.00
MPA	3672	7.73	7.73	7.57	7.46	7.91	7.68	2.25
	3673	7.04	7.14	7.19	7.05	7.25	7.13	1.27
EPA	3672	1.93	1.83	1.89	1.99	1.60	1.85	8.07
	3673	1.43	1.38	1.38	1.48	1.32	1.40	4.43
TCC	3672	0.21	0.21	0.22	0.22	0.23	0.22 *	3.20
	3673	2.63	2.67	3.05	2.82	2.47	2.73	8.00
B4-HBZ	3672	0.10	0.12	0.09	0.10	0.10	0.10 *	8.93
	3673	0.04	0.04	0.04	0.04	0.04	0.04 *	10.78
2,4-DCP	3672	2.49	2.35	2.67	2.55	2.32	2.48	5.74
	3673	1.57	1.46	1.44	1.47	1.64	1.51	5.85
TCP	3672	0.13	0.11	0.13	0.14	0.12	0.13 *	8.37

* : Less than LOQ

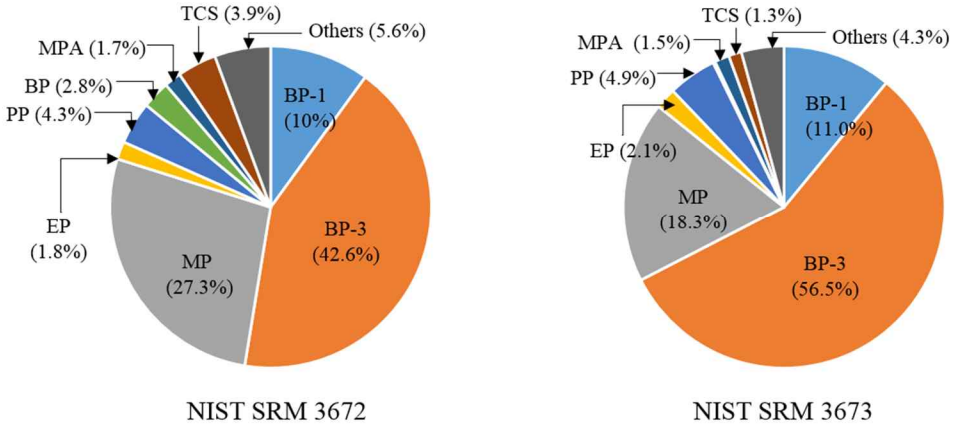

Figure 23. The concentration profile of environmental phenols in the NIST SRM (3672 and 3673) samples. Others (3672 / 3673): BPA (0.7% / 0.5%), BPF (0.5% / 0.6%), BPS (0.06% / 0.03%), OPP (0.03% / 0.08%), BP-8 (0.02%/ 0.02%), 4-HBP (0.3% / 0.2%), iPP (0.7% / 0.7%), iBP (0.2% / 0.05%), B4-HBZ (0.02% / 0.01%), EPA (0.4% / 0.3%), 4-TBP (1.3% / 0.7%), 4-PP (0.05% / 0.02%), PTOP (0.2% / 0.2%), NP (0.2% / 0.1%), TCC (0.05% / 0.6%), 2,4-DCP (0.6% / 0.3%), 2,5-DCP (0.4% / -), and TCP (0.03% / 0.02%)

4.3.3.3. Analytical performance comparison between methods

To evaluate an analytical performance of present multiclass method, we compared an analytical performance of recently published LC–ESI–MS/MS methods in terms of a coverage and sensitivity of multiclass phenols. We presented the analytical performances between our method with recently published LC–MS/MS methods for determining environmental phenols in human urine. In fact, it is not appropriate to compare the sensitivity only with the LOD reported in the literature because each analysis method used different calculation for LOD and the amount of sample loaded into the column was different. We expect that the sensitivity is related to the used sample volume and total number of analyzed phenols. Therefore, sample preparation, mobile phase condition, initial sample volume for preparation and analyzed phenols were shown in **Figure 24**. Generally, no additive mobile phase condition combined with SPE or LLE preparation was applied for simultaneous multi-phenols analysis, but most works have not determined alkylphenols. Among studies, our method simultaneously detected as many categories (5 categories) and numbers (38 analytes, including 7 alkylphenols) of phenols as possible. As shown in **Figure 24**, our 0.2 mL of urine for analysis is absolutely small volume when it comes to the consumption of biological sample. The required sample volume is very important issue. Because, the availability of sample amount for human biomonitoring is extremely limited due to ethical restriction and cost. Considering that only a small volume was used with simple dilute and shoot method, the expected sensitivity is sufficiently superior compared to other analytical methods. Consequently, our developed method significantly improved the simultaneous determination of environmental phenols in human urine.

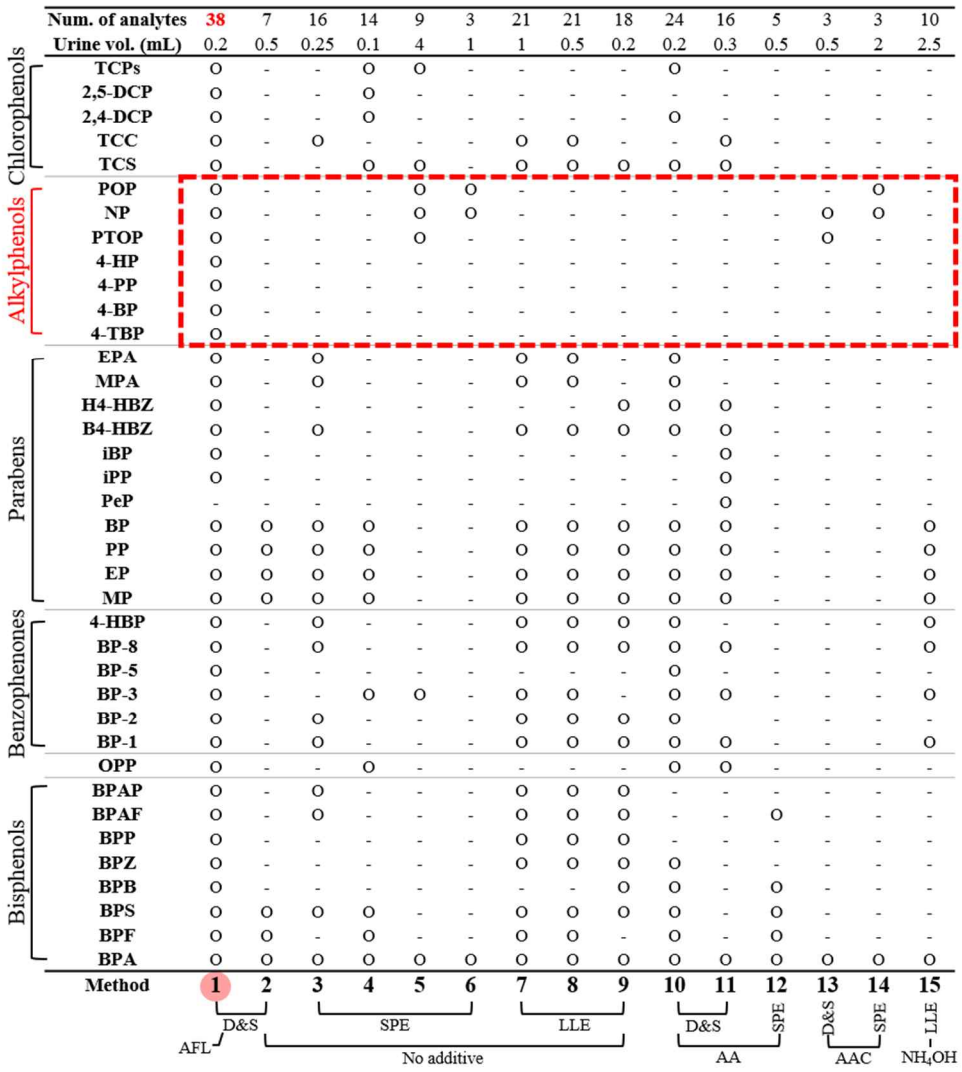

Figure 24. Comparison with other published methods for the determination of environmental phenols in human urine including the information of sample preparation methods, mobile phase composition, analyzed phenols, and used urine volume. 1:This work; 2:(Sanchis et al., 2019); 3: (Silveira et al., 2020); 4: (Zhou et al., 2014); 5: (Chen et al., 2012a); 6: (Xiao et al., 2011); 7: (Bocato et al., 2020); 8: (Rocha et al., 2018); 9: (Ao et al., 2021); 10: (Lee et al., 2022); 11: (Moos et al., 2014); 12: (Heffernan et al., 2016); 13: (Sukuroglu et al., 2022); 14: (Zhou et al., 2013); 15: (Jimenez-Diaz et al., 2016)

4.3.4 Application to sports-depending health risk assessment of athletes

It is commonly believed that athletes are in good physical health and they engage in activities in a safe environment. However, they are constantly exposed to specific phenols that may come from the environment (e.g., swimming pools) and personal care products (e.g., sunscreens). Furthermore, because environmental phenols are endocrine disruptors, they may affect the endogenous anabolic androgenic steroids of athletes. It is therefore important to assess the sports-related health risks of athletes. To assess the performance of our developed method on actual human samples, we monitored the levels of exposure of different types of athletes to environmental phenols.

We evaluated athletes engaged three sports (swimming, volleyball, and football) with different exercise environments (swimming pool, indoor gym, and outdoor sport facilities). Around 20 males for each sport were selected, and 19 females were additionally selected in swimming to compare results by gender. The mean, median, concentration range, as well as the detection frequency of the phenols found in the urine of athletes are summarized in **Table 19**, which lists the four categories of phenols detected at frequencies of over 5%. Statistical analysis was also performed to evaluate the differences in phenols in the four categories (**Figure 25**).

First, we were interested in comparing phenol levels in athletes engaged in aquatic (swimming) and land (volleyball and football) sports. As presented in **Figure 25**, higher levels of NP (nonylphenol) were found in aquatic athletes (median, 11.43 ng/mL for male and 15.74 ng/mL for female) compared to those engaged in other sports (median, 5.55 ng/mL for volleyball and 2.20 ng/mL for football). The value

was also much higher than the urinary level of 8.10 ng/mL (median) in Korean adults (Park and Kim, 2017). We propose that the higher level of NP in swimmers is caused by frequent exposure to the swimming pools. NP is an intermediate in the manufacture of the nonionic surfactants and is most likely present in aquatic environments, including swimming pools (Azzouz and Ballesteros, 2014). Therefore, it is likely that the higher NP level found in swimmers was influenced by a specific sports environment.

In addition, we found that BPA levels in male swimmers were higher (median, 3.45 ng/mL) than those in volleyball (median, 0.96 ng/mL) and football (median, 1.04 ng/mL) athletes. The level of BPA found in female swimmers was 1.59 ng/mL (median), which was close to that of the average Korean population (median, 1.17 ng/mL) (Park et al., 2017). This indicates that the higher BPA values found in male swimmers were associated with lifestyle rather than exposure to water in the swimming pool.

Second, we were interested in comparing phenol levels between athletes engaged in indoor and outdoor sports. Football athletes had very high levels (median, 6.05 ng/mL) of BP-3, which were approximately 10 times higher than that found in volleyball athletes (median, 0.55 ng/mL) and swimmers (median, 0.07 ng/mL for males and 0.66 ng/mL for females). BP-3 is a common ingredient in sunblock products (Kunisue et al., 2012), and football athletes are expected to extensively use such products as protection them from UV damage from the sun. In addition, the level of BP-1 (a metabolite of BP-3) in football athletes were also higher (median, 0.52 ng/mL) than those in athletes engaged in the other sports (median, from 0.11 to 0.18 ng/mL) (Jimenez-Diaz et al., 2016).

Overall, our developed method demonstrated sufficient analytical ability to detect and measure the levels of environmental phenols, including alkylphenols, in human urine. Moreover, the results of our assessment reveal that athletes can be exposed to specific types of environmental phenols associated with their sport, which can be a potential health risk.

Table 19. Urinary concentrations (ng/mL) and detection frequency of environmental phenols detected in volleyball (n=21), aquatics (male, n=23; female, n=19) and football (n=17)

Compounds	Volleyball			Aquatics (male)			Aquatics (female)			Football		
	Mean (Median)	Range	Detection Frequency(%)	Mean (Median)	Range	Detection Frequency(%)	Mean (Median)	Range	Detection Frequency(%)	Mean (Median)	Range	Detection Frequency(%)
BPA	1.23 (0.96)	0.05-5.02	90	4.15 (3.45)	0.14-13.9	100	1.84 (1.59)	0-4.68	95	1.89 (1.04)	0.44-7.44	100
BPF	0.82 (<LOD)	0-7.54	33	2.95 (<LOD)	0-23.3	39	3.95 (<LOD)	0-23.8	32	1.04 (<LOD)	0-8.74	53
BPS	0.83 (0.30)	0-5.12	81	0.35 (0.15)	0-1.89	61	0.79 (0.22)	0-6.37	68	2.61 (0.79)	0.06-19.5	94
BPB	<LOD (<LOD)	0-0.08	0	<LOD (<LOD)	0-0.05	0	<LOD (<LOD)	0-0.02	0	<LOD (<LOD)	<LOD	0
BPZ	<LOD (<LOD)	<LOD	0	<LOD (<LOD)	<LOD	0	<LOD (<LOD)	<LOD	0	<LOD (<LOD)	<LOD	0
BPP	<LOD (<LOD)	0-0.04	0	<LOD (<LOD)	<LOD	0	<LOD (<LOD)	0-0.04	0	0.01 (<LOD)	0-0.05	0
BPAF	0.10 (0.06)	0-0.47	19	0.10 (0.09)	0.03-0.25	43	0.14 (0.10)	0-0.43	47	0.10 (0.07)	0.03-0.44	29
BPAP	<LOD (<LOD)	<LOD	0	<LOD (<LOD)	<LOD	0	<LOD (<LOD)	<LOD	0	<LOD (<LOD)	<LOD	0
BP-1	0.34 (0.11)	0.03-2.50	86	0.28 (0.17)	0-1.09	91	0.37 (0.18)	0.06-2.14	100	36.5 (0.52)	0.03-408	94
BP-2	0.03 (0.02)	0-0.14	5	0.01 (0.01)	0-0.05	0	0.01 (<LOD)	0-0.06	0	0.01 (<LOD)	0-0.06	0

Table 19. (Continued)

Compounds	Volleyball			Aquatics (male)			Aquatics (female)			Football		
	Mean (Median)	Range	Detection Frequency(%)	Mean (Median)	Range	Detection Frequency(%)	Mean (Median)	Range	Detection Frequency(%)	Mean (Median)	Range	Detection Frequency(%)
BP-3	2.92 (0.55)	0-25.1	95	0.30 (0.07)	0-3.33	52	1.93 (0.66)	0-13.0	84	378 (6.05)	0-5048	100
BP-5	<LOD (<LOD)	<LOD	0	<LOD (<LOD)	<LOD	0	0.17 (<LOD)	0-3.30	5	3.49 (<LOD)	0-55.9	18
BP-8	<LOD (<LOD)	<LOD	0	<LOD (<LOD)	0-0.05	0	<LOD (<LOD)	0-0.07	0	0.05 (<LOD)	0-0.90	6
4-HBP	0.15 (0.13)	0.02-0.41	76	0.47 (0.11)	0-6.98	83	0.46 (0.21)	0.02-4.67	84	0.22 (0.14)	0.01-0.91	76
MP	73.6 (7.92)	2.14-628	100	75.9 (5.81)	1.56-943	100	88.0 (8.61)	0.71-923	100	237 (11.5)	1.28-2257	100
EP	200 (115)	2.20-1575	100	178 (100)	3.87-1028	100	171 (115)	1.38-742	100	236 (145)	12.7-1148	100
PP	7.78 (0.37)	0.05-79.9	100	8.17 (0.15)	0-137	74	15.1 (0.65)	0-215	89	15.3 (0.28)	0.04-228	94
BP	0.02 (0.02)	0-0.07	0	0.01 (0.01)	0-0.06	0	0.14 (0.04)	0-1.19	32	0.05 (0.03)	0-0.17	12
iPP	0.08 (0.04)	0-0.61	19	0.05 (0.03)	0-0.22	13	0.05 (0.03)	0-0.16	5	0.03 (<LOD)	0-0.10	6
iBP	<LOD (<LOD)	0-0.01	0	<LOD (<LOD)	0-0.02	0	<LOD (<LOD)	0-0.02	0	<LOD (<LOD)	0-0.04	0

Table 19. (Continued)

Compounds	Volleyball			Aquatics (male)			Aquatics (female)			Football		
	Mean (Median)	Range	Detection Frequency(%)	Mean (Median)	Range	Detection Frequency(%)	Mean (Median)	Range	Detection Frequency(%)	Mean (Median)	Range	Detection Frequency(%)
4-TBP	11.2 (8.66)	0-30.1	81	3.72 (<LOD)	0-23.7	35	4.04 (<LOD)	0-31.7	42	8.99 (9.84)	0-21.3	76
OPP	0.41 (<LOD)	0-4.74	19	0.31 (<LOD)	0-2.50	17	0.17 (<LOD)	0-2.61	11	0.32 (<LOD)	0-2.26	18
4-BP	0.06 (<LOD)	0-1.19	5	<LOD (<LOD)	<LOD	0	<LOD (<LOD)	<LOD	0	<LOD (<LOD)	<LOD	0
4-PP	0.11 (<LOD)	0-0.51	29	0.03 (<LOD)	0-0.36	9	0.06 (<LOD)	0-1.22	5	<LOD (<LOD)	<LOD	0
4-HP	0.03 (<LOD)	0-0.21	14	0.01 (<LOD)	0-0.14	9	0.01 (<LOD)	0-0.14	11	0.06 (<LOD)	0-0.46	29
PTOP	1.57 (0.88)	0-5.73	95	1.86 (1.66)	0.02-5.12	96	2.61 (2.05)	0.29-7.84	100	1.25 (1.21)	0-3.52	94
NP	7.95 (5.55)	0-33.0	95	13.5 (11.4)	0.13-32.4	96	17.6 (15.7)	0-42.2	95	5.07 (2.20)	0-42.5	76
POP	<LOD (<LOD)	<LOD	0	<LOD (<LOD)	<LOD	0	<LOD (<LOD)	<LOD	0	<LOD (<LOD)	<LOD	0
MPA	11.3 (7.57)	1.34-35.0	100	3.58 (2.12)	0.64-9.25	100	7.92 (5.04)	0.62-41.8	100	12.5 (6.69)	2.68-57.2	100
EPA	3.51 (3.36)	0.48-8.87	100	2.02 (1.39)	0.43-4.99	100	3.29 (2.33)	0.49-16.2	100	7.37 (4.20)	0.81-35.0	100

Table 19. (Continued)

Compounds	Volleyball			Aquatics (male)			Aquatics (female)			Football		
	Mean (Median)	Range	Detection Frequency(%)	Mean (Median)	Range	Detection Frequency(%)	Mean (Median)	Range	Detection Frequency(%)	Mean (Median)	Range	Detection Frequency(%)
TCS	2.03 (0.70)	0-10.4	52	1.08 (<LOD)	0-9.50	22	1.35 (<LOD)	0-11.5	21	2.35 (<LOD)	0-15.5	29
TCC	0.03 (<LOD)	0-0.38	5	<LOD (<LOD)	0-0.02	0	<LOD (<LOD)	0-0.06	0	<LOD (<LOD)	<LOD	0
B4-HBZ	0.10 (0.07)	0-0.44	38	0.07 (0.06)	0-0.27	17	0.06 (0.04)	0-0.25	21	0.13 (0.09)	0.03-0.81	53
H4-HBZ	<LOD (<LOD)	<LOD	0	<LOD (<LOD)	<LOD	0	<LOD (<LOD)	<LOD	0	<LOD (<LOD)	<LOD	0
2,4-DCP	<LOD (<LOD)	<LOD	0	<LOD (<LOD)	<LOD	0	<LOD (<LOD)	<LOD	0	<LOD (<LOD)	<LOD	0
2,5-DCP	<LOD (<LOD)	<LOD	0	<LOD (<LOD)	<LOD	0	<LOD (<LOD)	<LOD	0	<LOD (<LOD)	<LOD	0
2,4,5/2,4,6-TCP	0.06 (<LOD)	0-0.42	19	0.01 (<LOD)	0-0.17	4	0.01 (<LOD)	0-0.04	0	0.03 (<LOD)	0-0.33	12

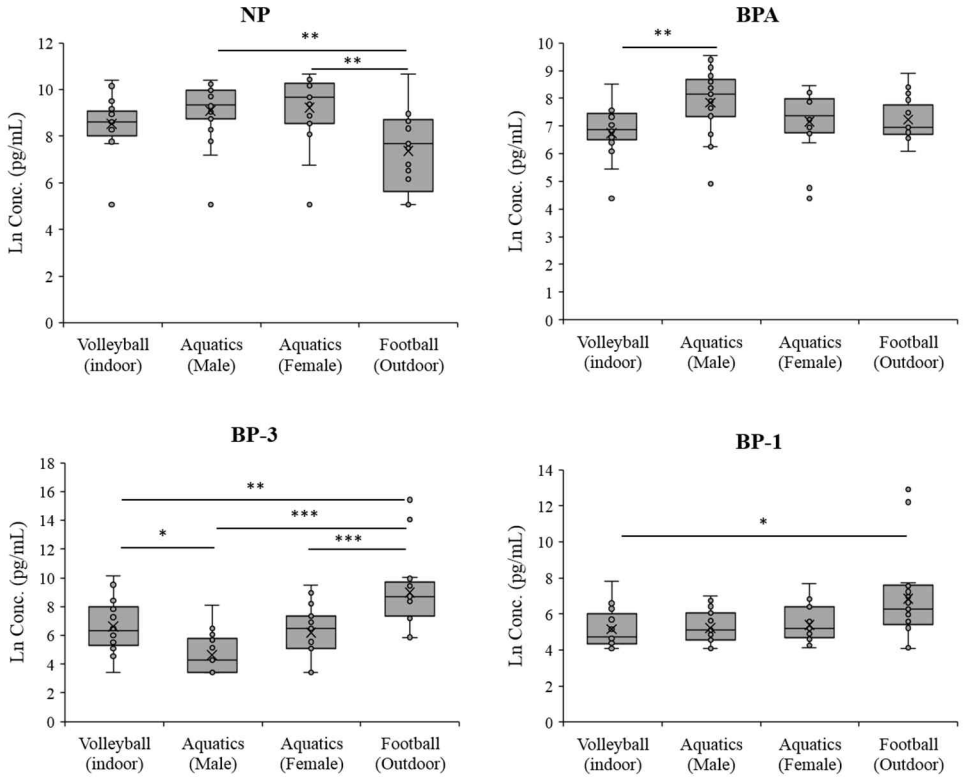

Figure 25. Statistical analysis graph of environmental phenols which showed statistical significance in four sports categories (volleyball, aquatics (male and female) and football). The box and whisker plots present the distribution of quantity of analytes that was transformed into the natural logarithm. The number of * symbol in the plots meant significant statistical differences at $P < 0.05$ for 1, $P < 0.01$ for 2, and $P < 0.001$ for 3, respectively. All data except BP-1 had been obtained via one-way analysis of variance and Scheffe post hoc test. BP-1 was observed using Kruskal-Wallis and Dunn's post hoc test, and its P-value was calculated using Bonferroni adjustment.

4.4 Conclusions

We evaluated the influence of mobile phase compositions on concurrent ionization and analytical sensitivity of LC–ESI–MS/MS for the analysis of multiple classes of phenols, resulting in the development of a sensitive method for analyzing bisphenols, parabens, chlorophenols, benzophenones, and alkylphenols in human urine. Our method relies on a water/MeOH system with AFL as an additive, which was the only phenol-specialized mobile phase composition that satisfied the requirements for concurrent ionization and sensitivity enhancement. In particular, the proposed method significantly improved the inherently poor ionization efficiencies of phenolic compounds with high pK_a values such as bisphenols and alkylphenols. Finally, the phenol-specialized mobile phase composition in our developed method provides a generic analytical platform for phenol analysis that can be very useful for integrating newly identified environmental phenols.

Chapter 5. Overall summary

In this study, mobile phase composition strategy was applied to explore and develop highly sensitive analytical method by using LC-ESI-MS/MS with negative mode. The water/MeOH system with ammonium fluoride additive developed in this dissertation have greatly enhanced ionization efficiency for phenolic compounds compared to commonly used conditions. Finally, the combination of simple sample preparation with outstanding ionization efficiency in negative ESI may help to design and develop high performance analytical platform for further practical applications in various research fields (**Figure 26**).

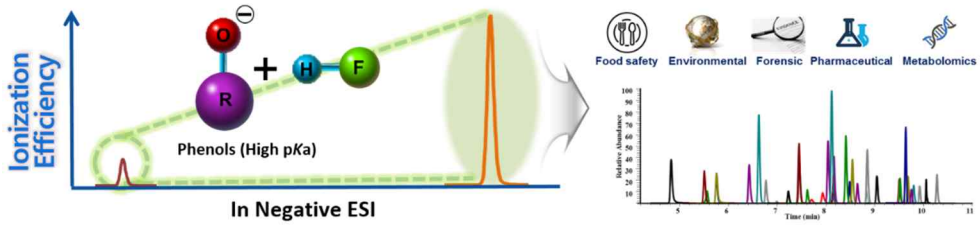

Figure 26. Overview of fluoride-assisted LC-ESI-MS/MS analysis of phenolic compounds for general analytical platform in various research fields

References

Ao, J.J., Zhang, Q.L., Tang, W.F., Yuan, T., Zhang, J., 2021. A simple, rapid and sensitive method for the simultaneous determination of eighteen environmental phenols in human urine. Chemosphere 278.

Asimakopoulos, A.G., Elangovan, M., Kannan, K., 2016. Migration of Parabens, Bisphenols, Benzophenone-Type UV Filters, Triclosan, and Triclocarban from Teethers and Its Implications for Infant Exposure. Environ Sci Technol 50, 13539-13547.

Azzouz, A., Ballesteros, E., 2014. Trace analysis of endocrine disrupting compounds in environmental water samples by use of solid-phase extraction and gas chromatography with mass spectrometry detection. J Chromatogr A 1360, 248-257.

Bajpai, L., Varshney, M., Seubert, C.N., Dennis, D.M., 2004. A new method for the quantitation of propofol in human plasma: efficient solid-phase extraction and liquid chromatography/APCI-triple quadrupole mass spectrometry detection. J Chromatogr B 810, 291-296.

Bajpai, L., Varshney, M., Seubert, C.N., Stevens, S.M., Johnson, J.V., Yost, R.A., Dennis, D.M., 2005. Mass spectral fragmentation of the intravenous anesthetic propofol and structurally related phenols. J Am Soc Mass Spectr 16, 814-824.

Bateman, B.T., Kesselheim, A.S., 2015. Propofol as a transformative drug in anesthesia: insights from key early investigators. Drug Discov Today 20, 1012-1017.

Beaudry, F., Guenette, S.A., Winterborn, A., Marier, J.F., Vachon, P., 2005. Development of a rapid and sensitive LC-ESI/MS/MS assay for the quantification of propofol using a simple off-line dansyl chloride derivatization reaction to enhance signal intensity. J Pharmaceut Biomed 39, 411-417.

Berge, T.L.L., Lygre, G.B., Jonsson, B.A.G., Lindh, C.H., Bjorkman, L., 2017. Bisphenol A concentration in human saliva related to dental polymer-based fillings. Clin Oral Invest 21, 2561-2568.

Binkley, R.W., Tevesz, M.J.S., Winnik, W., 1992. Reactions of Phenoxide Ion in the Gas-Phase. J Org Chem 57, 5507-5509.

Bocato, M.Z., Cesila, C.A., Lataro, B.F., de Oliveira, A.R.M., Campiglia, A.D., Barbosa, F., 2020. A fast-multiclass method for the determination of 21 endocrine disruptors in human urine by using vortex-assisted dispersive liquid-liquid microextraction (VADLLME) and LC-MS/MS. Environ Res 189.

Brodie, R.R., Hill, H.M., 2002. Validation issues arising from the new FDA guidance for industry on bioanalytical method validation. Chromatographia 55, S91-S94.

Cai, Y., Cole, R.B., 2002a. Stabilization of anionic adducts in negative ion electrospray mass spectrometry. Anal Chem 74, 985-991.

Cai, Y., Cole, R.B., 2002b. Stabilization of anionic adducts in negative ion electrospray mass spectrometry. Anal Chem 74, 985-991.

Cai, Y., Concha, M.C., Murray, J.S., Cole, R.B., 2002. Evaluation of the role of multiple hydrogen bonding in offering stability to negative ion adducts in electrospray mass spectrometry. J Am Soc Mass Spectr 13, 1360-1369.

Castro, G.T., Giordano, O.S., Blanco, S.E., 2003. Determination of the pK(a) of hydroxy-benzophenones in ethanol-water mixtures. Solvent effects. J Mol Struc-Theochem 626, 167-178.

Cech, N.B., Enke, C.G., 2001. Practical implications of some recent studies in electrospray ionization fundamentals. Mass Spectrom Rev 20, 362-387.

Chen, D., Kannan, K., Tan, H.L., Zheng, Z.G., Feng, Y.L., Wu, Y., Widelka, M., 2016. Bisphenol Analogues Other Than BPA: Environmental Occurrence, Human Exposure, and Toxicity-A Review. Environ Sci Technol 50, 5438-5453.

Chen, M., Tao, L., Collins, E.M., Austin, C., Lu, C.S., 2012a. Simultaneous determination of multiple phthalate metabolites and bisphenol-A in human urine by liquid chromatography-tandem mass spectrometry. J Chromatogr B 904, 73-80.

Chen, M.J., Zhu, P.F., Xu, B., Zhao, R.C., Qiao, S.L., Chen, X.J., Tang, R., Wu, D., Song, L., Wang, S.L., Xia, Y.K., Wang, X.R., 2012b. Determination of Nine Environmental Phenols in Urine by Ultra-High-Performance Liquid ChromatographyTandem Mass Spectrometry. J Anal Toxicol 36, 608-615.

Cheng, X., Zhou, J.L., Shi, Z.Q., Yin, Y.H., Liu, J.Q., Chen, H.X., Li, P., Liu, L.F., Xin, G.Z., 2019. Ammonium fluoride-induced stabilization for anion attachment mass spectrometry: Facilitating the pseudotargeted profiling of bile acids submetabolome. Anal Chim Acta 1081, 120-130.

Chung, S.H., Ding, W.H., 2018. Isotope-dilution gas chromatography-mass spectrometry coupled with injection-port butylation for the determination of 4-t-octylphenol, 4-nonylphenols and bisphenol A in human urine. J Pharmaceut Biomed 149, 572-576.

Cohen, S., Lhuillier, F., Mouloua, Y., Vignal, B., Favetta, P., Guitton, J., 2007. Quantitative measurement of propofol and in main glucuroconjugate metabolites in human plasma using solid phase extraction-liquid chromatography-tandem mass spectrometry. J Chromatogr B 854, 165-172.

Cole, R.B., Harrata, A.K., 1993. Solvent Effect on Analyte Charge-State, Signal Intensity, and Stability in Negative-Ion Electrospray Mass-Spectrometry -

Implications for the Mechanism of Negative-Ion Formation. J Am Soc Mass Spectr 4, 546-556.

Cornwall, W., 2020. Can do. Science 367, 380-383.

Dewalque, L., Pirard, C., Dubois, N., Charlier, C., 2014. Simultaneous determination of some phthalate metabolites, parabens and benzophenone-3 in urine by ultra high pressure liquid chromatography tandem mass spectrometry. J Chromatogr B 949, 37-47.

Dziadosz, M., 2019. The study and application of analyte adduct based ionisation of propofol in the analysis with liquid chromatography-tandem mass spectrometry. J Chromatogr B 1114, 1-4.

Eggink, M., Wijtmans, M., Ekkebus, R., Lingeman, H., de Esch, I.J.P., Kool, J., Niessen, W.M.A., Irth, H., 2008. Development of a Selective ESI-MS Derivatization Reagent: Synthesis and Optimization for the Analysis of Aldehydes in Biological Mixtures. Anal Chem 80, 9042-9051.

Fan, X.H., Kubwabo, C., Wu, F., Rasmussen, P.E., 2019. Analysis of Bisphenol A, Alkylphenols, and Alkylphenol Ethoxylates in NIST SRM 2585 and Indoor House Dust by Gas Chromatography-Tandem Mass Spectrometry (GC/MS/MS). J Aoac Int 102, 246-254.

Favetta, P., Dufresne, C., Desage, M., Paisse, O., Perdrix, J.P., Boulieu, R., Guitton, J., 2000. Detection of new propofol metabolites in human urine using gas chromatography/mass spectrometry and liquid chromatography/mass spectrometry techniques. Rapid Commun Mass Sp 14, 1932-1936.

Fiers, T., Casetta, B., Bernaert, B., Vandersypt, E., Debock, M., Kaufman, J.M., 2012. Development of a highly sensitive method for the quantification of estrone and

estradiol in serum by liquid chromatography tandem mass spectrometry without derivatization. J Chromatogr B 893, 57-62.

Frederiksen, H., Nielsen, J.K.S., Morck, T.A., Hansen, P.W., Jensen, J.F., Nielsen, O., Andersson, A.M., Knudsen, L.E., 2013. Urinary excretion of phthalate metabolites, phenols and parabens in rural and urban Danish mother-child pairs. Int J Hyg Envir Heal 216, 772-783.

Gao, C.Z., He, H.H., Qiu, W.H., Zheng, Y., Chen, Y.Y., Hu, S.Y., Zhao, X., 2021. Oxidative Stress, Endocrine Disturbance, and Immune Interference in Humans Showed Relationships to Serum Bisphenol Concentrations in a Dense Industrial Area. Environ Sci Technol 55, 1953-1963.

Gely, C.A., Huesca, A., Picard-Hagen, N., Toutain, P.L., Berrebi, A., Gauderat, G., Gayrard, V., Lacroix, M.Z., 2021. A new LC/MS method for specific determination of human systemic exposure to bisphenol A, F and S through their metabolites: Application to cord blood samples. Environ Int 151.

Heffernan, A.L., Thompson, K., Eaglesham, G., Vijayasarathy, S., Mueller, J.F., Sly, P.D., Gomez, M.J., 2016. Rapid, automated online SPE-LC-QTRAP-MS/MS method for the simultaneous analysis of 14 phthalate metabolites and 5 bisphenol analogues in human urine. Talanta 151, 224-233.

Henriksen, T., Juhler, R.K., Svensmark, B., Cech, N.B., 2005. The relative influences of acidity and polarity on responsiveness of small organic molecules to analysis with negative ion electrospray ionization mass spectrometry (ESI-MS). J Am Soc Mass Spectr 16, 446-455.

Hua, Y., Jenke, D., 2012. Increasing the sensitivity of an LC-MS method for screening material extracts for organic extractables via mobile phase optimization. J Chromatogr Sci 50, 213-227.

Huffman, B.A., Poltash, M.L., Hughey, C.A., 2012. Effect of Polar Protic and Polar Aprotic Solvents on Negative-Ion Electrospray Ionization and Chromatographic Separation of Small Acidic Molecules. Anal Chem 84, 9942-9950.

Iwersen-Bergmann, S., Rosner, P., Kuhnau, H.C., Junge, M., Schmoldt, A., 2001. Death after excessive propofol abuse. Int J Legal Med 114, 248-251.

Jiang, Y.J., Cole, R.B., 2005. Oligosaccharide analysis using anion attachment in negative mode electrospray mass spectrometry. J Am Soc Mass Spectr 16, 60-70.

Jimenez-Diaz, I., Artacho-Cordon, F., Vela-Soria, F., Belhassen, H., Arrebola, J.P., Fernandez, M.F., Ghali, R., Hedhili, A., Olea, N., 2016. Urinary levels of bisphenol A, benzophenones and parabens in Tunisian women: A pilot study. Sci Total Environ 562, 81-88.

Khedr, A., Abd El-Hay, S.S., Kammoun, A.K., 2017. Liquid chromatography-tandem mass spectrometric determination of propofol in rat serum and hair at attogram level after derivatization with 3-bromomethyl-propyphenazone. J Pharmaceut Biomed 134, 195-202.

Kim, J., In, S., Park, Y., Park, M., Kim, E., Lee, S., 2013. Quantitative analysis of propofol-glucuronide in hair as a marker for propofol abuse. Anal Bioanal Chem 405, 6807-6814.

Kim, S., Hahn, S., Jang, M.J., Choi, Y., Hong, H., Lee, J.H., Kim, H.S., 2019. Evaluation of the safety of using propofol for paediatric procedural sedation: A systematic review and meta-analysis. Sci Rep-Uk 9.

Kingman, A., Hyman, J., Masten, S.A., Jayaram, B., Smith, C., Eichmiller, F., Arnold, M.C., Wong, P.A., Schaeffer, J.M., Solanki, S., Dunn, W.J., 2012. Bisphenol A and other compounds in human saliva and urine associated with the placement of composite restorations. J Am Dent Assoc 143, 1292-1302.

Kloepfer, A., Quintana, J.B., Reemtsma, T., 2005. Operational options to reduce matrix effects in liquid chromatography-electrospray ionization-mass spectrometry analysis of aqueous environmental samples. J Chromatogr A 1067, 153-160.

Kruve, A., Kaupmees, K., Liigand, J., Leito, I., 2014. Negative Electrospray Ionization via Deprotonation: Predicting the Ionization Efficiency. Anal Chem 86, 4822-4830.

Kunisue, T., Chen, Z., Louis, G.M.B., Sundaram, R., Hediger, M.L., Sun, L.P., Kannan, K., 2012. Urinary Concentrations of Benzophenone-type UV Filters in U.S. Women and Their Association with Endometriosis. Environ Sci Technol 46, 4624-4632.

Lee, K.M., Kim, H.J., Jeong, E.S., Yoo, H.H., Kwon, O.S., Jin, C., Kim, D.H., Lee, J., 2011. Simple and accurate quantitative analysis of seven prohibited threshold substances in human urine by liquid chromatography/tandem mass spectrometry in doping control. Rapid Commun Mass Sp 25, 2261-2267.

Lee, S., Lee, K.M., Han, S.M., Lee, H.J., Sung, C., Min, H., Im, H., Han, S.B., Cha, S., Lee, J., 2022. Comprehensive LC-MS/MS method combined with tandem hybrid hydrolysis for multiple exposure assessment of multiclass environmental pollutants. Environ Res 211.

Lee, S.Y., Park, N.H., Jeong, E.K., Wi, J.W., Kim, C.J., Kim, J.Y., In, M.K., Hong, J., 2012. Comparison of GC/MS and LC/MS methods for the analysis of propofol and its metabolites in urine. J Chromatogr B 900, 1-10.

Lei, Z., Chen, Y.S., Liu, Z.W., Ji, W.J., Zhao, S.Q., 2018. A highly sensitive and quantitative detection method for bisphenol A (BPA) by competitive

immunoassay based on surface-enhanced Raman spectroscopy. Pigm Resin Technol 47, 38-46.

Li, H., Huang, K., Jin, S.N., Peng, Y., Liu, W.Y., Wang, M., Zhang, H.L., Zhang, B., Xia, W., Li, Y.Y., Lu, S., Xu, S.Q., 2019a. Environmental cadmium exposure induces alterations in the urinary metabolic profile of pregnant women. Int J Hyg Envir Heal 222, 556-562.

Li, J.F., Wu, C.S., Zhao, H.Z., Zhou, Y.Q., Cao, G.D., Yang, Z.Y., Hong, Y.J., Xu, S.Q., Xia, W., Cai, Z.W., 2019b. Exposure Assessment of Bisphenols in Chinese Women during Pregnancy: A Longitudinal Study. Environ Sci Technol 53, 7812-7820.

Li, M.Z., He, Y.N., Sun, J., Li, J., Bai, J.H., Zhang, C.D., 2019c. Chronic Exposure to an Environmentally Relevant Triclosan Concentration Induces Persistent Triclosan Resistance but Reversible Antibiotic Tolerance in Escherichia coli. Environ Sci Technol 53, 3277-3286.

Li, X., Ying, G.G., Zhao, J.L., Chen, Z.F., Lai, H.J., Su, H.C., 2013. 4-Nonylphenol, bisphenol-A and triclosan levels in human urine of children and students in China, and the effects of drinking these bottled materials on the levels. Environ Int 52, 81-86.

Lin, H., Chen, X., Ma, J., Zhang, X., Li, T., Zhang, Y., Wang, H., 2021. Determination of propofol in human plasma with C18 pipette-tip based solid-phase extraction followed by liquid chromatography atmospheric-pressure chemical ionization tandem mass spectrometry analysis. J Pharm Biomed Anal 193, 113714.

Lindner, J.M., Vogeser, M., Grimm, S.H., 2017. Biphenyl based stationary phases for improved selectivity in complex steroid assays. J Pharmaceut Biomed 142, 66-73.

Maas, A., Maier, C., Iwersen-Bergmann, S., Madea, B., Hess, C., 2017a. Simultaneous extraction of propofol and propofol glucuronide from hair followed by validated LC-MS/MS analyses. J Pharmaceut Biomed 146, 236-243.

Maas, A., Maier, C., Michel-Lauter, B., Madea, B., Hess, C., 2017b. 1,2-Dimethylimidazole-4-sulfonyl chloride (DMISC), a novel derivatization strategy for the analysis of propofol by LC-ESI-MS/MS. Anal Bioanal Chem 409, 1547-1554.

Maurer, F., Shopova, T., Wolf, B., Kiefer, D., Huppe, T., Volk, T., Sessler, D.I., Kreuer, S., 2018. Design and validation of an automated solid phase extraction liquid chromatography coupled mass spectrometry method for the quantification of propofol in plasma. J Pharmaceut Biomed 150, 341-346.

Moos, R.K., Anger, J., Wittsiepe, J., Wilhelm, M., Bruning, T., Koch, H.M., 2014. Rapid determination of nine parabens and seven other environmental phenols in urine samples of German children and adults. Int J Hyg Envir Heal 217, 845-853.

Mulabagal, V., Wilson, C., Hayworth, J.S., 2017. An ultrahigh-performance chromatography/tandem mass spectrometry quantitative method for trace analysis of potential endocrine disrupting steroid hormones in estuarine sediments. Rapid Commun Mass Sp 31, 419-429.

Neven, L., Barich, H., Sleegers, N., Canovas, R., Debruyne, G., De Wael, K., 2022. Development of a combi-electrosensor for the detection of phenol by combining photoelectrochemistry and square wave voltammetry. Anal Chim Acta 1206.

Orzel, J., Swit, P., 2021. Comparison of Quantitative Detection Methods Based on Molecular Fluorescence Spectroscopy and Chromatographic Techniques Used for the Determination of Bisphenol Compounds. Int J Mol Sci 22.

Park, C., Choi, W., Hwang, M., Lee, Y., Kim, S., Yu, S., Lee, I., Paek, D., Choi, K., 2017. Associations between urinary phthalate metabolites and bisphenol A levels, and serum thyroid hormones among the Korean adult population - Korean National Environmental Health Survey (KoNEHS) 2012-2014. Sci Total Environ 584-585, 950-957.

Park, H., Kim, K., 2017. Urinary Levels of 4-Nonylphenol and 4-t-Octylphenol in a Representative Sample of the Korean Adult Population. Int J Environ Res Public Health 14.

Peng, F.L., Ji, W.L., Zhu, F., Peng, D.H., Yang, M., Liu, R., Pu, Y.P., Yin, L.H., 2016. A study on phthalate metabolites, bisphenol A and nonylphenol in the urine of Chinese women with unexplained recurrent spontaneous abortion. Environ Res 150, 622-628.

Plummer, G.F., 1987. Improved Method for the Determination of Propofol in Blood by High-Performance Liquid-Chromatography with Fluorescence Detection. J Chromatogr-Biomed 421, 171-176.

Preindl, K., Braun, D., Aichinger, G., Sieri, S., Fang, M.L., Marko, D., Warth, B., 2019. A Generic Liquid Chromatography-Tandem Mass Spectrometry Exposome Method for the Determination of Xenoestrogens in Biological Matrices. Anal Chem 91, 11334-11342.

Rainville, P.D., Smith, N.W., Cowan, D., Plumb, R.S., 2012. Comprehensive investigation of the influence of acidic, basic, and organic mobile phase compositions on bioanalytical assay sensitivity in positive ESI mode LC/MS/MS. J Pharm Biomed Anal 59, 138-150.

Regueiro, J., Breidbach, A., Wenzl, T., 2015. Derivatization of bisphenol A and its analogues with pyridine-3-sulfonyl chloride: multivariate optimization and

fragmentation patterns by liquid chromatography/Orbitrap mass spectrometry. Rapid Commun Mass Spectrom 29, 1473-1484.

Rocha, B.A., de Oliveira, A.R.M., Barbosa, F., 2018. A fast and simple air-assisted liquid-liquid microextraction procedure for the simultaneous determination of bisphenols, parabens, benzophenones, triclosan, and triclocarban in human urine by liquid chromatography-tandem mass spectrometry. Talanta 183, 94-101.

Sanchis, Y., Coscolla, C., Yusa, V., 2019. Analysis of four parabens and bisphenols A, F, S in urine, using dilute and shoot and liquid chromatography coupled to mass spectrometry. Talanta 202, 42-50.

Seger, C., Salzmann, L., 2020. After another decade: LC-MS/MS became routine in clinical diagnostics. Clin Biochem 82, 2-11.

Shopova, T., Kiefer, D., Wolf, B., Maurer, F., Sessler, D.I., Volk, T., Fink, T., Kreuer, S., 2019. Simultaneous quantification of propofol, ketamine and rocuronium in just 10 mu L plasma using liquid chromatography coupled with quadrupole mass spectrometry and its pilot application to a pharmacokinetic study in rats. Biomed Chromatogr 33.

Silveira, R.S., Rocha, B.A., Rodrigues, J.L., Barbosa, F., 2020. Rapid, sensitive and simultaneous determination of 16 endocrine-disrupting chemicals (parabens, benzophenones, bisphenols, and triclocarban) in human urine based on microextraction by packed sorbent combined with liquid chromatography tandem mass spectrometry (MEPS-LC-MS/MS). Chemosphere 240.

Smith, R.D., Loo, J.A., Edmonds, C.G., Barinaga, C.J., Udseth, H.R., 1990. New Developments in Biochemical Mass-Spectrometry - Electrospray Ionization. Anal Chem 62, 882-899.

Sohoni, P., Tyler, C.R., Hurd, K., Caunter, J., Hetheridge, M., Williams, T., Woods, C., Evans, M., Toy, R., Gargas, M., Sumpter, J.P., 2001. Reproductive effects of long-term exposure to bisphenol a in the fathead minnow (Pimephales promelas). Environ Sci Technol 35, 2917-2925.

Sorensen, L.K., Hasselstrom, J.B., 2015. Simultaneous determination of propofol and its glucuronide in whole blood by liquid chromatography-electrospray tandem mass spectrometry and the influence of sample storage conditions on the reliability of the test results. J Pharmaceut Biomed 109, 158-163.

Sosvorova, L.K., Chlupacova, T., Vitku, J., Vlk, M., Heracek, J., Starka, L., Saman, D., Simkova, M., Hampl, R., 2017. Determination of selected bisphenols, parabens and estrogens in human plasma using LC-MS/MS. Talanta 174, 21-28.

Sukuroglu, A.A., Battal, D., Kocadal, K., Sungur, M.A., Cok, I., Unlusayin, I., 2022. Biomonitoring of bisphenol A, 4-nonylphenol, and 4-t-octylphenol in Turkish population: exposure and risk assessment. Environ Sci Pollut R 29, 26250-26262.

Takkis, K., Aro, R., Korgvee, L.T., Varendi, H., Lass, J., Herodes, K., Kipper, K., 2017. Signal Enhancement in the HPLC-ESI-MS/MS analysis of spironolactone and its metabolites using HFIP and NH4F as eluent additives. Anal Bioanal Chem 409, 3145-3151.

Teeguarden, J.G., Twaddle, N.C., Churchwell, M.I., Yang, X.X., Fisher, J.W., Seryak, L.M., Doerge, D.R., 2015. 24-hour human urine and serum profiles of bisphenol A: Evidence against sublingual absorption following ingestion in soup. Toxicol Appl Pharm 288, 131-142.

Thayer, K.A., Doerge, D.R., Hunt, D., Schurman, S.H., Twaddle, N.C., Churchwell, M.I., Garantziotis, S., Kissling, G.E., Easterling, M.R., Bucher, J.R.,

Birnbaum, L.S., 2015. Pharmacokinetics of bisphenol A in humans following a single oral administration. Environ Int 83, 107-115.

Thieme, D., Sachs, H., Schelling, G., Hornuss, C., 2009. Formation of the N-methylpyridinium ether derivative of propofol to improve sensitivity, specificity and reproducibility of its detection in blood by liquid chromatography-mass spectrometry. J Chromatogr B 877, 4055-4058.

Thurman, E.M., Ferrer, I., Barcelo, D., 2001. Choosing between atmospheric pressure chemical ionization and electrospray ionization interfaces for the HPLC/MS analysis of pesticides. Anal Chem 73, 5441-5449.

Tuzimski, T., Pieniazek, D., Buszewicz, G., Teresinski, G., 2019. QuEChERS-Based Extraction Procedures for the Analysis of Bisphenols S and A in Breast Milk Samples by LC-QqQ-MS. J Aoac Int 102, 23-32.

Ulrich, S., 2000. Solid-phase microextraction in biomedical analysis. J Chromatogr A 902, 167-194.

Vaiano, F., Busardo, F.P., Pascali, J., Fioravanti, A., Mortali, C., Mari, F., Bertol, E., 2017. Hair testing of propofol by liquid chromatography-tandem mass spectrometry and azo-coupling derivatization. Drug Test Anal 9, 1080-1084.

Vaiano, F., Mari, F., Busardo, F.P., Bertol, E., 2014. Enhancing the sensitivity of the LC-MS/MS detection of propofol in urine and blood by azo-coupling derivatization. Anal Bioanal Chem 406, 3579-3587.

Vaiano, F., Serpelloni, G., Focardi, M., Fioravanti, A., Mari, F., Bertol, E., 2015. LC-MS/MS and GC-MS methods in propofol detection: Evaluation of the two analytical procedures. Forensic Sci Int 256, 1-6.

Vlase, L., Popa, D.S., Siserman, C., Zaharia, D., 2011. High-throughput toxicological analysis of propofol in human whole blood by LC-MS. Rom J Leg Med 19, 145-150.

Vokel, W., Colnot, T., Csanady, G.A., Filser, J.G., Dekant, W., 2002. Metabolism and kinetics of bisphenol A in humans at low doses following oral administration. Chem Res Toxicol 15, 1281-1287.

Walfish, S., 2006. A statistical perspective on the ICH Q2A and Q2B guidelines for validation of analytical methods. Biopharm Int 19, 28-+.

Walorczyk, S., 2014. Validation and use of a QuEChERS-based gas chromatographic-tandem mass spectrometric method for multiresidue pesticide analysis in blackcurrants including studies of matrix effects and estimation of measurement uncertainty. Talanta 120, 106-113.

Walsh, C.T., 2018. Propofol: Milk of Amnesia. Cell 175, 10-13.

Wang, H.X., Wang, B., Zhou, Y., Jiang, Q.W., 2013. Rapid and sensitive analysis of phthalate metabolites, bisphenol A, and endogenous steroid hormones in human urine by mixed-mode solid-phase extraction, dansylation, and ultra-performance liquid chromatography coupled with triple quadrupole mass spectrometry. Anal Bioanal Chem 405, 4313-4319.

Wang, J.A., Aubry, A., Bolgar, M.S., Gu, H.D., Olah, T.V., Arnold, M., Jemal, M., 2010. Effect of mobile phase pH, aqueous-organic ratio, and buffer concentration on electrospray ionization tandem mass spectrometric fragmentation patterns: implications in liquid chromatography/tandem mass spectrometric bioanalysis. Rapid Commun Mass Sp 24, 3221-3229.

Wang, W.Q., Cole, R.B., 2009. Enhanced Collision-Induced Decomposition Efficiency and Unraveling of Fragmentation Pathways for Anionic Adducts of

Brevetoxins in Negative Ion Electrospray Mass Spectrometry. Anal Chem 81, 8826-8838.

Wang, Y.S., Meng, L., Pittman, E.N., Etheredge, A., Hubbard, K., Trinidad, D.A., Kato, K., Ye, X.Y., Calafat, A.M., 2017. Quantification of urinary mono-hydroxylated metabolites of polycyclic aromatic hydrocarbons by on-line solid phase extraction-high performance liquid chromatography-tandem mass spectrometry. Anal Bioanal Chem 409, 931-937.

Wilm, M., 2011. Principles of Electrospray Ionization. Mol Cell Proteomics 10.

Wilson, C., Canning, P., Caravati, E.M., 2010. The abuse potential of propofol. Clin Toxicol 48, 165-170.

Wu, J.W., Chen, H.C., Ding, W.H., 2013. Ultrasound-assisted dispersive liquid-liquid microextraction plus simultaneous silylation for rapid determination of salicylate and benzophenone-type ultraviolet filters in aqueous samples. J Chromatogr A 1302, 20-27.

Wu, Z.R., Gao, W.Q., Phelps, M.A., Wu, D., Miller, D.D., Dalton, J.T., 2004. Favorable effects of weak acids on negative-ion electrospray ionization mass spectrometry. Anal Chem 76, 839-847.

Xiao, J., Shao, B., Wu, X.Y., Sun, X.J., Wu, Y.N., 2011. A Study on Bisphenol A, Nonylphenol, and Octylphenol in Human Urine amples Detected by SPE-UPLC-MS. Biomed Environ Sci 24, 40-46.

Xue, J.C., Liu, W.B., Kannan, K., 2017. Bisphenols, Benzophenones, and Bisphenol A Diglycidyl Ethers in Textiles and Infant Clothing. Environ Sci Technol 51, 5279-5286.

Yanes, O., Tautenhahn, R., Patti, G.J., Siuzdak, G., 2011. Expanding Coverage of the Metabolome for Global Metabolite Profiling. Anal Chem 83, 2152-2161.

Yang, J., Zhao, X.J., Lu, X., Lin, X.H., Xu, G.W., 2015. A data preprocessing strategy for metabolomics to reduce the mask effect in data analysis. Front Mol Biosci 2.

Yang, X.J., Qu, Y., Yuan, Q., Wan, P., Du, Z., Chen, D., Wong, C., 2013. Effect of ammonium on liquid- and gas-phase protonation and deprotonation in electrospray ionization mass spectrometry. Analyst 138, 659-665.

Yang, Y.J., Guan, J., Yin, J., Shao, B., Li, H., 2014. Urinary levels of bisphenol analogues in residents living near a manufacturing plant in south China. Chemosphere 112, 481-486.

Yao, Y., Shao, Y.J., Zhan, M., Zou, X.L., Qu, W.D., Zhou, Y., 2018. Rapid and sensitive determination of nine bisphenol analogues, three amphenicol antibiotics, and six phthalate metabolites in human urine samples using UHPLC-MS/MS. Anal Bioanal Chem 410, 3871-3883.

Ye, X.Y., Wong, L.Y., Kramer, J., Zhou, X.L., Jia, T., Calafat, A.M., 2015. Urinary Concentrations of Bisphenol A and Three Other Bisphenols in Convenience Samples of US Adults during 2000-2014. Environ Sci Technol 49, 11834-11839.

Zhang, J.Y., Dang, X.P., Dai, J.H., Hu, Y.L., Chen, H.X., 2021. Simultaneous detection of eight phenols in food contact materials after electrochemical assistance solid-phase microextraction based on amino functionalized carbon nanotube/polypyrrole composite. Anal Chim Acta 1183.

Zhang, L., Zhou, L.H., Ji, W.J., Song, W., Zhao, S.Q., 2017. Cysteamine-Assisted Highly Sensitive Detection of Bisphenol A in Water Samples by Surface-Enhanced Raman Spectroscopy with Ag Nanoparticle-Modified Filter Paper as Substrate. Food Anal Method 10, 1940-1947.

Zhang, Y.V., Wei, B., Zhu, Y., Zhang, Y.H., Bluth, M.H., 2016. Liquid Chromatography-Tandem Mass Spectrometry An Emerging Technology in the Toxicology Laboratory. Clin Lab Med 36, 635-+.

Zhou, F.Q., Zhang, L., Liu, A., Shen, Y., Yuan, J.P., Yu, X.J., Feng, X., Xu, Q., Cheng, C.G., 2013. Measurement of phenolic environmental estrogens in human urine samples by HPLC-MS/MS and primary discussion the possible linkage with uterine leiomyoma. J Chromatogr B 938, 80-85.

Zhou, X.L., Kramer, J.P., Calafat, A.M., Ye, X.Y., 2014. Automated on-line column-switching high performance liquid chromatography isotope dilution tandem mass spectrometry method for the quantification of bisphenol A, bisphenol F, bisphenol S, and 11 other phenols in urine. J Chromatogr B 944, 152-156.

Zhu, H.K., Chinthakindi, S., Kannan, K., 2021. A method for the analysis of 121 multi-class environmental chemicals in urine by high-performance liquid chromatography-tandem mass spectrometry. J Chromatogr A 1646.

Zhu, J.H., Cole, R.B., 2000. Formation and decompositions of chloride adduct ions, [M+Cl](-), in negative ion electrospray ionization mass spectrometry. J Am Soc Mass Spectr 11, 932-941.

Zhu, J.H., Cole, R.B., 2001. Ranking of gas-phase acidities and chloride affinities of monosaccharides and linkage specificity in collision-induced decompositions of negative ion electrospray-generated chloride adducts of oligosaccharides. J Am Soc Mass Spectr 12, 1193-1204.

Zimmers, S.M., Browne, E.P., O'Keefe, P.W., Anderton, D.L., Kramer, L., Reckhow, D.A., Arcaro, K.F., 2014. Determination of free Bisphenol A (BPA) concentrations in breast milk of US women using a sensitive LC/MS/MS method. Chemosphere 104, 237-243.

국문초록

액체 크로마토그래피(LC)-전자분무 이온화(ESI)-질량 분석법(MS)은 환경, 제약 및 생물학적 영역과 같은 생명 과학 응용 분야를 위해 널리 사용되는 분석 플랫폼이다. 우리 일상 생활의 기술 발전에 따라 고급 정보에 대한 보다 민감하고 강력한 분석 방법론에 대한 요구가 증가하고 있다. 따라서 최근의 분석 경향은 소량의 마이크로 샘플링만을 사용하여 다중 잔류물의 동시분석에 초점을 맞추고 있으며 이를 위한 핵심 요구 사항은 표적 분석물의 고감도 검출 한계이다. LC-ESI-MS/MS 분석에서 이동상 조성은 ESI 의 액상 스프레이 기반 이온화 과정으로 인해 분석물의 이온화 효율과 크로마토그래피 거동에 영향을 미치는 핵심 매개변수이다. 그러나 포지티브 ESI 분석모드에 대해 효과적으로 잘 알려진 이동상 첨가제(예: 아세트산 또는 포름산)와 대조적으로, 네거티브 ESI 모드에 대한 최상의 이동상 조성을 선택하기 위한 명확한 연구가 거의 없었다. 많은 생체 분자가 포지티브 ESI 분석을 선호하지만 네가티브 ESI 에서 쉽게 이온화될 수 있는 상당수의 작은 분자도 있다. 따라서 본 연구에서는 네가티브 ESI 모드에서 이동상 조성과 이온화 효율 사이의 상관 관계를 설명하였다.

이온화 효율에 대한 이동상 조성의 영향을 조사하기 위해 프로포폴 및 환경성 페놀류를 대상 물질로 분석하였다. 왜냐하면 약한 산인 페놀 구조는 ESI 에서 쉽게 음전하 이온으로 이온화되기 때문이다. 프로포폴은 널리 사용되는 마취제이지만 오락 목적으로 자주 남용되어 심각한 사회적 문제가 되고 있다. 환경성 페놀류 (예: 비스페놀, 파라벤, 벤조페논,

클로로페놀 및 알킬페놀)는 노출된 개인의 건강에 악영향을 줄 수 있는 중요한 내분비 교란 화학물질이다. 그러나 생물학적 시료의 프로포폴 측정은 프로포폴의 높은 휘발성과 질량분석기의 낮은 이온화 효율과 관련된 문제가 있다. 환경성 페놀류 또한 LC-ESI-MS/MS 를 사용하여 포괄적이고 민감한 분석 방법을 개발하는 데 한계가 있다. 그 이유는 상당량의 페놀, 특히 알킬페놀이 ESI 감도가 부족하기 때문이다.

본 연구에서, 우리는 이동상 조성의 체계적인 조사를 통해 페놀 화합물의 측정을 위한 민감하고 정확한 불소 보조 LC-MS/MS 방법을 개발하였다. 개발된 분석법은 극적으로 개선된 이온화 효율로 인해 간단한 희석을 통한 전처리가 가능하였다. 프로포폴의 경우 이동상의 ammonium fluoride 의 최적 농도는 메탄올 조건에서 1 mM 이었다. 유효성 검증시험에서 직선성은 양호했고 (R^2≥0.999) 일중 및 일간 정밀도는 1.9~8.7% 사이였다. 정확도는 87.5%에서 105.4% 범위였으며 소변 내 프로포폴의 검출 및 정량 한계는 각각 0.15 및 0.44 ng/mL 이었다. 개발된 분석법은 인간의 소변에 성공적으로 적용되었으며 투여 후 48 시간 동안 프로포폴과 프로포폴의 2 상 대사체를 동시분석할 수 있는 충분한 감도를 보였다. 환경성 페놀류의 경우 최적의 조건은 0.5 mM ammonium fluoride 를 첨가한 메탄올 이동상이었다. 이 이동상 조성은 38 개의 페놀류를 동시 이온화 및 특히 이온화 효율이 낮은 비스페놀 및 알킬페놀에 대한 감도 향상을 허용하였다. 개발된 분석법은 유효성 확인시험을 통해 검증되었으며 모든 물질은 좋은 직선성을 나타내는 R^2의 0.99 이상을 만족하였다. 대상 분석물에 대한 일중 및 일간 시험에서 정밀도는 0.4~14.6%,

정확도는 85.4~113.0%이었다. 또한, 수중(수영) 및 육상(실내 배구 및 야외 축구) 운동 선수로부터 얻은 80 개의 소변 샘플을 분석한 결과 특정 운동 선수는 스포츠 활동 유형에 따라 특정 환경 페놀에 노출될 수 있음을 발견하였다.

결과적으로, 페놀류에 특화된 이동상 조성물은 네가티브 ESI 에서 높은 p*K*a 값을 갖는 페놀 화합물의 본질적으로 열악한 이온화 효율을 크게 개선하였다. 게다가, 개발된 분석법은 새로 확인된 페놀 화합물을 통합 분석하는 데 매우 유용할 수 있는 일반 분석 플랫폼으로서의 잠재력을 가지고 있다.

주요어 : 플루오르화물 (fluoride), 이온화 효율, 프로포폴, 환경성 페놀류, 알킬페놀, 네가티브 이온화

학번 : 2015-30505

Fluoride-assisted liquid chromatography-tandem mass spectrometry method for simultaneous analysis of propofol and its metabolites without derivatization in urine

Author: Kang Mi Lee,Sang Moon Han,Seunghwa Lee,Tae Young Jeong,Ho Jun Kim,Hophil Min,Ki Hun Kim,Sangwon Cha,Won Keun Oh,Jaeick Lee

Publication: Journal of Chromatography A

Publisher: Elsevier

Date: 30 August 2021

Influence of mobile phase composition on the analytical sensitivity of LC–ESI–MS/MS for the concurrent analysis of bisphenols, parabens, chlorophenols, benzophenones, and alkylphenols

Author:
Kang Mi Lee,Sang Moon Han,Hyeon-Jeong Lee,Minsik Kang,Tae Young Jeong,Junghyun Son,Hophil Min,Sangwon Cha,Han Bin Oh,Won Keun Oh,Jaeick Lee

Publication: Environmental Research

Publisher: Elsevier

Date: 15 March 2023